UNIVERSITÀ DEGLI STUDI DI SALERNO

UNIVERSITÀ DEGLI STUDI DI SALERNO
Dipartimento di Farmacia

Dottorato di ricerca
in Scienze Farmaceutiche
Ciclo XII NS — Anno di discussione 2014

Coordinatore: Chiar.mo Prof. *Gianluca Sbardella*

Design, synthesis and biological studies of novel heterocyclic compounds as anticancer drugs

settore scientifico disciplinare di afferenza: CHIM/08

Dottorando

Dott.
Antonio Botta

Tutore

Chiar.mo Prof.
Carmela Saturnino

Contents

Abstract

Heterocyles are an essencial class of molecules, assuming a role in many aspect of our life. Indeed heterocyclic nucleus is a common feature of several biomolecule and bioactive compounds including agrochemical products and drugs.

In this work we focused on two important class of heterocyclic compounds: carbazoles and NHCs (N-heterocyclic carbenes).

Carbazoles, prevalent as structural motifs in various synthetic materials and naturally occurring alkaloids, as is known, have many applications such as optoelectronic materials, conducting polymers and especially as promising bioactive compounds due to their biological properties, known since 1965.

Furthermore NHCs are a class of stable carbenes that over the last few years have entered the field as "new" ligands for bioactive coordination compounds. It has been demonstrated that metal NHC complexes can be used to develop highly efficient metal based drugs with possible applications in the treatment of cancer or infectious diseases.

We aimed to design, synthesize and characterize novel carbazole derivatives and NHC metal complexes with the purpose of identify new biologically active heterocyclic compounds.

Introduction

Heterocycles

Heterocycles are a class of compounds, making up more than half of all known organic compounds. Heterocycles are prevalent in a broad variety of drugs, vitamins, natural products, biomolecules, and biologically active compounds, including anticancer, antibiotic, anti-inflammatory, antimalarial, anti-HIV, antimicrobial, antibacterial, antifungal, antiviral, antidiabetic, herbicidal, fungicidal, and insecticidal agents. Most of the heterocycles are involved in important applications regarding materials science such as dyestuff, fluorescent sensor, brightening agents, plastics, and analytical reagents. In addition, they have applications in polymer chemistry, especially in conjugated polymers. Indeed, they behave as organic conductors, semiconductors, molecular wires, photovoltaic cells, and organic light-emitting diodes (OLEDs), light harvesting systems, optical data carriers, chemically controllable switches, and liquid crystalline compounds. Heterocycles are also of considerable interest because of their synthetic utility as synthetic intermediates, protecting groups, chiral auxiliaries, organ catalysts, and metal ligands in asymmetric catalysts inorganic synthesis. Therefore, substantial attention has been paid to develop efficient new methods to synthesize heterocycles.

Heterocycles are common structural units in marketed drugs and in medicinal chemistry in the drug discovering process. The majority of pharmaceuticals and biologically active agrochemicals are heterocyclic while countless additives and modifiers used in industrial applications from cosmetics, reprography, information storage and plastics are heterocyclic in nature. One structural features inherent to heterocycles, which continue to be exploited to great advantage by the drug industry, lies in their ability to manifest substituents around a core scaffold in defined three dimensional representations. For more than a century, heterocycles have constituted one the largest areas of research in organic chemistry.

Among the approximately 20 million chemical compounds identified to this day, more than two-thirds are fully or partially aromatic and approximately half are heterocyclic. The presence of heterocycles in all kinds of organic compounds of interest in electronics, biology, optics, pharmacology, material sciences and so on is very well known. Between them, sulfur and nitrogen-containing heterocyclic compounds have maintained the interest of researchers through decades of historical development of organic synthesis. Many natural drugs [1,2,3,4] such as papaverine, theobromine, quinine, emetine, theophylline, atropine, procaine, codeine, reserpine and morphine are heterocycles. Almost all the compounds known as synthetic drugs such as diazepam, chlorpromazine, isoniazid, metronidazole, azidothymidine, barbiturates, antipyrine are also heterocycles. Synthetic heterocycles have therapeutic applications such as antibacterial, antifungal, antimycobacterial, trypanocidal, anti-HIV activity, antitubercular, antimalarial, herbicidal, analgesic, antiinflammatory, muscle relaxants, anticonvulsant, anticancer and lipid peroxidation inhibitor, hypnotics, antidepressant, antitumoral, anthelmintic and insecticidal agents [5,6,7,8,9]. In fact, heterocyclic motif is present in the structures of all top 10 brand name small molecule drugs (Figure 1).

Moreover heterocycles are used as bioisosteres for a variety of functional groups in drug candidates. The pharmacological benefits of employing heterocycles for better potency and specificity can in many cases be explained by their ability to participate in hydrogen bonding with the target protein, where the heterocycle can play the role of either H-acceptor as in heteroaromatic compounds or H-donor as in saturated N-heterocycles.

Hydrogen bonding is relevant not only for pharmacological properties, but also for physicochemical and transport properties of drug molecules. In their review, Laurence et al. have convincingly explained the importance of HB basicity, i.e., HB acceptor ability, in drug molecule design. The strongest HB acceptors among the heterocycles are N-methylimidazole, N-methylpyrazole, and pyridine, while the weakest HB acceptors include furan and thiophene. Steric and electronic effects influence the HB of heterocycles. It is also important to realize that HB basicity does not always correlate with proton basicity. Pyridine is much

more basic than pyridazine; however, their HB acceptor properties are comparable. [10]

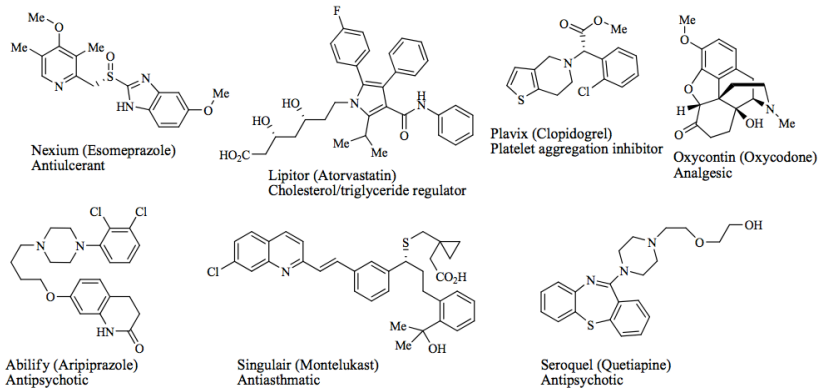

Figure 1 *All top 10 brand name small molecule drugs*

Chapter I

1 Carbazoles

Carbazoles are a class of aromatic heretocyclic nuclei (Figure 2), isolated first from coal tar in 1872 by Graebe and Glazer. In 1965, Chakraborty et al. described the isolation and biological properties of murrayanine from Murraya koenigii Spreng. The isolation of murrayanine was the first report of a naturally occurring carbazole alkaloid. Since then there has been a strong interest in this compounds due to the alluring structural features and promising biological activities exhibited by many carbazole alkaloids. They are prevalent as structural motifs in various synthetic materials and naturally occurring alkaloids.

Most carbazole alkaloids have been isolated from the taxonomically related higher plants of the genus Murraya, Glycosmis, and Clausena from the family Rutaceae. The genus Murraya represents the richest source of carbazole alkaloids from terrestrial plants. The lower plants from which carbazole alkaloids have been isolated include several different Streptomyces species. Further natural sources for carbazole alkaloids are, for example, the blue-green algae Hyella caespitosa, Aspergillus species, Actinomadura species, and the ascidian Didemnum granulatum. [11]

Carbazoles exhibit material properties as optoelectronic [12] materials, conducting polymers [13], and synthetic dyes [14]. For example, polyvinylcarbazoles (PVK) [15] have been extensively studied for their applications in photorefractive materials and xerography. Recently, some poly(2,7-carbazole) derivatives have been used in polymer solar cells [16]. They are also widely used in organic light-emitting diodes as green, red, and white emitters. The molecular and optical properties of carbazoles can be engineered by structural modifications on the C-2, -3, -6, -7, and -9 positions [17]. Moreover some benzo-carbazoles have been utilized as molecular platforms for luminescent, hole-transporting, and host materials in organic light-emitting devices [18].

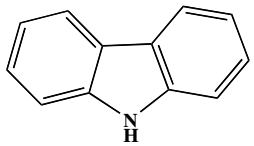

Figure 2 *Structure of carbazole*

A large number of carbazoles from plants are endowed with profound biological activities, which include antitumor, psychotropic, antiinflammatory, antihistaminic, antibiotic, and anti-oxidative activities. The structural attributes of such carbazole-based natural products are multifarious. One of their most important features is the presence of nuclear hydroxyl groups, as well as the quinone functionality.

In addition, phenyl groups are often found in some natural carbazoles. A large group of bioactive carbazole natural products and synthetic derivatives are found to contain annulated rings such as those in ellipticine derivatives (1) (Figure 3), staurosporine (2),carbazomycin B (3), carbazomadurin A (4), clausenamine A (5), etc. Moreover, the carbazole moiety is considered as one of the pharmacophores in the cardiovascular pharmaceuticals carvedilol (6), and carazolol (7), which are used in the treatment of hypertension, ischemic heart disease, and congestive heart failure [19].

Considering the evidences of carbazoles bioactivities, several synthetic strategies has been reported in the literature. In recent years, the synthesis of these carbazole alkaloids has been extensively reviewed by Knolker et al. [20] [21]. Traditionally, the synthesis of carbazoles could be carry out upon nitrene insertion, Fischer indolization, Pummerer cyclization, Diels-Alder reaction, dehydrogenative cyclization of diarylamines, etc. In more recent years, transition metal-mediated C-C and C-N bond formation, cyclotrimerization, benzannulation, Suzuki-Miyaura coupling, ring-closing metathesis, etc. have been investigated. These reactions follow two modes: (i) the formation of an A or C ring from substituted indole derivatives and (ii) the formation of a B ring from benzene derivatives. Many of these strategies are continuously innovated to address issues related to regiochemical selectivity and efficiency [19].

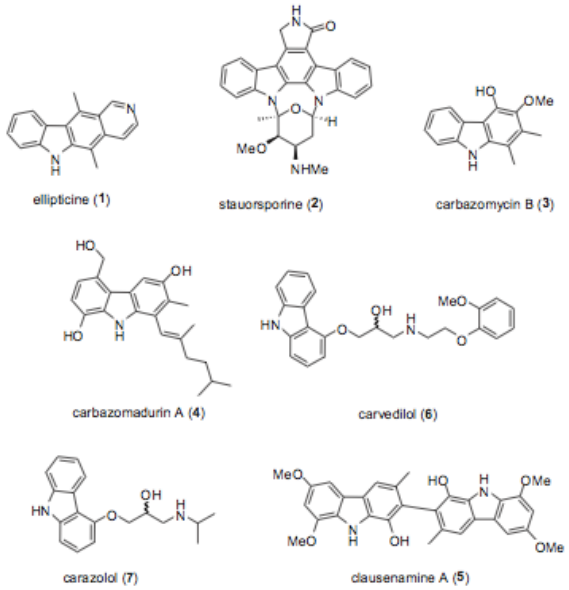

Figure 3 *Bioactive carbazole natural products and synthetic derivatives*

Several working hypotheses have been proposed to account for the biogenesis of carbazole alkaloids, but no evidences have been observed. A comparison of the structural features of the carbazole alkaloids isolated from higher plants suggests that 3-methylcarbazole may represent the key intermediate in their biosynthesis. On the other hand, 2-methylcarbazole appears to be the common biogenetic precursor of the conventional tricyclic carbazoles isolated from lower plants. However the biogenetic precursor of the carbazole nucleus in nature is not clear.

The isolation of several 3-methylcarbazole derivatives from higher plants [22] and of carbazole from Glycosmis pentaphylla [23] shows that the aromatic methyl group can be eliminated oxidatively from the key intermediate 3-methylcarbazole via -CH_2OH, -CHO, and -COOH functionalities [24]. The isolation of 3-methylcarbazole from the genus Clausena [25] the co-occurrence of murrayafoline A (**2**), koenoline (**3**), murrayanine (**4**), and mukoeic acid (**5**) in M. koenigii, as well as the subsequent isolation of mukonine (**6**) and mukonidine (**9**) and the discovery of 2-hydroxy-3-methylcarbazole (**7**) and mukonal (**8**) in M. koenigii support the hypothesis of biomimetic hydroxylation of 3-

methylcarbazole. Congeners that differ in the oxidation state of the C-3 methyl group, i.e. -CH_2OH, -CHO, -COOH, and -COOMe, were found for various alkaloids, a fact which indicates an in vivo oxidation of carbazole alkaloids (Figure 4). The occurrence of heptaphylline (**10**) [26] and murrayacine (**11**) [27] (Figure 5) in Clausena heptaphylla is circumstantial evidence for the origin of the pyran ring from the phenylated congener. This explains the formation of pyranocarbazoles from 2-hydroxy-3-methylcarbazole as shown by Popli and Kapil [28] The co-occurrence of 2-hydroxy-3-methylcarbazole (**7**) [29] mukonal (**8**), [30] and mukonidine (**9**) [31] provides clear evidence for the in vivo oxidation of the methyl group in 2-hydroxy-3-methylcarbazole. All these findings strongly suggest 3-methylcarbazole as the key precursor for the carbazoles isolated from higher plants.

A classical method that has been often utilized for the synthesis of aromatic carbazoles is the dehydrogenation of 1,2,3,4-tetrahydrocarbazoles prepared by Fischer-Borsche synthesis. Many carbazole alkaloids were synthesized from a variety of indole precursors or by oxidative cyclization of diarylamines.

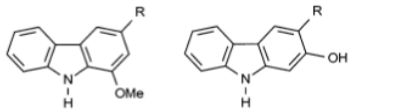

2 Murrayafoline A
R = Me
3 Koenoline
R = CH_2OH
4 Murrayanine
R = CHO
5 Mukoeic acid
R = COOH
6 Mukonine
R = COOMe

7 2-Hydroxy-3-methylcarbazole
R = Me
8 Mukonal
R = CHO
9 Mukonidine
R = COOMe

Figure 4 *Carbazole alkaloids*

10 Heptaphylline **11** Murrayacine

Figure 5 *Carbazole alkaloids (1)*

Carbazole, the active compound of coal tar and its *N*-alkyl derivatives, decreased IL-6-stimulated STAT3 activation and DNA-binding activity in embryonic kidney or human monocytic leukaemia cells through undefined mechanisms, without affecting phosphorylation of STAT3 [32] [33].

1.1 STAT proteins: novel molecular targets for cancer drug discovery

Signal Transducers and Activators of Transcription (STATs) are a family of cytoplasmic proteins with roles as signal messengers and transcription factors that participate in normal cellular responses to cytokines and growth factors. Frequently, however, abnormal activity of certain STAT family members, particularly Stat3 and Stat5, is associated with a wide variety of human malignancies, including hematologic, breast, head and neck, and prostate cancers.

STATs were originally discovered as latent cytoplasmic transcription factors that mediate cellular responses to diverse cytokines and growth factors [34] [35] [36].

STATs are activated by tyrosine phosphorylation following the binding of cytokines or growth factors to cognate receptors on the cell surface (Figure 6).Tyrosine kinases that mediate STAT activation include growth factor receptors and cytoplasmic tyrosine kinases, particularly Janus kinase (JAK) and Src kinase families. Once tyrosine phosphorylated, two STAT monomers form dimers through reciprocal phosphotyrosine-SH2 interactions, translocate to the nucleus, and bind to STAT-specific DNA-response elements of target genes to induce gene transcription. To date, there are seven STAT family members identified in mammals, designated Stat1, Stat2, Stat3, Stat4, Stat5a, Stat5b and Stat6. STATs have diverse normal biological functions, which include roles in cell differentiation, proliferation, development, apoptosis, and inflammation [37] [38].

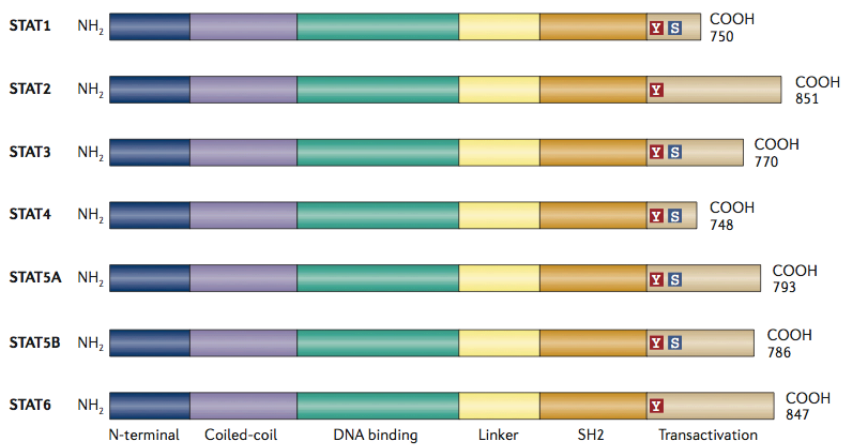

STAT proteins are involved in some fundamental cellular processes, including cell growth and differentiation, development, apoptosis, immune responses and inflammation [39](Figure 6). STAT1 signaling is activated in response to interferon (IFN) stimulation and supports immune function by controlling the growth and apoptosis of immune cells [40]. STAT1 signaling regulates T helper type 1 (TH1) cell-specific cytokine production that alters both immune function and inflammatory responses by shifting the balance between TH1 and TH2 cells [41]. Indeed, STAT1 deficiency abrogates IFN responsiveness, leading mice to succumb to bacterial and viral infections [42]. Furthermore, the loss of responsiveness to IFNγ due to STAT1 deficiency provides malignant cells with a growth advantage and leads to increased tumour formation [40]. This outcome suggests that STAT1 has a tumour-suppressive function; although recent data indicate that the protein has a more complex role in carcinogenesis [40]. Moreover, in STAT1-null mouse models of atherosclerosis-susceptible bone-marrow transplantation, these mice have reduced foam cell formation and atherosclerosis, which suggests that STAT1 has a pro-atherogenic function [43]. By contrast, gain-of-function mutations in the STAT1 gene which lead to STAT1 hyperactivation and defective nuclear dephosphorylation affect TH1 and TH17 cell responses and cause chronic mucocutaneous candidiasis [44].

STAT2 signalling is important for the induction of antiviral effects. STAT2-null mice and STAT2-null cell lines have defective antiviral

responses to IFNα and IFNβ, as well as blunted apoptotic effects to IFNα and IFNβ [45]. Evidence further suggests that altered STAT2 signalling may partly contribute to carcinogenesis through the upregulation of interleukin-6 (IL-6) production, which promotes STAT3 activation [45]. Notably, the colon of STAT2-deficient mice showed markedly lower levels of IL-6, which was associated with diminished tumour progression [45]. By contrast, the reconstitution of STAT2 in the null background upregulated IL-6 production and increased the levels of pSTAT3.

STAT3 function is essential for early embryonic development, which is clearly demonstrated by the death on day 8.5 of STAT3-deficient mouse embryos [46]. The biological importance of STAT3 was further studied using tissue-specific STAT3-deficient mice [47]. In vitro cultured STAT3-deficient T cells did not respond to IL-6 stimulation and could not be rescued by IL-6 from apoptotic cell death, indicating that STAT3 functions are essential for IL-6-mediated anti-apoptotic responses [48]. Furthermore, STAT3-deficient keratinocytes showed a poor wound-healing response in vitro and in vivo, which was due to the limited migration of the cells [49]. In addition, the dysregulation of the role of STAT3 in keratinocyte physiology is thought to contribute to the induction of skin carcinogenesis [50]. STAT3 function is often aberrant in the context of cancer, and this abnormality represents an underlying mechanism of STAT3 for promoting malignant transformation and progression. Of clinical significance, constitutively active STAT3 is detected in numerous malignancies, including breast, melanoma, prostate, head and neck squamous cell carcinoma (HNSCC), multiple myeloma, pancreatic, ovarian, and brain tumours [51] [52] [53] [54] [55].

Aberrant STAT3 signalling promotes tumorigenesis and tumour progression partly through dysregulating the expression of critical genes that control cell growth and survival, angiogenesis, migration, invasion or metastasis [51] [52] [53] [54]. These genes include those that encode p21WAF1/CIP2, cyclin D1, MYC, BCL-XL, BCL-2, vascular endothelial growth factor (VEGF), matrix metalloproteinase 1 (MMP1), MMP7 and MMP9, and survivin [51] [52] [53] [54]. Evidence also supports a role of STAT3 in the suppression of tumour immune surveillance [56] [57]. Consequently, the genetic and pharmacological modulation of persistently active STAT3 was shown to control the tumour phenotype and to lead to tumour regression in vivo [53] [54] [55], [58] [59]. Of further clinical

significance, mutations within the SH2 domain-coding sequence in STAT3 occur in patients with a rare primary immunodeficiency, hyperimmunoglobulin E syndrome, and in large granular lymphocytic leukaemia [60]. These mutations reportedly increase the stability of the functional STAT3–STAT3 dimers and are associated with the disease pathogenesis [60] [61].

STAT4 is a crucial mediator of IL-12 function that regulates the differentiation of TH1 cells and their inflammatory responses [41]. Accordingly, STAT4 signalling is associated with autoimmune diseases, such as experimental autoimmune encephalomyelitis (EAE) induction, an animal model of multiple sclerosis [62]. Indeed, mice deficient in the Stat4 gene were protected from developing EAE35. Additionally, STAT4-null lymphocytes showed decreased proliferation and had an impaired response to IL-12 [63]. Treatment with a STAT4-specific antisense oligonucleotide (ASO) led to an improvement in the systemic lupus erythematosus (SLE) phenotype, severe lupus nephritis in mouse models, which suggests that STAT4 also has an important role in SLE, even though STAT4 knockout had no effect on the clinical presentation of the disease in mouse models [63].

STAT5 has two isoforms, STAT5A and STAT5B, which are encoded by distinct genes and share 96% sequence homology, with notable differences occurring in the transactivation domain [64]. Normal STAT5 signalling is important in mammary gland development and milk production, and in haematopoiesis [65]. Mice deficient in both STAT5A and STAT5B show defects in IL-2 receptor-α expression in T lymphocytes [47]. By contrast, mice that are deficient in STAT5B only showed loss of sexual dimorphism of body growth rate, which was accompanied by a decreased expression in male-specific liver genes [66] and the attenuation of the cytolytic activity of natural killer cells [67]. Constitutive STAT5 activation is also implicated in the pathogenesis of HNSCC, chronic myelogenous leukaemia (CML) [68], breast [69], prostate and uterine cancers [54]. The aberrant STAT5 activation by BCR–ABL in CML43 is particularly noteworthy. It is widely recognized that STAT5 and STAT3 share similar functions in promoting cancer, including the induction of pro-proliferative and anti-apoptotic genes [70] [71].

STAT6 signalling is induced by IL-4 and IL-13 and supports immune function, notably regulating the balance between inflammatory and allergic immune responses [72] [73] [74] [75]. Beyond the immune system, STAT6 signalling promotes luminal mammary epithelium development and is implicated in the pathology of lung and airway disease, including the promotion of airway hyperactivity and mucus production in the lung epithelium, and the regulation of allergic skin inflammation [72] [76] [77] [78].

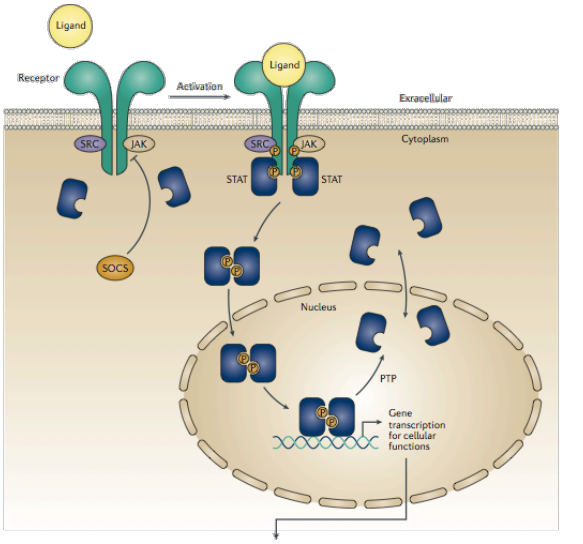

STAT	Cellular functions	Major diseases
1	• Cell growth and apoptosis • T_H1 cell-specific cytokine production • Antimicrobial defence	• Atherosclerosis • Infection • Immune disorders
2	• Mediation of IFNα/IFNβ signalling	• Cancer • Infection • Immune disorders
3	• Cell proliferation and survival • Inflammation • Immune response • Embryonic development • Cell motility	• Cancer
4	• T_H1 cell differentiation • Inflammatory responses • Cell proliferation	• Experimental autoimmune encephalomyelitis (multiple sclerosis) • Systemic lupus erythematosus
5A	• Cell proliferation and survival • IL-2Rα expression in T lymphocytes • Mammary gland development • Lactogenic signalling	• Cancer • Chronic myelogenous leukaemia
5B	• Cell proliferation and survival • IL-2Rα expression in T lymphocytes • Sexual dimorphism of body growth rate • NK cell cytolytic activity	• Cancer • Chronic myelogenous leukaemia
6	• Inflammatory and allergic immune response • B cell and T cell proliferation • T_H2 cell differentiation	• Asthma • Allergy

Figure 6 *Stat proteins activation and their diseases involving*

1.1.1 Approaches to inhibit STAT proteins

Since the discovery of the first peptide inhibitor of a STAT protein [71], the achievement to target STAT signalling for therapeutic purposes continue.
Several inhibitory strategies against STAT signalling and function are being pursued (Corporature 7).
A validated model for the inhibition of STATs patways is represented by small-molecule dimerization disruptors (SMDDs) or phospho-peptidomimetic inhibitors (PPMIs) that target the phospho-Tyr-SH2 domain interaction at the interface of dimers of signal transducer and activator of transcription (STAT) proteins. This leads to the disruption of STAT–STAT dimers and the formation of STAT–SMDD or STAT–PPMI heterocomplexes, leading to a suppression of STAT signalling and function. Instead the binding of ligands, such as growth factors and cytokines, to their cognate receptors on the cell surface induces STAT tyrosine phosphorylation and activation. Tyrosine kinases that mediate STAT phosphorylation, leading to STAT–STAT dimer formation, are the targets of small-molecule tyrosine kinase inhibitors. The overall effect of these modulators is to block the induction of STAT phosphorylation and signalling [79].

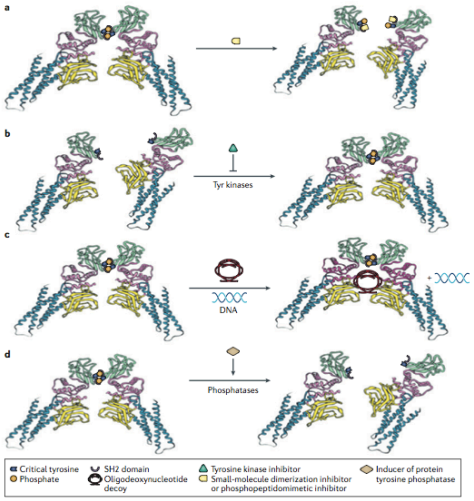

Corporature 7 *Various inhibitory strategies against STAT signalling*

Most of

these focus on inhibiting STAT dimerization using peptides or peptidomimetics generated through structure-based design, small molecules identified by molecular modelling, virtual or library screening, or natural products. STAT dimerization and signalling can also be blocked by inhibiting tyrosine kinases that phosphorylate STAT proteins, or by inducing phosphatases that dephosphorylate STAT proteins.
Other approaches, include the use of oligodeoxynucleotide (ODN) decoys as specific STAT DNA-binding domain inhibitors and ASOs that interfere with STAT mRNA [79].

1.1.2 STATs and oncogenesis

Studies of the molecular basis of oncogenesis by oncoproteins like v-Src have provided insights into changes in intracellular signaling proteins that participate in malignant transformation. The initial finding that Stat3 is constitutively activated in v-Src transformation [79] [80] suggested that aberrant STATs may have key roles in oncogenesis [81] [82]. Moreover, a constitutively activated Stat3 mutant alone is sufficient to induce transformation, and cells transformed this way can form tumors in nude mice [83], providing genetic evidence that Stat3 has oncogenic potential. Certainly these evidences confirm that the abnormal Stat3 activation can induce permanent changes in gene expression programs that ultimately lead to the malignant phenotype. Hence, constitutive Stat3 signaling contributes to transformation by oncogenic tyrosine kinases.
In addition to v-Src, other transforming tyrosine kinases, such as v-Eyk [84], v-Ros [85], v-Fps [86], Etk/ BMX [87], and Lck [88], all activate Stat3 in the context of oncogenesis.
Furthermore, constitutive Stat3 activation is also associated with transformation induced by tumor viruses, including HTLV-1 [89],polyomavirus middle T antigen [86], EBV [90], and herpesvirus saimiri [88], that directly or indirectly activate JAKs or Src family tyrosine kinases. Due of its central position in the signaling pathways from protein tyrosine kinases, aberrant Stat3 activity is a key mediator in the transforming process induced by oncogenic tyrosine kinases. In contrast, Stat3-independent mechanisms mediate transformation by oncoproteins that are not tyrosine kinases themselves or do not activate tyrosine kinase signaling pathways, including v-Ras and v-Raf [86].
With regard to other STATs, constitutive activation of both Stat1 and Stat5 accompanies transformation of pre-B lymphocytes by the v-Abl tyrosine kinase [91]. The transforming BCR-Abl fusion protein also activates Stat1 and/or Stat5 [92] and constitutive Stat5 activity is essential for BCR-Abl-induced transformation [93] [94]. Consistent with these findings, mutationally activated forms of Stat5 are sufficient to induce certain properties of transformed cells [95]. That being so, it can be resumed that Stat3 and Stat5 are the STAT family members with intrinsic oncogenic potential and most strongly associated with human cancer.

Mounting evidence gives credence to Stat3 as a bona fide mediator of oncogenesis that participates in human malignancies. In the context of human cancer, there is a high frequency of activation of Stat1, Stat3 and Stat5 (Table 1), with higher incidence of abnormal Stat3 activation in almost all the tumors studied [97].

Tumor type	*Activated STATs*	*References*
Breast cancer		
Tumors	Stats 1,3	(Garcia *et al.*, 2000; Watson and Miller, 1995) (J Bromberg and JE Darnell, unpublished results; P Chaturvedi and EP Reddy, unpublished results; R Garcia, C Muro-Cacho, S Minton, C Cox, N Ku, R Falcone, T Bowman and R Jove, unpublished results)
Cell lines	Stat 3	(Garcia *et al.*, 1997; Sartor *et al.*, 1997)
Head and neck cancer		
Cell lines and tumors	Stats 1,3	(Grandis *et al.*, 1998, 2000a)
Malignant melanoma		
Cell lines and tumors	Stats 1,3	(Florenes *et al.*, 1999; Kirkwood *et al.*, 1999; Pansky *et al.*, 2000)
Pituitary tumors		
Cell lines	Stat 1	(Ray *et al.*, 1998)
Brain tumors (primary tumors)		
Gliomas	Stats 1,3	(Cattaneo *et al.*, 1998)
Medulloblastomas	Stat 3	(Cattaneo *et al.*, 1998)
Cerebral menangiomas	Stats 1,3,5	(Magrassi *et al.*, 1999; Schrell *et al.*, 1998)
Multiple myeloma		
Cell lines and tumors	Stats 1,3	(Catlett-Falcone *et al.*, 1999b)
Lymphomas (tumors and cell lines)		
Anaplastic large T cell lymphoma	Stats 3,5	(Zhang *et al.*, 1996c)
Sezary syndrome	Stats 3,5	(Zhang *et al.*, 1996c)
EBV-related Burkitt's lymphoma	Stat 3	(Weber-Nordt *et al.*, 1996)
HSV Saimiri-dependent (T cell)	Stat 3	(Lund *et al.*, 1997b, 1999)
Cutaneous T cell lymphoma	Stat 3	(Sun *et al.*, 1998)
LSTRA T cell lymphoma (mouse)	Stat 5	(Yu *et al.*, 1997)
Mycosis fungoides	Stat 3	(Nielsen *et al.*, 1997)
Leukemias (tumors and cell lines)		
HTLV-I-dependent	Stats 3,5	(Migone *et al.*, 1995; Takemoto *et al.*, 1997)
Erythroleukemia	Stats 1,5	(Carlesso *et al.*, 1996)
Acute lymphocytic leukemia (ALL)	Stats 1,5	(Gouilleux-Gruart *et al.*, 1996; Weber-Nordt *et al.*, 1996)
Chronic lymphocytic leukemia (CLL)	Stats 1,3	(Frank *et al.*, 1997)
Acute myelogenous leukemia (AML)	Stats 1,3,5	(Chai *et al.*, 1997; Gouilleux-Gruart *et al.*, 1996; Weber-Nordt *et al.*, 1996)
Chronic myelogenous leukemia (CML)	Stat 5	(Carlesso *et al.*, 1996; Chai *et al.*, 1997; Shuai *et al.*, 1996a)
Megakaryocytic leukemia	Stats 1,3,5	(Liu *et al.*, 1999)
Large granular lymphocyte (LGL) leukemia	Stat 3	(Epling-Burnette *et al.*, 2000)
Other cancers (tumors and cell lines)		
Prostate	Stat 3	L Mora, R Garcia, J Seigne, T Bowman, M Huang, G Niu,
Renal cell carcinoma	Stat 3	J Pow-Sang, J Diaz, C Muro-Cacho, D Coppola, T Yeatman,
Pancreatic adenocarcinoma	Stat 3	J Cheng, S Nicosia, S Shivers, T Landowski, D Reintgen,
Ovarian carcinoma	Stat 3	W Dalton, H Yu and R Jove, unpublished results
Melanoma		

Table 1 *Activation of STAT proteins in tumor*

1.1.3 Targeting STAT3

Several human cancers could benefit from therapeutics that target aberrantly active STAT3. Owing to its therapeutic significance, STAT3 is the target in many drug discovery research efforts.
An important factor determining STAT3 functional heterogeneity is probably the existence of two alternatively spliced isoforms: the full-length STAT3α and the truncated STAT3β, which lacks the C-terminal activation domain and is generally considered a dominant negative form [96,97]. Mice specifically lacking STAT3β are hypersensitive to endotoxin-induced inflammation and undergo both up- and down-regulation of gene subsets, indicating specific functions for the STAT3β isoform [98]. To assess the specific functions of STAT3α and STAT3β, V. Poli and co. [99] generated mice that can produce only one isoform or the other. They confirmed that STAT3β is not required for viability but is involved in inflammation. In contrast, STAT3α-deficient mice died within 24 h of birth, showing that this isoform is required for postnatal functions but that STAT3β can rescue the embryonic lethality of a complete STAT3 deletion. Indeed, their data indicate that STAT3β is not a dominant negative factor, as it can activate specific STAT3 target genes. However, STAT3α has nonredundant roles in modulating IL-6 signaling and mediating IL-10 functions.
Several studies highlighted the oncogenic importance of Stat3 and established a direct link to tumor progression. Aberrant Stat3 signaling is obligatory for growth and survival of various human tumor cells, including multiple myelomas (MM), breast carcinomas, head and neck squamous cell carcinomas (HNSCC), the T cell lymphoma mycosis fungoides, and large granular lymphocyte (LGL) leukemia [100] [101].
STAT3 drug discovery research has mostly focused on targeting the pTyr-SH2 domain interaction [102] [103] given its importance in promoting STAT3 dimerization and function, and these efforts have generated various inhibitory agents.
However, there are many reported STAT3 inhibitors that may induce their effects through multiple mechanisms.

1.1.3.1 Peptides and peptidomimetics

A semirational, structure-based design approach identified the first SH2 domain-binding peptides and peptidomimetics that disrupt the STAT3 pTyr-SH2 domain interactions and STAT3–STAT3 dimerization [102,103,104]. The native, parent pTyr peptide, PY*LKTK (where Y* stands for pTyr) and its modified forms blocked the DNA-binding and transcriptional activities of STAT3 at high micromolar concentrations [104]. Peptidomimetic and non-peptide analogues, including ISS-610 and S3I-M2001, exhibited improved potency against STAT3 activity in vitro and against diverse malignant cells harbouring aberrantly active STAT3 [58,103,104]. S31-M2001 inhibited the growth of human breast tumour xenografts, while ISS-610 inhibited cell growth and induced apoptosis in vitro [58].

Furthermore, phosphopeptide binding sequences with the primary structure pTyr-Xxx-Xxx-Gln (where Xxx represents any amino acid) derived from leukaemia inhibitory factor (LIF), IL-10 receptor, epidermal growth factor receptor (EGFR), granulocyte colony-stimulating factor (GCSF) receptor or glycoprotein 130 (gp130), similarly inhibited STAT3 activation [105,106]. In these studies, the peptidomimetic Ac-pTyr-Leu-Pro-Gln-Thr-Val-NH2 was derived, which inhibited STAT3 activity (IC50 values of 150 nM) [106,107]. Moreover, a 28-mer native peptide identified as SPI, derived from the STAT3 SH2 domain, inhibited the STAT3 pTyr-SH2 domain interaction and signalling. The activity of SPI was moderate, but it did suppress cell viability and induced apoptosis of human breast, pancreatic, prostate and non-small cell lung cancer (NSCLC) cells in vitro [108].

1.1.3.2 Small molecules

Many small-molecule inhibitors of STAT3 activity have been identified through computational modelling, docking studies and virtual screening of chemical libraries (Table 2). In most cases, these agents function as disruptors of STAT3–STAT3 dimerization. STA-21 (also known as NSC628869) was identified from the screening of the National Cancer Institute (NCI) chemical library as an inhibitor of STAT3 dimerization, DNA-binding activity and transcriptional function in breast cancer cells,

with a potency of 20 μM [109]. Its structural analogue, LLL-3 (which showed improved membrane permeability), decreased cell viability *in vitro* and intracranial tumour size *in vivo* in glioblastoma animal models [110]. A catechol (1,2-dihydroxybenzene) compound was identified from Wyeth's proprietary small-molecule collection as a STAT3 SH2 domain inhibitor, and this agent was active at 106 μM against a multiple myeloma cell line [111]. Furthermore, a structure-based, virtual screen of the NCI chemical library targeting the STAT3 SH2 domain discovered S3I-201 (also known as NSC74859) as a STAT3–STAT3 dimerization disruptor, with a potency of 60–110 μM [58]. S3I-201 inhibited STAT3 DNA-binding and transcriptional activities, induced growth inhibition and apoptosis of tumour cells harbouring constitutively active STAT3, and suppressed the growth of human breast cancer xenografts [58]. Several of its derivatives, including S3I-201.1066, BP-1-102 and S3I-1757, showed improved potencies, with IC50 values of 35 μM (S3I-201.1066), 6.8 μM (BP-1-102) and 13.5 μM (S3I-1757), and inhibited cell growth, malignant transformation, survival, migration and invasiveness *in vitro* of malignant cells harbouring aberrantly active STAT3.

Virtual ligand screening identified Cpd30 (4-(5-((3-ethyl-4-oxo-2-thioxo-1,3-thiazolidin-5-ylidene)methyl)-2-furyl)benzoic acid), which selectively inhibited STAT3 with moderate potency, blocked STAT3 nuclear translocation upon IL-6 stimulation, and induced apoptosis in breast cancer cells harbouring constitutively active STAT3 . The related agent, Cpd188(4-((3-((carboxymethyl)thio)-4-hydroxy-1-naphthyl)amino)sulphonyl)benzoic acid), in combination with docetaxel, decreased tumour growth in chemotherapy-resistant human breast cancer xenograft models.

Stattic, a non-peptide small molecule discovered through virtual screening of chemical libraries, targets the STAT3 SH2 domain and inhibits STAT3 signalling at 10 μM [112]. It induced apoptosis of STAT3-dependent breast cancer and HNSCC cells and inhibited growth of orthotopic HNSCC tumour xenografts [112]. STX-0119, another STAT3 SH2 domain antagonist, induced antitumour cell effects *in vitro* and antitumour effects *in vivo* in a human lymphoma model, possibly by disrupting STAT3–STAT3 dimerization [113], with little effect on STAT3 phosphorylation [113]. Fragments of STX-0119 and stattic were chemically fused to generate HJC0123 [114], which suppressed STAT3

phosphorylation and transcriptional activity in breast cancer cells and induced antitumour cell effects against breast and pancreatic cancer cells *in vitro* at IC50 values of 0.1–1.25 μM. The oral administration of HJC0123 led to inhibition of growth of human breast cancer xenografts [114].

Furthermore, an agent identified as OBP-31121 was reported to inhibit STAT1, STAT3 and STAT5 phosphorylation. OBP-31121 induced loss of viability and apoptosis *in vitro* and inhibited tumour growth *in vivo* in gastric cancer models, and it further sensitized gastric cancer cells to cisplatin and 5-fluorouracil [115]. OBP-31121 has progressed to a Phase I clinical trial to determine the maximum tolerated dose.

1.1.3.3 Natural product inhibitors

Natural products have been an important resource in STAT3 inhibitor discovery and these efforts have yielded several lead candidates (Table 3).In many of these cases, however, the mechanism of action of these candidates with regard to STAT3 activity are unclear. It is possible that they inhibit STAT3 indirectly and are likely to block several targets.

Curcumin, a phenolic compound derived from the perennial herb *Curcuma longa* was shown to suppress JAK–STAT signalling at 15 μM, induce cell cycle arrest and inhibit cell invasion *in vitro* in a small cell lung cancer model [116]. In mice bearing gastric cancer xenografts, treatment with curcumin inhibited IL-6 production by IL-1β-stimulated myeloid-derived suppressor cells, which was associated with decreased activation of STAT3 and nuclear factor-κB (NF-κB).

Curcumin analogues with improved bioavailability and stability, such as FLLL32, had enhanced potency (IC50 values of 0.75–1.45 μM) in suppressing both pSTAT3 and total STAT3, and they also induced STAT3 ubiquitylation and possible proteasomal degradation in canine and human osteosarcoma cells *in vitro* [117]. Another curcumin analogue, HO-3867, similarly downregulated STAT3 signalling in cisplatin-resistant human ovarian cancer cells, thereby promoting enhanced sensitivity to cisplatin [118]. HO-3867 also induced apoptosis in BRCA1-mutated human ovarian cancer cells that harbour aberrantly active STAT3 [119].

Studies suggest that LLL12 (Table 2), another small-molecule inhibitor of STAT3 signalling that is based on curcumin [120], might suppress STAT3 activation by blocking its recruitment to the receptor and thereby preventing phosphorylation by tyrosine kinases, and by interfering with dimerization [121]. LLL12 suppressed cell viability, induced apoptosis, and repressed colony formation and migration *in vitro* in studies of glioblastoma, osteosarcoma and breast cancer cells84,86. It also inhibited angiogenesis, tumour vasculature development, and tumour growth *in vivo* in osteosarcoma xenograft models [120,121]. Except for the finding that the analogues FLLL32 and FLLL62 may interact with the STAT3 SH2 domain, questions remain regarding how curcumin or its analogues inhibit STAT3 signalling.

Resveratrol (3,5,4′-trihydroxystilbene), a polyphenolic compound found in red grapes and several other plants, was reported to inhibit STAT3 signalling at high micromolar concentrations, and it is likely that this effect contributes to the antitumour cell responses to this agent.

Constitutive and IL-6-induced STAT3 activation in multiple myeloma, leukaemia and other tumour cell types were inhibited on resveratrol treatment, leading to a decreased expression of BCL-2 and other anti-apoptotic proteins, and apoptosis induction *in vitro* [122]. The resveratrol derivative LYR71 suppressed breast cancer cell viability (IC50 value of 20 μM), and inhibited STAT3-mediated MMP9 expression [123]. Reports also showed that the inhibition of the JAK–STAT3 pathway by resveratrol or its analogue, piceatannol (3,3′,4,4′-transtrihydroxystilbene), decreased BCL-XL and BCL-2 expression and sensitized lung carcinoma, multiple myeloma, prostate and pancreatic cancer and the glioblastoma multiforme patient-derived CD133-positive cells to radiation or chemotherapy *in vitro*. Despite these observations, the mechanisms for the inhibition of STAT3 signalling by resveratrol or its analogues remain poorly understood.

Carbazole, the active compound of coal tar and its *N*-alkyl derivatives, decreased IL-6-stimulated STAT3 activation and DNA-binding activity in embryonic kidney or human monocytic leukaemia cells through undefined mechanisms, without affecting phosphorylation of STAT3 [32,33].

In Table 3 other natural compounds that inhibits STAT3 pathways are reported.

Molecule	Target	Effect	Indication (clinical trial phase)
Peptide and peptidomimetics			
PY*LKTK	STAT3 SH2 domain	Inhibits STAT3–STAT3 dimerization	Not applicable
Ac-pTyr-Leu-Pro-Gln-Thr-Val-NH_2	STAT3 SH2 domain	Inhibits STAT3–STAT3 dimerization	Not applicable
ISS-610	STAT3 SH2 domain	Inhibits STAT3–STAT3 dimerization	Not applicable
PM-73G	STAT3 SH2 domain	Inhibits phosphorylation of STAT3	Not applicable
CJ-1383	STAT3 SH2 domain	Inhibits phosphorylation of STAT3	Not applicable
ISS-840	STAT1 SH2 domain	Inhibits STAT1–STAT1 dimerization	Not applicable
Non-peptide small molecules			
S3I-M2001	STAT3 SH2 domain	Inhibits STAT3–STAT3 dimerization	Not applicable
STA-21	STAT3 SH2 domain	Inhibits STAT3–STAT3 dimerization	Psoriasis (Phase I/II)
Catechol moiety	STAT3 SH2 domain	Inhibits STAT3 DNA binding	Not applicable
Stattic	STAT3 SH2 domain	Inhibits phosphorylation of STAT3	Not applicable
LLL12	STAT3 SH2 domain	Inhibits STAT3–STAT3 dimerization	Not applicable
FLLL32	STAT3 SH2 domain	Inhibits STAT3–STAT3 dimerization	Not applicable
S3I-201	STAT3 SH2 domain	Inhibits STAT3–STAT3 dimerization	Not applicable
BP-1-102	STAT3 SH2 domain	Inhibits STAT3–STAT3 dimerization	Not applicable
S3I-201.1066	STAT3 SH2 domain	Inhibits STAT3–STAT3 dimerization	Not applicable
Pravastatin	STAT1	Inhibits phosphorylation of STAT1, decreases levels of IFNγ	Schizophrenia (Phase IV), pre-eclampsia (Phase I), hyperlipidaemia (Phase I/II/III/IV), cirrhosis (Phase II/III), gastroesophageal cancer (Phase IV), myeloid leukaemia (Phase I/II), pneumonia (Phase 0)
Pimozide	STAT5	Inhibits phosphorylation of STAT5	Schizophrenia (Phase II/IV), Tourette's syndrome (Phase II), psychosis (Phase III), post-operative nausea (phase not provided)
Chromone nicotinyl hydrazone	STAT5 DNA-binding domain	Inhibits phosphorylation of STAT5	Not applicable
AS1517499[51]	STAT6	Inhibits phosphorylation of STAT6	Not applicable

Table 2 *Peptide, peptidomimetics and small molecules as STAT inhibitors*

Natural products			
Capsaicin	STAT3, gp130	Inhibits STAT3 expression, depletes gp130	Chronic obstructive pulmonary disease (Phase 0/I/II), psoriasis (Phase IV), chronic neck pain (Phase II), rhinitis (Phase I/II/IV), pulmonary hypertension (Phase II), HIV infections (Phase II/III), peripheral nervous system diseases (Phase II/III), migraine (Phase I), burning mouth syndrome (Phase 0)
Curcumin	JAK1, JAK2, JAK3, STAT3	Inhibits phosphorylation of STAT3	Pancreatic cancer (Phase II/III), colon cancer (Phase I/II/III), breast cancer (Phase II), head and neck cancer (Phase 0), osteosarcoma (Phase I/II), multiple myeloma (Phase II), atopic asthma (phase not provided), dermatitis (Phase II/III), type 2 diabetes (Phase IV), schizophrenia (Phase I/II), Alzheimer's disease (Phase I/II), multiple sclerosis (Phase II), rheumatoid arthritis (Phase 0)
Avicin D	JAK1, JAK2, STAT3	Inhibits phosphorylation of STAT3	Not applicable
Resveratrol	JAK1, STAT3	Inhibits phosphorylation of STAT3	Colorectal cancer (Phase I), follicular lymphoma (Phase II), cardiovascular diseases (Phase I/II), type 2 diabetes (Phase I/II/III), obesity (Phase II), Alzheimer's disease (Phase II/III), memory impairment (phase not provided)
Piceatannol	JAK1, STAT3	Inhibits phosphorylation of STAT3	Not applicable
Sanguarine	JAK2, SRC, STAT3	Inhibits phosphorylation of STAT3	Not applicable
Celastrol	JAK2, SRC, STAT3	Inhibits phosphorylation of STAT3	Not applicable
Withaferin A	JAK2, STAT3	Inhibits phosphorylation of STAT3	Schizophrenia (phase not provided)
Cucurbitacin I	JAK2, STAT3	Inhibits phosphorylation of STAT3	Not applicable
Cucurbitacin B	JAK2, STAT3	Inhibits phosphorylation of STAT3	Not applicable
Evodiamine	JAK2, SHP1, STAT3	Decreases JAK2 phosphorylation, increases SHP1 expression leading to inhibition of activated STAT3	Not applicable
Cryptotanshinone	STAT3 SH2 domain	Inhibits STAT3–STAT3 dimerization	Polycystic ovary syndrome (phase not provided)
Honokiol	EGFR, SHP1, STAT3	Decreases EGFR expression, increases SHP1 expression leading to inhibition of activated STAT3	Not applicable
Berbamine	JAK2, SRC, STAT3	Inhibits phosphorylation of STAT3, decreases level of STAT4, induces STAT6 activation	Not applicable
Cinnamon bark	STAT4	Inhibits phosphorylation of STAT4, decreases levels of IFNγ	Polycystic ovary syndrome (Phase I), hypercholesterolaemia and type 2 diabetes (Phase II)
Indirubin	JAK, STAT3 DNA-binding domain, STAT5 DNA-binding domain	Inhibits phosphorylation of STAT3, inhibits phosphorylation of STAT5	Not applicable
TMC-264	STAT6 DNA-binding domain,	Inhibits phosphorylation of STAT6, decreases IL-4 signal transduction	Not applicable

Table 3 *Natural products as STAT inhibitors*

Chapter II

2 Aims of the project

Since the discovery, by Arbisier and co., in 2006 [32] of a relationship between carbazole and STAT3, many attention has been focused on carbazoles as a potential anticancer drug.
Starting from these assumptions it seems that the carbazole moiety can be regarded as a privileged structure in the search of new antiproliferative chemotypes and several modifications of the carbazole scaffold led to different activity profiles against different tumor cell lines. Nevertheless, analysis of these studies reveals that the N9 position was never targeted and functionalized. Therefore, we synthesized and characterized some N-alkylcarbazole derivatives. In the present work a small series of new carbazoles modified by N-alkylation with C5, C6, C7 alkyl chains was obtained. Such a structural modification was also attempted to modulate the lipophilic properties of the carbazole ligands. Moreover, the alkyl chains were functionalized with dimethyl 5-hydroxyisophthalate or methyl salicylate as substituents. The characterization and biological evaluation of new N-alkylcarbazole derivatives as potential STAT3 inhibitors is also reported.
We have demonstrated that some of these compounds suppress, with different effectiveness, the STAT3 phosphorylation and its nuclear translocation [33].
These compounds (**9a**, **9b** and **9c** in the Figure 8) represent a new class of carbazole leads endowed with antiproliferative activities.
To assess how different substituents on the carbazole nucleus can alter the activity of these compounds, we decided to design, synthesize, characterize by nuclear magnetic resonance (NMR), and elemental analysis the 1,4-dimethyl-carbazoles derivatives showed Figure 8 (compounds **10**-**23**).Moreover in order to elucidate the role of the heteroatom, we decide to synthesize and characterize by nuclear magnetic resonance (NMR), and elemental analysis compounds 24 and 25 (Figure 10), starting from dibenzofuran a bioisoster of carbazoles.

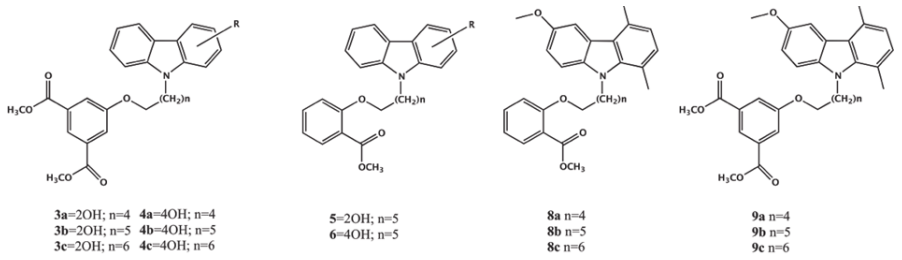

Figure 8 *Structures of synthesized compounds 3a-3c, 4a-c, 5,6 8a-8c and 9a-9c*

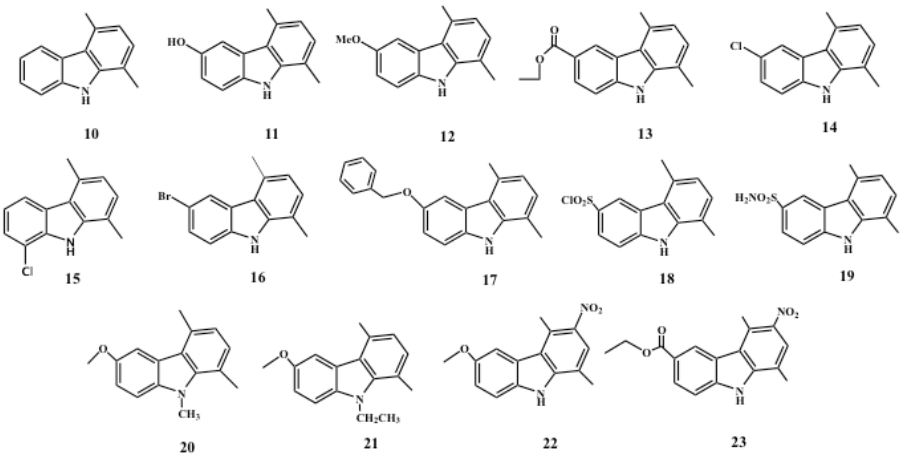

Figure 9 *Structures of synthesized compounds 10-23*

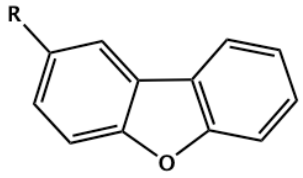

24. R= Cl
25. R= OCH_3

Figure 10 *Structures of synthesized compounds 24-25*

Chapter III

3 Results and discussion

3.1 Molecular docking

In order to find new lead compounds to develop new inhibitors of STAT3, we designed and screened by molecular docking 1,4-dimethyl-carbazole-based compounds (10-23).
Our aim is to discover new ligands of SH2 domain of STAT3, as this domain is responsible of the protein dimerization, where a monomer recognizes the Pro-pTyr-Leu-Lys-Thr-Lys sequence of its partner. In the recognition process a key role is played by phosphoryl Tyr705. Thus for our virtual screening we have considered the protein accommodating the Pro-pTyr-Leu-Lys-Thr-Lys sequence and specially the interactions involving the phosphoryl Tyr705. pY705 makes crucial interactions with the side chains of K591, R609, S611 and S613, as well as with the backbone NH group of Glu612 and L706, and with the main chain C=O of S636.
In order to establish a minimum of structure-activity relationship, we started from 1,4-dimethyl-carbazole and then we have designed compounds with substituents at position 6 and on the carbazole nitrogen.
From our theoretical calculation, we observe that the compound **10** is not able to establish interactions where the pTyr705 takes place (Figure 11a). Compound **10** establishes hydrophobic contacts with side chains of Lys591, Ile634, Gln635 and Ser636; and is hydrogen bonded with backbone CO of Ile634 ((Figure 11a).. Compared to **11-19**, the compound **1** shows the carbazole ring rotated of 180°, and presents the methyl groups overlapped with the same substituents at C-1 and C-4 of **11-19** (Figure 11a). The docked poses of **11-19** are superimposable in the binding SH2 domain of STAT3, where Pro-pTyr-Leu-Lys-Thr-Lys peptide binds (Figure 11a,b)

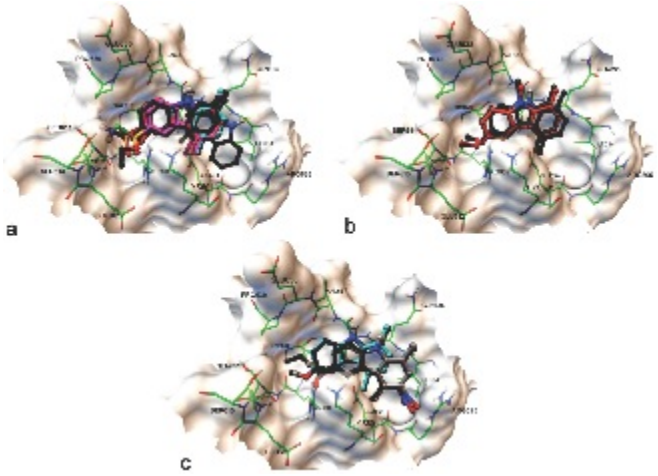

Figure 11 *Superimposition in the STAT3 SH2 domain*

The carbazole ring is in close contacts with Glu594, Ser636, Pro639, Lys591, Gln635 (Figure 11a,b). The methyl groups at positions 1 and 4 extend the Van der Walls contacts of the carbazole (Figure 11a,b). In particular the methyl at position 1 interacts with Gln635, whereas the methyl at C-4 interacts with hydrophobic portion of side chain of Lys591 and Glu594 (Figure 11a,b). The Ly591 forms a Cation-π interaction with the carbazole. The hydroxyl group of Thr620 faces the electron π system of carbazole (Figure 11a,b). The different substituents at position 6 of **11-19** occupies the site of phosphate group of Tyr705, establishing the key interactions with Arg609 (Figure 11a,b). Moreover, only the NH of carbazole core of **11-19** is hydrogen bonded to backbone CO of Ser636 (Figure 11a).

The compound **11** forms two hydrogen bonds with Arg609 by the hydroxyl. The same interactions are made by **12** through its methoxy group (Figure 11a). The compound **12** gives a further contact by the methyl group with the side chain of Ser611 (Figure 11a). **13** presents at C-6 an ethyl ester, and is hydrogen bonded by the two oxygen of the ester group with Arg609 (Figure 11a). Due to the ethyl group, the CO does not present an optimal orientation to form H-bonds. Moreover, the ethyl

group does not favour the interaction of the other oxygen of the ester group with backbone NH of Glu612 (Figure 11a). The ethyl contributes to the binding giving Van der Walls interactions with hydrophobic moiety of Lys591, Ser611 and Glu612 (Figure 11a).

It is interesting the insertion of the chlorine at C-6 (14).We observed that the guanidine group of Arg609 is nearly normal to Cl—C-6 (Figure 11a) bond giving a halogen bond contact. Further contacts could be established with Ser611 and Ser613. The compound **6** interact by its sulfon with the side chain of Lys591 and Arg609, with backbone NH of Glu612 (Figure 11a). The chlorine atom could further interact with Ser611 and Ser613. Similarly to **6**, the compound **7** is engaged in H-bonds with Lys591 and Arg609, and with NH backbone of Glu612 by the sulfon group (Figure 11a). The NH_2 of sulphonamide establishes two hydrogen bonds with Ser611 and Ser613 (Figure 11a). As found for **12**, the methoxy group of **20** and **21** gives a hydrogen bond with Arg609 and Van der Walls interaction with Ser611 (Figure 11b). The compounds **20** and **21** structurally differ from **3** for the alkylation of the carbazole nitrogen. This chemical modification causes the loss of a hydrogen bond with backbone CO of Ser636 (Figure 11b), without giving any further contacts with protein. The introduction of nitro group at position 3 in compounds **22** and **23** allows the interaction with Arg595 (Figure 11c), but does not favour the H-bond with the backbone CO of Ser636 (Figure 11c). Moreover, we observe that the methoxy group interacts with Arg609, but does not fill the site occupied by Pro-pTyr-Leu-Lys-Thr-Lys peptide (Figure 11c). The docked poses of **22** and **23** show the carbazole ring not superimposable with the tricyclic system of **11-19** (Figure 11c)

3.2 Chemistry

The synthesis of N-alkylcarbazole derivatives was accomplished using two different carbazole scaffolds. The compounds **3a-c**, **4a-c** and **5**, **6** were achieved from the 2 or 4 hydroxycarbazoles **1**, commercially available, in two steps of reaction as shown in (Scheme 1). The first step was the N-alkylation of the hydroxycarbazoles with 1,5-dibromopentane; 1,6-dibromohexane or 1,7-dibromoheptane, to obtain the intermediates **2a-c**. These N-alkylated derivatives, in the second step were reacted to dimethyl 5- hydroxyisophthalate or methyl salicylate to give the final products. The compounds **8a-c** and **9a-c** were obtained from the same reactions, as shown in (Scheme 2), from the 6-methoxy-1,4-dimethyl-9H-carbazole **7**. The compound **7** was synthesized from 5-methoxy-1H-indole, hexane-2,5-dione and 4-methylbenzenesulfonic acid dissolved in ethanol as shown in (Scheme 2).

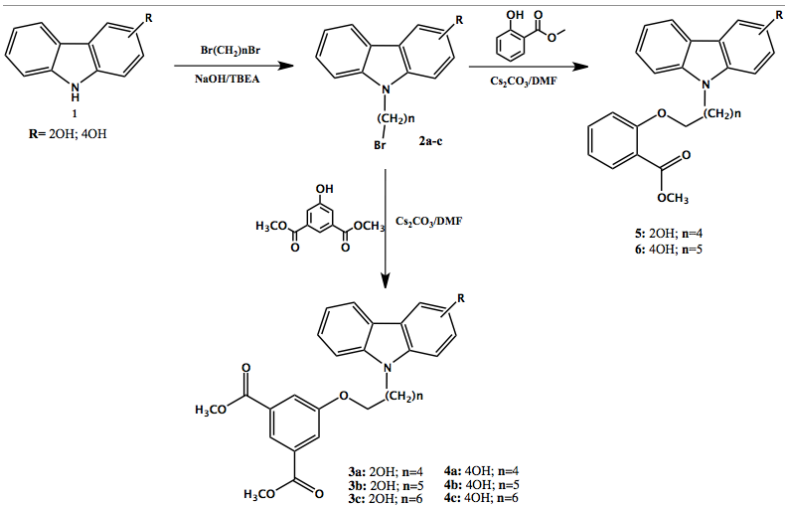

Scheme 1 *Synthetic route for the preparation of compounds 3a-c and 4a-c*

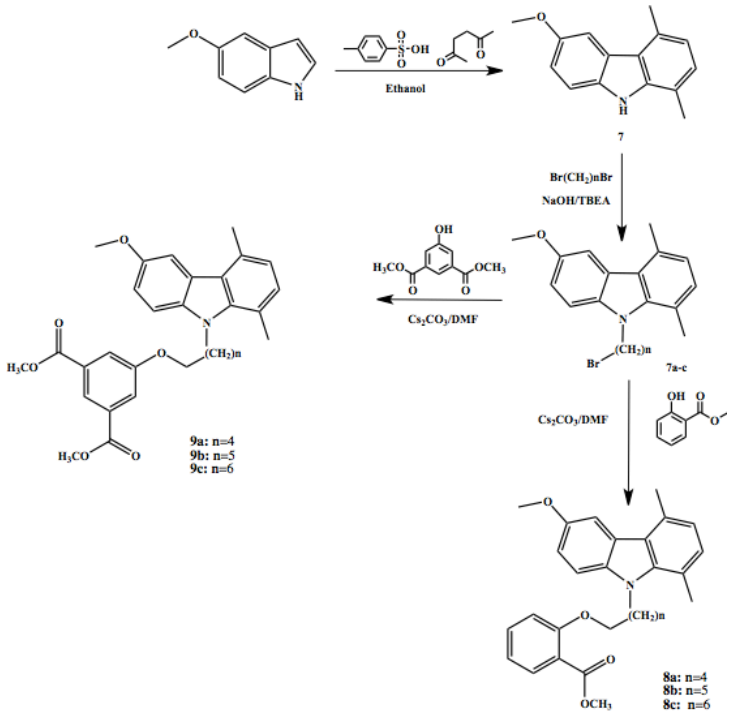

Scheme 2 *Synthetic route for the preparation of compounds 9a-c and 8a-c*

In order to investigate how and which substituents are necessary and which positions should be taken in account, starting from promising **9a-c** compounds, we synthesized compounds **10-23.**

The first of these (**10**) is the core carbazole compound used in the derivatives previously reported [33], while compounds **11-17** have different substituents in position 6, compared to **1**, i.e. chloride, bromide, carboxy-ethyl, phenyl-methoxyl. The compound **15** has the same substituent of the compound **14** (chloride), but in position 8 rather than 6. This comparison may be indicative of the most suitable position in which to place the substituent. The compound **18** has a sulfonyl chloride in position 6 and the compound **19** is his sulfonamidi-derivative. The compounds **20** and **21** have the same carbazole-nucleous as **1**, but have two alkyl groups linked to nitrogen atom. This could allow us to evaluate

the influence on H bonds formation of our compounds, since they loss an hydrogen bond donor than **1**. Compounds **22** and **23** have a as substituents a nitro group and a methoxyl or carboxyethyl in the position 3 and 6, respectively. This compound could give us information on whether an additional polar substituent could influence the activity.
Compounds **10-17** were synthesized according to the Cronwell and Saxton reaction (Scheme 3) [124].

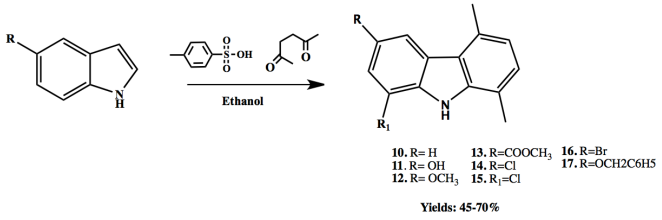

Scheme 3 *Synthetic route for the preparation of compounds 10-17*

Compounds **18** was synthesized starting from compound **10** by reaction with chlorosulfonic acid at 0° C (Scheme 4).Compound **19** was obtained from **18** by reaction with a stoichiometric amount of a 2M ammonia solution in ethanol (Scheme 4).

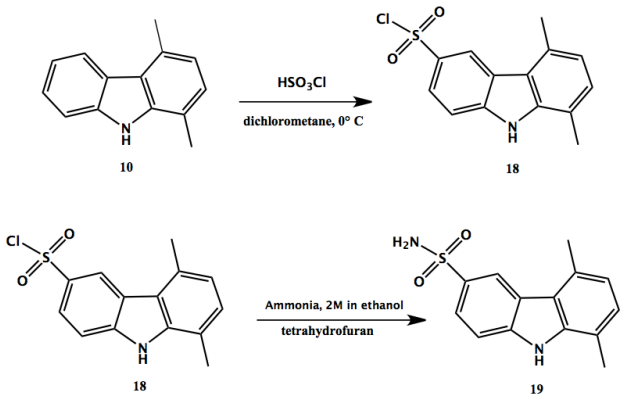

Scheme 4 *Synthetic route for the preparation of compounds 18-19*

Compounds **20** and **21** were synthesized starting from compound **12** by reaction with sodium hydride at 0° C in DMF and iodomethane to obtain compound **20** and with sodium hydride at 0° C in DMF and iodoethane to obtain compound **21** (Scheme 5).

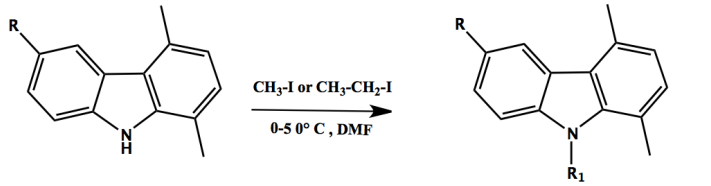

20. R= OCH_3; R_1= CH_3
21. R= OCH_3; R_1= CH_2CH_3

Scheme 5 *Synthetic route for the preparation of compounds 20-21*

Compound **22** and **23** were synthesized by reaction of compound **12** and **13** with a stoichiometric amount of fuming nitric acid in acetic anhydride [124] (Scheme 6).

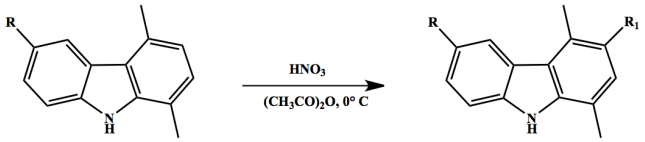

22. R= OCH_3; R_1= NO_2
23. R= OCH_3; R_1= NO_2

Scheme 6 *Synthetic route for the preparation of compounds 22-23*

The analysis carried out on the synthesized compounds was in accord with the proposed formulations.
As an example, ^{1}H NMR, ^{13}C NMR and MS spectra of compound **9a** are reported.

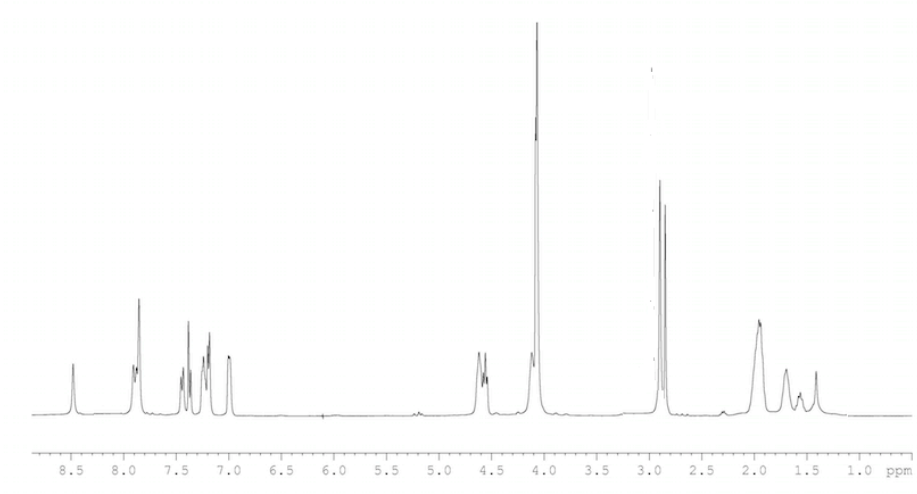

Figure 12 ***^{1}H NMR of compound 9a***

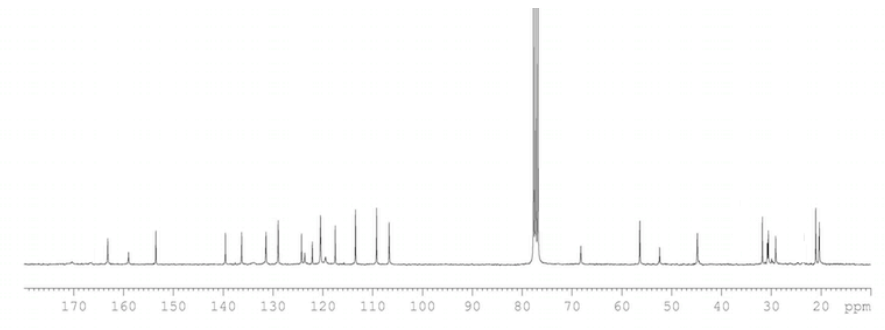

Figure 13 ^{13}C NMR of compound ***9a***

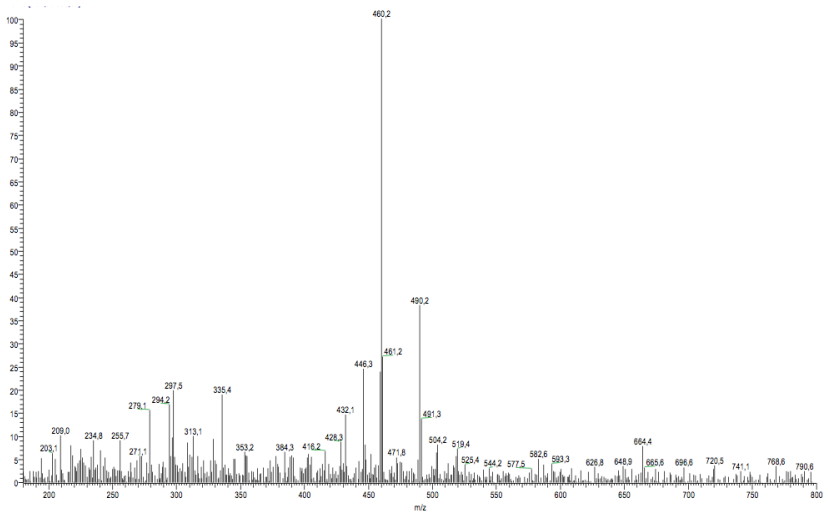

Figure 14 *MS spectrum of compound* ***9a***

Compound **24** and **25** were synthesized according to a literature procedure [125,126](Scheme 7).

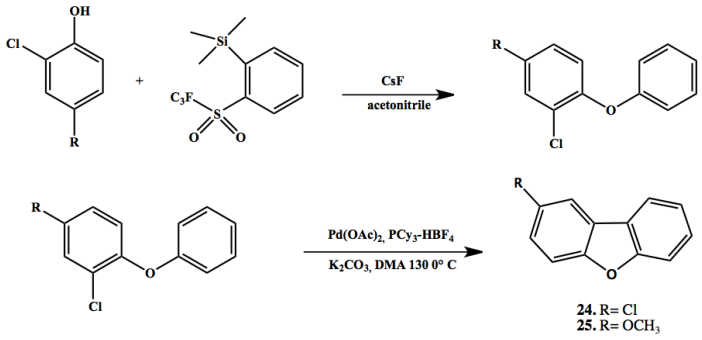

Scheme 7 *Synthetic route for the preparation of compounds 24-25*

The analysis carried out on the synthesized compounds was in accord with the proposed formulations.

As an example, ^{1}H NMR, ^{13}C NMR and MS spectra of compound **25** are reported.

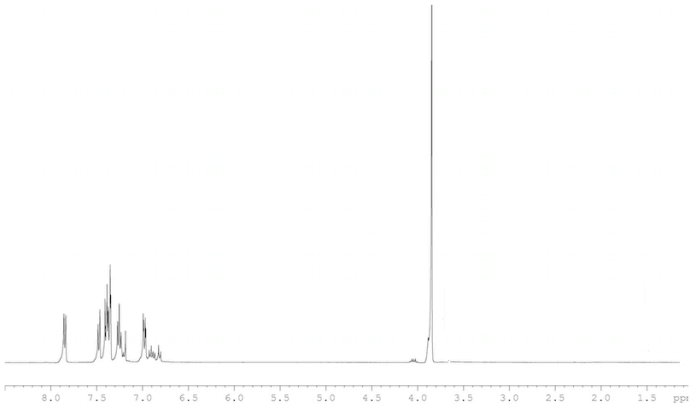

Figure 15 *^{1}H NMR of compound **25***

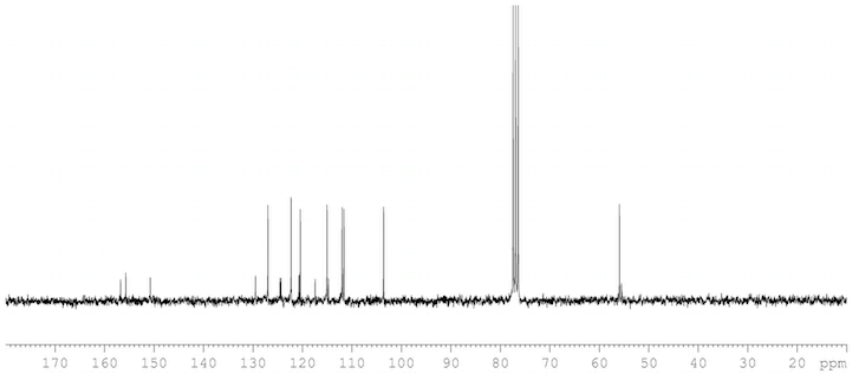

Figure 16 *^{13}C NMR of compound **9a***

3.3 Pharmacology

3.3.1 Stat3 inhibition studies

In order to analyse the effect of a new set of N-alkylcarbazole derivatives on STAT3 signalling pathway, EMSA and Western blot analysis were performed in THP-1 cells treated with IL-6 (20 ng/ ml) for 15 min. IL-6 increased predominantly the STAT3 DNA- binding activity as indicated by EMSA/supershift experiments with anti-STAT3 antibody (data not shown) in line with previous report [127]. Among different compounds examined only **9a**, **9b** and **9c** were able to inhibit, with different effectiveness, STAT3.
DNA-binding activity at 50 mM (Figure 17a) whereas all other compounds were ineffective also at higher doses (100 mM) (**Table 4**).

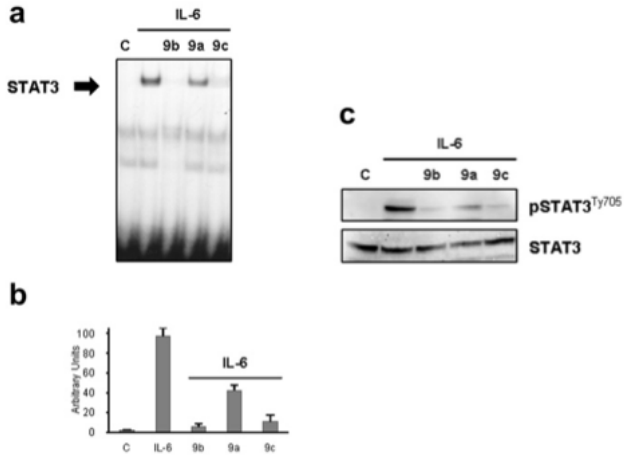

Figure 17 *Effect of compounds 9a-c on STAT3 activation in THP-1 cell line*

Effect of examined compounds on STAT3 activation in THP-1 cell line.[a]

Compound	Dose (μM)	% of STAT 3 inhibition
3a	100	1 ± 0.5
3b	100	1 ± 0.5
3c	100	5 ± 1.1
4a	100	20 ± 2.2
4b	100	5 ± 1.2
4c	100	6 ± 1.3
5	100	1 ± 0.3
6	100	3 ± 0.4
8a	100	3 ± 0.3
8b	100	1 ± 0.3
8c	100	6 ± 1.2
9a	50	50 ± 5.2
9b	50	95 ± 3.2
9c	50	90 ± 6.5

[a] THP-1 cells (1.5×10^6/mL) were pretreated with 50 μM or 100 μM of all the synthesized compounds for 30 min and then stimulated with IL-6 (20 ng/mL) for 15 min. Nuclear extracts were subjected to EMSA analysis. Densitometric analysis of the gels were performed as described in experimental protocols (Section 4.6) and the inhibition of STAT3 DNA-binding is reported as mean percentage ± SD respect to IL-6 induction alone.

Table 4 *Effect of examined compounds on STAT3 activation in THP-1 cell line*.

Moreover, the compounds **9a**, **9b** and **9c** were unable to inhibit IFNy induced STAT1 nor TNF-a þ LPS-induced NF-kB activation (**Figure 18**a,b). One of the critical steps leading to the activation of STATs is their phosphorylation on specific tyrosine residues and successive translocation into the nucleus. In line with above described data, Western Blot analysis showed that the compounds **9a**, **9b** and **9c** decreased, in different grade, IL-6-induced tyrosine705 phosphorylation of cytosolic STAT3 without affecting the total amount of STAT3 protein (Figure 17).
Among non N-alkylated derivatives only **12** and **14** were able to inhibit, with different effectiveness, STAT3.

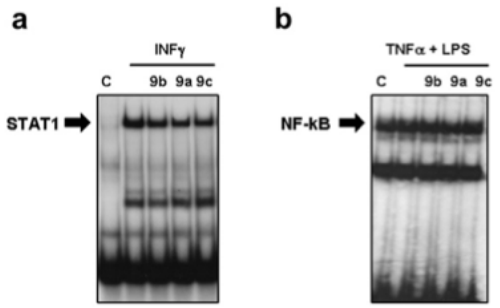

Figure 18 *Effect of compounds 9a-c on STAT1 and NF-kB activation in THP-1 cell line.*

3.3.2 Cytotoxic studies

In order to analyze the biological activity of new set of carbazole derivatives, antiproliferative assay has been carried out on all synthesized coumpounds to screen their cytotoxic activity.

All compounds have been tested on on human epithelial lung adenocarcinoma (A549), human melanoma (A375) and human epithelial cervix adenocarcinoma (HeLa) cell lines.

The IC50 value, express as μM, is the concentration of compound that affords a 50% reduction in cell growth as compared to control cells. Doxorubicin is also included for comparison and it was chosen for testing the susceptibility of our cell lines to cytotoxicity.

Tables shows the results, expressed as IC_{50} (μM) values, indicating the concentration of each compound that reduce cell growth by 50% as compared to control cells. Results are expressed as mean ± SEM from at least three independent experiments, each performer in triplicate. Data were analyzed by Student's t test. ** denotes $P<0.005$ and *** denotes $P<0.001$ *vs* Doxorubicin on the same cell line.

Compounds **9a-c**, the only compounds that are able to inhibit STAT3 at 50 mM, do not show cytotoxic activity (Table 5).

	Cytotoxicity (IC50, µM)		
compound	**A375**	**A549**	**HeLa**
9a	>100	>100	>100
9b	90	>100	>100
9c	>100	>100	90
Doxorubicin	87	89	48

Table 5 *Effect of compound 9a-c on cancer cell lines*

As it is possible to observe in **Table 6**, the compounds **12** and **14** show a comparable and in some cases better activity than doxorubicin on all three cell lines tested. In particular, **12** and **14** perform better than doxorubicin against A375 and A549 cell lines. The compound **13** presents a similar antiproliferative activity to doxorubicin *vs* A375, and a better biological profile against A549 than the reference compound. Comparable cell growth inhibition activity to doxorubicin are shown by **23** and **17**. The latter, inhibits the cell growth of A549 cell lines with a lower IC_{50} value compared to doxorubicin.

	Cytotoxicity (IC_{50}, µM)		
compound	**A375**	**A549**	**HeLa**
10	80 ± 2.1	>100	>100
11	90 ± 3	90 ± 0.79	80 ± 1.5
12	50 ± 2.6 ***	60 ± 4.2 **	70 ± 1.2
13	90 ± 3.9	60 ± 2.7 **	60 ± 3.7
14	60 ± 1.9 **	60 ± 4.1 **	60 ± 0.98
15	90 ± 1.5	90 ± 3.2	72 ± 0.69
16	90 ± 4.8	>100	>100
17	87 ± 2.7	50± 1.2	40± 3.2
18	>100	90 ± 3.1	90 ± 4.1
19	>100	>100	>100
20	>100	>100	>100
21	80 ± 1.9	>100	>100
22	>100	>100	>100
23	80 ± 4.6	90 ± 1.1	90 ± 5.1
24	>100	>100	>100
25	>100	>100	>100
Doxorubicin	87 ± 3.3	89 ± 2.8	48 ± 3.1

Table 6 *Effect of compounds 10-25 on cancer cell lines. IC50 (µM) values, indicating the concentration of each compound that reduce cell growth by 50% as compared to control cells. Results are expressed as mean ± SEM from at least three independent experiments, each performer in triplicate. Data were analyzed by Student's t test. ** denotes P<0.005 and *** denotes P<0.001 vs Doxorubicin on the same cell line.*

Conclusions

In this first section, design, synthesis and characterization of 25 carbazole derivatives are reported.
Antiproliferative assay and western blot analysis have been carried out on all synthesized coumpounds to screen their cytotoxic activity.
First of all, starting from the literature data showing a correlation between STAT3 inhibition and hydroxy-carbazole, we synthesized some N-alkylcarbazole derivatives using two different carbazole scaffolds (2 or 4 hydroxycarbazoles and 1,4-dimethylcarbazole).
We demonstrated that some of the tested compounds suppressed, with different effectiveness, the STAT3 phosphorylation and its nuclear translocation. In particular, compound 9a, 9b and 9c revealed to inhibit the STAT3 activation for the 50%, 90% and 95%, respectively. The addition of an N-alkyl chain provided an additional interaction point to the target protein as small modifications of its terminal phenyl ring cause dramatic changes in the activity profile (compare 8a, 8b and 8c with 9a, 9b and 9c). Also among the active ligand the length of the alkyl linker seems to be critical for the activity (compare 9a with 9b and 9c).
Starting from these results we aimed to simplify the lead compound. For this purpose we have designed some carbazole derivative using as scaffold scaffold the 1,4-dimethyl-carbazole, and we inserted different substituents in the position 3, 6 and 9. The key interactions are made by the substituents in position 6, because they are accommodated where the phoshoryl group of Tyr705 takes place. In particular, we observed that the substituents at C-6 differently interact with macromolecular counterparts, influencing the affinity for the protein and the consequent STAT3 modulation. We found that the methoxyl group and chlorine in C-6 are better than the other substituents because the methoxyl could give Van der Walls contacts along with two hydrogen bonds, while the chlorine atom gives close contacts with Arg609. According to pharmacological assays, the chlorine atom in position 6 give a good antiproliferative activity to the scaffold , in all the three cell lines tested, and shows a notable inhibition activity

on STAT3 signaling patways. We observed that the 1,4-dimethyl-carbazole can establish hydrophobic contacts and cation-π interactions with the amino acids residues of SH2 domain. Moreover, the NH of carbazole is hydrogen bonded with CO of Ser636. This hydrogen bond is also observable by the Pro-pTyr-Leu-Lys-Thr-Lys peptide. All these compounds showed an interesting antiproliferative activity on all three used cell lines (IC_{50} value ≥60μM). The **20** and **21** have the carbazole nitrogen alkylated, and for this chemical feature they loss the hydrogen bond with the CO of Ser636. According to MTT assay and western blot analysis compound 8 and 9 display a loss of antiproliferative activity and STAT3-inhibition capability compared to the not alkylated ones. On the compounds **22** and **23** we inserted a nitro group at C-3 with the aim to give interactions with Arg595. The docked poses of **22** and **23** show electrostatic contacts between the nitro group of at C-3 and the Arg595, but the interactions of the remaining ligand moieties are affected. Indeed, the H bond with the backbone CO of Ser636 is not favoured, and the methoxyl group does not fill the pocket experienced by the phosphoryl group of Pro-pTyr-Leu-Lys-Thr-Lys peptide. In our biological experiments appear that compound 22 and 23 do not show antiproliferative activity. Despite of computational data, unexpectedly, compound 23 seems to have considerable STAT3-inhibition effect. Finally, we can assume that the 1,4-dimethyl-carbazole is a suitable scaffold to develop STAT3 inhibitors. Our analysis suggests that the chlorine, methoxyl, chlorosulfonic and sulfonamide groups are optimal substituents at C-6 to mimic to phosphoryl group of Tyr705. In particular compound 12 and 14, exhibit the best antiproliferative and STAT3-inhibition activity among synthesized compounds.The carbazole nitrogen has to be not alkylated, in order to give hydrogen bonds with Ser6363. Moreover, substituents at C-3 could be inserted to give other important interactions with Arg595, but without altering the contacts given by the other structural portions of the ligands. It is noteworthy that the used scaffold can be easily substituted in different positions, such as 1,3,4,8 allowing the obtainment of more potent ligands of STAT3.

Chapter IV

4 Experimental section

4.1 Computational studies

All ligands (**10-23**) were sketched using the graphical interface Maestro version 6.0, Schrödinger, LLC, New York, NY, 2003, and their geometries optimized through Macro-Model 8.5 by using the MMFFs force field and the Polak–Ribier conjugate gradient algorithm (maximum derivative less than 0.001 kcal/mol). A GB/SA (generalized Born/surface area) solvent treatment33 was used, mimicking the presence of H_2O in the geometry optimization.
The crystal structure of Stat3β homodimer bound to DNA (1BG1, pdb ID) and was used as macromolecule in theoretical studies.
Molecular docking studies were performed using AutoDock4.2. To achieve a representative conformational space during the docking studies and taking into account the variable number of active torsions, 10 calculations consisting of 256 runs were performed, obtaining 2560 structures for each ligand (**10-23**). The Lamarckian genetic algorithm was employed for dockings. An initial population of 700 randomly placed individuals was used. The maximum number of energy evaluations and of generations was set up at 6×10^6 and 7×10^6, respectively. A mutation rate of 0.02 and a crossover rate of 0.8 were used, and the local search frequency was set up at 0.26. Results differing by less than 2 Å in positional root-mean-square deviation (rmsd) were clustered together and ranked by free energy of binding. For all the docked structures, all bonds were treated as active torsional bonds except the amide bonds. The grid box was sized at 64 x 64 x 64 number of points, by using 0.375 Å between the grid points. The x, y, and z coordinates of grid center were: 96.616, 73.201 and 68.027.

4.2 Chemistry

All reagents and solvents were purchased from Sigma-Aldrich s.r.l. (Milan, Italy). The elemental analyses for C, H and N were recorded on a ThermoFinnigan Flash EA 1112 series and performed according to standard microanalytical procedures. ^{1}H NMR, homodecoupled ^{1}H NMR, ^{1}HCOSY and ^{13}C NMR spectra were recorded at 298 K on a Bruker Avance 300 Spectrometer operating at 300 MHz (^{1}H) and 75 MHz (^{13}C) and referred to internal tetramethylsilane.

4.2.1 General procedures for the synthesis of compounds 7 and 10-17 [124]

5-substituted-1H-indole (6.60 mmol) was dissolved in ethanol (20 mL) and stirred at room temperature. To this solution hexan-2,5-dione (8.18 mmol) and 4-methylbenzenesulfonic acid (8.24 mmol) were added. The mixture was stirred under reflux for 4 h. After the reaction, the solution was cooled, and the solvent was evaporated, poured into water and extracted with diethyl ether (3 x 30 ml). The organic layer was dried over anhydrous $MgSO_4$, filtered and the solvent removed by evaporation. The resulting residue was purified on a silica gel column chromatography in hexane/ethyl acetate (7:3).
All NMR data are in according to literature ones.

4.2.2 General procedures for the synthesis of compounds 2a-c and 7a-c

TBEA (benzyltriethylamonium bromide) (2.73 mmol), was dissolved in an aqueous solution of NaOH 50% p/p (15 ml) and toluene (20 ml) and stirred for 15 min. After was added a solution of a suitable hydroxycarbazole or 6-methoxy-1,4-dimethyl-9H- carbazole (5.45 mmol) in toluene (20 ml). To this mixture was added 1,5-dibromopentane or 1,6-dibromohexane or 1,7- dibromoheptane (16.3 mmol) and was stirred at reflux for 48 h. After the reaction, the solvent was evaporated, poured into water and extracted with chloroform (5 50 ml). The organic layer was dried over anhydrous $MgSO_4$, filtered and the solvent removed by

evaporation. The resulting residue was purified on a silica gel column chromatography in petroleum ether/ethyl acetate (9/1) to give as white/yellow solid (60% yield) (7a-c). The resulting residue was extracted with hexane (3 20 ml), ethyl acetate, and diethyl ether. Final product was purified on a silica gel column chromatography in chloroform to give as yellow/orange solid (60% yield) (2a-c).

4.2.3 General procedures for the synthesis of compounds 3a-c, 4a-c and 9a-c

Dimethyl 5-hydroxyisophthalate (l.35 mmol) and Cs2CO3 (2.7 mmol) were dissolved in DMF (10 ml). A solution of N-bromoalkyl-substituted carbazole (1.35 mmol) in DMF was added at room temperature. The mixture was stirred for 20 h. After the reaction, the solvent was evaporated, poured into water and extracted with chloroform (5 50 ml). The organic layer was dried over anhydrous MgSO4, filtered and the solvent removed by evaporation. Final product was an orange/brown solid (80% yield).

4.2.3.1 Dimethyl-5-(5-(2-hydroxy-9H-carbazol-9-yl)pentyloxy)isophthalate (3a)

^{1}H NMR (d ppm, $CDCl_3$): 4.20 [(OH-$C_{12}H_7N$)-CH_2e$(CH_2)_3$-CH_2O-C_6H_3-$(OCOCH_3)_2$, 1H, s]; 4.10 [(OH-$C_{12}H_7N$)-CH_2-$(CH_2)_3$-CH_2O-C_6H_3-$(OCOCH_3)_2$, 2H, t]; 4.03 [(OH-$C_{12}H_7N$)-CH_2e$(CH_2)_3$-CH_2O-C_6H_3-$(OCOCH_3)_2$, 2H, t]; 3.94 [(OH-$C_{12}H_7N$)-CH_2-$(CH_2)_3$-CH_2O-C_6H_3-$(OCOCH_3)_2$, 6H, s]; 1.27-2.02 [(OH-$C_{12}H_7N$)-CH_2-$(CH_2)_3$-CH_2O-C_6H_3-$(OCOCH_3)_2$, 6H, m]; 6.80-8.22 [(OH-$C_{12}H_7N$)-CH_2-$(CH_2)_3$-CH_2O-C_6H_3-$(OCOCH_3)_2$, 10H,m].
Mass spectrum: 461.51 [(OH-$C_{12}H_7N$)-CH_2-$(CH_2)_3$-CH_2O-C_6H_3-$(OCOCH_3)_2$].
Elemental analysis of 3a: Calcd. for $C_{27}H_{27}NO_6$ (%): C 70.27, H 5.90, N 3.03. Found (%): C 70.14, H 5.96, N 3.12.

4.2.3.2 Dimethyl-5-(6-(2-hydroxy-9H-carbazol-9-yl)hexyloxy)isophthalate (3b)

^{1}H NMR (d ppm, $CDCl_3$): 4.17 [(OH-$C_{12}H_7N$)-CH_2-$(CH_2)_4$-CH_2O-C_6H_3-$(OCOCH_3)_2$, 1H, s]; 4.05 [(OH-$C_{12}H_7N$)-CH_2-$(CH_2)_4$-CH_2O-C_6H_3-$(OCOCH_3)_2$, 2H, t]; 3.93 [(OH-$C_{12}H_7N$)-CH_2-$(CH_2)_4$-CH_2O-C_6H_3-$(OCOCH_3)_2$, 2H, t]; 3.88 [(OH-$C_{12}H_7N$)-CH_2-$(CH_2)_4$-CH_2O-C_6H_3-$(OCOCH_3)_2$, 6H, s]; 1.27-2.00 [(OH-$C_{12}H_7N$)-CH_2-$(CH_2)_4$-CH_2O-C_6H_3-$(OCOCH_3)_2$, 8H, m]; 6.70-8.30 [(OH-$C_{12}H_7N$)-CH_2-$(CH_2)_4$-CH_2O-C_6H_3-$(OCOCH_3)_2$, 10H,m].
Mass spectrum: 475.53 [(OH-$C_{12}H_7N$)-CH_2-$(CH_2)_4$-CH_2O-C_6H_3-$(OCOCH_3)_2$].
Elemental analysis of 3b: calcd. for $C_{28}H_{29}NO_6$ (%): C 70.72, H 6.15, N 2.95. Found (%): C 70.54, H 6.23, N 2.86.

4.2.3.3 Dimethyl-5-(7-(2-hydroxy-9H-carbazol-9-yl)heptyloxy)isophthalate (3c)

^{1}H NMR (d ppm, $CDCl_3$): 4.20 [(OH-$C_{12}H_7N$)-CH_2-$(CH_2)_5$-CH_2O-C_6H_3-$(OCOCH_3)_2$, 1H, s]; 4.11 [(OH-$C_{12}H_7N$)-CH_2-$(CH_2)_5$-CH_2O-C_6H_3-$(OCOCH_3)_2$, 2H, t]; 3.94 [(OH-$C_{12}H_7N$)-CH_2-$(CH_2)_5$-CH_2O-C_6H_3-$(OCOCH_3)_2$, 2H, t]; 3.91 [(OH-$C_{12}H_7N$)-CH_2-$(CH_2)_5$-CH_2O-C_6H_3-$(OCOCH_3)_2$, 6H, s]; 1.12-1.94 [(OH-$C_{12}H_7N$)-CH_2-$(CH_2)_5$-CH_2O-C_6H_3-$(OCOCH_3)_2$, 10H, m]; 6.80-8.30 [(OH-$C_{12}H_7N$)-CH_2-$(CH_2)_5$-CH_2O-C_6H_3-$(OCOCH_3)_2$, 10H, m].
Mass spectrum: 489.56 [(OH-$C_{12}H_7N$)-CH_2-$(CH_2)_5$-CH_2O-C_6H_3-$(OCOCH_3)_2$].
Elemental analysis of 3c: Calcd. for $C_{29}H_{31}NO_6$ (%): C 71.15, H 6.38, N 2.86. Found (%): C 71.02, H 6.49, N 2.92.

4.2.3.4 Dimethyl-5-(5-(4-hydroxy-9H-carbazol-9-yl)pentyloxy)isophthalate (4a)

^{1}H NMR (d ppm, $CDCl_3$): 4.22 [(OH-$C_{12}H_7N$)-CH_2-$(CH_2)_3$-$CH_2OeC_6H_3$-$(OCOCH_3)_2$, 1H, s]; 4.16[(OH-$C_{12}H_7N$)-CH_2-$(CH_2)_3$-CH_2O-C_6H_3-$(OCOCH_3)_2$, 2H, t]; 3.96 [(OH-$C_{12}H_7N$)-CH_2-$(CH_2)_3$-CH_2O-C_6H_3-

$(OCOCH_3)_2$, 2H, t]; 3.90 [(OH-$C_{12}H_7N$)-CH_2-$(CH_2)_3$-CH_2O-C_6H_3-$(OCOCH_3)_2$, 6H, s]; 1.23-2.11 [(OH-$C_{12}H_7N$)-CH_2-$(CH_2)_3$-CH_2O-C_6H_3-$(OCOCH_3)_2$, 6H, m]; 6.56-8.41 [(OH-$C_{12}H_7N$)-CH_2-$(CH_2)_3$-CH_2O-C_6H_3-$(OCOCH_3)_2$, 10H, m].

Mass spectrum: 461.51 [(OH-$C_{12}H_7N$)-CH_2-$(CH_2)_3$-CH_2O-C_6H_3-$(OCOCH_3)_2$].

Elemental analysis of 4a: calcd. for $C_{27}H_{27}NO_6$ (%): C 70.27, H 5.90, N 3.03. Found (%): C 70.15, H 5.98, N 3.14.

4.2.3.5 Dimethyl-5-(6-(4-hydroxy-9H-carbazol-9-yl)hexyloxy)isophthalate (4b)

^{1}H NMR (d ppm, $CDCl_3$): 4.10 [(OH-$C_{12}H_7N$)-CH_2-$(CH_2)_4$-CH_2O-C_6H_3-$(OCOCH_3)_2$, 1H, s]; 4.32 [(OH-$C_{12}H_7N$)-CH_2-$(CH_2)_4$-CH_2O-C_6H_3-$(OCOCH_3)_2$, 2H, t]; 3.99 [(OH-$C_{12}H_7N$)-CH_2-$(CH_2)_4$-CH_2O-C_6H_3-$(OCOCH_3)_2$, 2H, t]; 3.88 [(OH-$C_{12}H_7N$)-CH_2-$(CH_2)_4$-CH_2O-C_6H_3-$(OCOCH_3)_2$, 6H, s]; 1.21-2.12 [(OH-$C_{12}H_7N$)-CH_2-$(CH_2)_4$-CH_2O-C_6H_3-$(OCOCH_3)_2$, 8H, m]; 6.57-8.50 [(OH-$C_{12}H_7N$)-CH_2-$(CH_2)_4$-CH_2O-C_6H_3-$(OCOCH_3)_2$, 10H, m].

Mass spectrum: 475.53 [(OH-$C_{12}H_7N$)-CH_2-$(CH_2)_4$-CH_2O-C_6H_3-$(OCOCH_3)_2$].

Elemental analysis of 4b: calcd. for $C_{28}H_{29}NO_6$ (%): C 70.72, H 6.15, N 2.95. Found (%): C 70.59, H 6.27, N 2.84.

4.2.3.6 Dimethyl-5-(7-(4-hydroxy-9H-carbazol-9-yl)heptyloxy)isophthalate (4c)

^{1}H NMR (d ppm, $CDCl_3$): 4.23 [(OH-$C_{12}H_7N$)-CH_2-$(CH_2)_5$-CH_2O-C_6H_3-$(OCOCH_3)_2$, 1H, s]; 4.25 [(OH-$C_{12}H_7N$)-CH_2-$(CH_2)_5$-CH_2O-C_6H_3-$(OCOCH_3)_2$, 2H, t]; 3.98 [(OH-$C_{12}H_7N$)-CH_2-$(CH_2)_5$-CH_2O-C_6H_3-$(OCOCH_3)_2$, 2H, t]; 3.93 [(OH-$C_{12}H_7N$)-CH_2-$(CH_2)_5$-CH_2O-C_6H_3-$(OCOCH_3)_2$, 6H, s]; 1.20-2.10 [(OH-$C_{12}H_7N$)-CH_2-$(CH_2)_5$-CH_2O-C_6H_3-$(OCOCH_3)_2$, 10H, m]; 6.50-8.40 [(OH-$C_{12}H_7N$)-CH_2-$(CH_2)_5$-CH_2O-C_6H_3-$(OCOCH_3)_2$, 10H, m]].

Mass spectrum: 489.56 [(OH-$C_{12}H_7N$)-CH_2-$(CH_2)_5$-CH_2O-C_6H_3-$(OCOCH_3)_2$].
Elemental analysis of 4c: calcd. for $C_{29}H_{31}NO_6$ (%): C 71.15, H 6.38, N 2.86. Found (%): C 71.02, H 6.49, N 2.97.

4.2.3.7 Dimethyl-5-(5-(6-methoxy-1,4-dimethyl-9H-carbazol-9-yl)-pentyloxy)isophthalate (9a)

^{1}H NMR(d ppm $CDCl_3$): 4.06 [$(CH_3O$-C_6H_3-C_6H_3-$(CH_3)_2$-N)-CH_2-$(CH_2)_3$-CH_2O-C_6H_3-$(OCOCH_3)_2$, 3H, s]; 4.56 [(C H_3O-C_6H_3-C_6H_3-$(CH_3)_2$-N)-CH_2-$(CH_2)_3$-CH_2O-C_6H_3-(OCOC $H_3)_2$, 2H, t]; 4.10 [$(CH_3O$-C_6H_3-C_6H_3-$(CH_3)_2$-N)-CH_2-$(CH_2)_3$-CH_2O-C_6H_3-$(OCOCH_3)_2$, 2H, t]; 4.00 [$(CH_3O$-C_6H_3-C_6H_3-$(CH_3)_2$-N)-CH_2-$(CH_2)_3$-CH_2O-C_6H_3-$(OCOCH_3)_2$, 6H, s]; 2.79 [$(CH_3O$-C_6H_3-C_6H_3-$(CH_3)_2$-N)-CH_2-$(CH_2)_3$-CH_2O-C_6H_3-$(OCOCH_3)_2$, 3H, s]; 2.74 [$(CH_3O$-C_6H_3-C_6H_3-$(CH_3)_2$-N)eCH$_2$-$(CH_2)_3$-CH_2O-C_6H_3-$(OCOCH_3)_2$, 3H, s]; 1.21-2.00 [$(CH_3O$-C_6H_3-C_6H_3-$(CH_3)_2$-N)-CH_2-$(CH_2)_3$-CH_2O-C_6H_3-$(OCOCH_3)_2$, 6H, m]; 6.91-8.50 [$(CH_3O$-C_6H_3-C_6H_3-$(CH_3)_2$-N)eCH$_2$e\-$(CH_2)_3$-CH_2O-C_6H_3-$(OCOCH_3)_2$, 8H, m].
^{13}C NMR(d ppm $CDCl_3$): 166.5 [$(CH_3O$-C_6H_3-C_6H_3-$(CH_3)_2$-N)-CH_2-$(CH_2)_3$-CH_2O-C_6H_3-$(OCOCH_3)_2$] 159, 153.5, 139.5, 136.2, 131.4, 128.9, 124.28, 123.6, 122.1, 120.4, 117.5, 113.4, 109.2, 106.6 [$(CH_3O$-C_6H_3-C_6H_3-$(CH_3)_2$-N)-CH_2-$(CH_2)_3$-CH_2O-C_6H_3-$(OCOCH_3)_2$]; 68.2[$(CH_3O$-C_6H_3-C_6H_3-$(CH_3)_2$-N)-CH_2-$(CH_2)_3$-CH_2O-C_6H_3-$(OCOCH_3)_2$]; 56.3[$(CH_3O$-C_6H_3-C_6H_3-$(CH_3)_2$-N)-CH_2-$(CH_2)_3$-CH_2O-C_6H_3-$(OCOCH_3)_2$]; 52.4[$(CH_3O$-C_6H_3-C_6H_3-$(CH_3)_2$-N)-- $(CH_2)_3$-CH_2O-$C_6H_3(OCOCH_3)_2$]; 44.8[$(CH_3O$-C_6H_3-C_6H_3-$(CH_3)_2$-N)-CH_2-$(CH_2)_3$-CH_2O-C_6H_3-$(OCOCH_3)_2$]; 30.7, 30.5, 29.1[$(CH_3O$-C_6H_3-C_6H_3-$(CH_3)_2$-N)-CH_2-$(CH_2)_3$-CH_2O-$(OCOCH_3)_2$]; 20.3[$(CH_3O$-C_6H_3-C_6H_3-$(CH_3)_2$-N)-CH_2-$(CH_2)_3$-CH_2O-C_6H_3-$(OCOCH_3)_2$]; 20.4[$(CH_3O$-C_6H_3-C_6H_3-$(CH_3)_2$-N)-CH_2-$(CH_2)_3$-CH_2O-C_6H_3-$(OCOCH_3)_2$].
Mass spectrum: 503.59 [$(CH_3O$-C_6H_3-C_6H_3-$(CH_3)_2$-N)-CH_2-$(CH_2)_3$-CH_2O-C_6H_3-$(OCOCH_3)_2$].
Elemental analysis of 9a: Calcd. for $C_{30}H_{33}NO_6$ (%): C 71.55, H 6.61, N 2.78. Found (%): C 71.44, H 6.81, N 2.91.

4.2.3.8 Dimethyl-5-(6-(6-methoxy-1,4-dimethyl-9H-carbazol-9-yl) hexyloxy)isophthalate (9b)

^{1}H NMR (d ppm $CDCl_3$): 3.95 [$(CH_3O\text{-}C_6H_3\text{-}C_6H_3\text{-}(CH_3)_2\text{-}N)\text{-}CH_2\text{-}(CH_2)_4\text{-}CH_2O\text{-}C_6H_3\text{-}(OCOCH_3)_2$, 3H, s]; 4.52 [$(CH_3O\text{-}C_6H_3\text{-}C_6H_3\text{-}(CH_3)_2\text{-}N)\text{-}CH_2\text{-}(CH_2)_4\text{-}CH_2O\text{-}C_6H_3\text{-}(OCOCH_3)_2$, 2H, t]; 4.05 [$(CH_3O\text{-}C_6H_3\text{-}C_6H_3\text{-}(CH_3)_2\text{-}N)\text{-}CH_2\text{-}(CH_2)_4\text{-}CH_2O\text{-}C_6H_3\text{-}(OCOCH_3)_2$, 2H, t]; 3.94 [$(CH_3O\text{-}C_6H_3\text{-}C_6H_3\text{-}(CH_3)_2\text{-}N)\text{-}CH_2\text{-}(CH_2)_4\text{-}CH_2O\text{-}C_6H_3\text{-}(OCOCH_3)_2$,6H, s]; 2.79 [$(CH_3O\text{-}C_6H_3\text{-}C_6H_3\text{-}(CH_3)_2\text{-}N)\text{-}CH_2\text{-}(CH_2)_4\text{-}CH_2O\text{-}C_6H_3\text{-}(OCOCH_3)_2$, 3H, s]; 2.83 [$(CH_3O\text{-}C_6H_3\text{-}C_6H_3\text{-}(CH_3)_2\text{-}N)\text{-}CH_2\text{-}(CH_2)_4\text{-}CH_2O\text{-}C_6H_3\text{-}(OCOCH_3)_2$, 3H, s]; 1.21-1.90 [$(CH_3O\text{-}C_6H_3\text{-}C_6H_3e\text{-}(CH_3)_2\text{-}N)\text{-}CH_2\text{-}(CH_2)_4\text{-}CH_2O\text{-}C_6H_3\text{-}(OCOCH_3)_2$, 8H, m]; 6.80-8.30 [$(CH_3O\text{-}C_6H_3\text{-}C_6H_3\text{-}(CH_3)_2\text{-}N)\text{-}CH_2\text{-}(CH_2)_4\text{-}CH_2O\text{-}C_6H_3\text{-}(OCOCH_3)_2$, 8H, m].

^{13}C NMR (d ppm $CDCl_3$ 300 MHz): 166.5 [$(CH_3O\text{-}C_6H_3\text{-}C_6H_3\text{-}(CH_3)_2\text{-}N)\text{-}CH_2\text{-}(CH_2)_4\text{-}CH_2O\text{-}C_6H_3\text{-}(OCOCH_3)_2$] 159, 153.5, 139.5, 136.2, 131.4, 128.9, 124.28, 123.6, 122.1, 120.4, 117.5, 113.4, 109.2, 106.6 [$(CH_3O\text{-}C_6H_3\text{-}C_6H_3\text{-}(CH_3)_2\text{-}N)\text{-}CH_2\text{-}(CH_2)_4\text{-}CH_2O\text{-}C_6H_3\text{-}(OCOCH_3)_2$]; 68.2[$(CH_3O\text{-}C_6H_3\text{-}C_6H_3\text{-}(CH_3)_2\text{-}N)\text{-}CH_2\text{-}(CH_2)_4\text{-}CH_2O\text{-}C_6H_3\text{-}(OCOCH_3)_2$]; 56.3[$(CH_3O\text{-}C_6H_3\text{-}C_6H_3\text{-}(CH_3)_2\text{-}N)\text{-}CH_2\text{-}(CH_2)_4\text{-}CH_2O\text{-}C_6H_3\text{-}(OCOCH_3)_2$]; 52.4[$(CH_3O\text{-}C_6H_3\text{-}C_6H_3\text{-}(CH_3)_2\text{-}N)\text{-}CH_2\text{-}(CH_2)_4\text{-}CH_2O\text{-}C_6H_3\text{-}(OCOCH_3)_2$]; 44.8[$(CH_3O\text{-}C_6H_3\text{-}C_6H_3\text{-}(CH_3)_2\text{-}N)\text{-}CH_2\text{-}(CH_2)_4\text{-}CH_2O\text{-}C_6H_3\text{-}(OCOCH_3)_2$]; 30.8, 29.2, 26.9, 26.1[$(CH_3O\text{-}C_6H_3\text{-}C_6H_3\text{-}(CH_3)_2\text{-}N)\text{-}CH_2\text{-}(CH_2)_4\text{-}CH_2O\text{-}C_6H_3\text{-}(OCOCH_3)_2$]; 20.3[$(CH_3O\text{-}C_6H_3\text{-}C_6H_3\text{-}(CH_3)_2\text{-}N)\text{-}CH_2\text{-}(CH_2)_4\text{-}CH_2O\text{-}C_6H_3\text{-}(OCOCH_3)_2$]; 20.4[$(CH_3O\text{-}C_6H_3\text{-}C_6H_3\text{-}(CH_3)_2\text{-}N)\text{-}CH_2\text{-}(CH_2)_4\text{-}CH_2O\text{-}C_6H_3\text{-}(OCOCH_3)_2$].

Mass spectrum: 517.61 [$(CH_3O\text{-}C_6H_3\text{-}C_6H_3\text{-}(CH_3)_2\text{-}N)\text{-}CH_2\text{-}(CH_2)_4\text{-}CH_2O\text{-}C_6H_3\text{-}(OCOCH_3)_2$].

Elemental analysis of 9b: calcd. for $C_{31}H_{35}NO_6$ (%): C 71.93, H 6.82, N 2.71. Found (%): C 71.82, H 6.96, N 2.59.

4.2.3.9 Dimethyl-5-(7-(6-methoxy-1,4-dimethyl-9H-carbazol-9-yl) heptyloxy)isophthalate (9c)

^{1}H NMR (d ppm $CDCl_3$): 3.95 [$(CH_3O\text{-}C_6H_3\text{-}C_6H_3\text{-}(CH_3)_2\text{-}N)\text{-}CH_2\text{-}(CH_2)_5\text{-}CH_2O\text{-}C_6H_3(OCOCH_3)_2$, 3H, s]; 4.48 [$(CH_3O\text{-}C_6H_3\text{-}C_6H_3\text{-}(CH_3)_2\text{-}N)\text{-}CH_2\text{-}(CH_2)_5\text{-}CH_2O\text{-}C_6H_3\text{-}(OCOCH_3)_2$, 2H, t]; 4.00 [$(CH_3O\text{-}C_6H_3\text{-}C_6H_3\text{-}(CH_3)_2\text{-}N)\text{-}CH_2\text{-}(CH_2)_5\text{-}CH_2O\text{-}C_6H_3\text{-}(OCOCH_3)_2$, 2H, t]; 3.93 [$(CH_3O\text{-}C_6H_3\text{-}C_6H_3\text{-}(CH_3)_2\text{-}N)\text{-}CH_2\text{-}(CH_2)_5\text{-}CH_2O\text{-}C_6H_3\text{-}(OCOCH_3)_2$, 6H, s]; 2.77 [$(CH_3O\text{-}C_6H_3\text{-}C_6H_3\text{-}(CH_3)_2\text{-}N)\text{-}CH_2\text{-}(CH_2)_5\text{-}CH_2O\text{-}C_6H_3\text{-}(OCOCH_3)_2$, 3H, s]; 2.84 [$(CH_3O\text{-}C_6H_3\text{-}C_6H_3\text{-}(CH_3)_2\text{-}N)\text{-}CH_2\text{-}(CH_2)_5\text{-}CH_2O\text{-}C_6H_3\text{-}(OCOCH_3)_2$, 3H, s]; 1.23-1.87 [$(CH_3O\text{-}C_6H_3\text{-}C_6H_3\text{-}(CH_3)_2\text{-}N)\text{-}CH_2\text{-}(CH_2)_5\text{-}CH_2O\text{-}C_6H_3\text{-}(OCOCH_3)_2$, 10H, m]; 6.80-8.40 [$(CH_3O\text{-}C_6H_3\text{-}C_6H_3\text{-}(CH_3)_2\text{-}N)\text{-}CH_2\text{-}(CH_2)_5\text{-}CH_2O\text{-}C_6H_3\text{-}(OCOCH_3)_2$, 8H, m].

^{13}C NMR (d ppm $CDCl_3$): 166.5 [$(CH_3O\text{-}C_6H_3\text{-}C_6H_3\text{-}(CH_3)_2\text{-}N)\text{-}CH_2\text{-}(CH_2)_5\text{-}CH_2O\text{-}C_6H_3\text{-}(OCOCH_3)_2$] 159, 153.5, 139.5, 136.2, 131.4, 128.9, 124.28, 123.6, 122.1, 120.4, 117.5, 113.4, 109.2, 106.6 [$(CH_3O\text{-}C_6H_3\text{-}C_6H_3\text{-}(CH_3)_2\text{-}N)\text{-}CH_2\text{-}(CH_2)_5\text{-}CH_2O\text{-}C_6H_3\text{-}(OCOCH_3)_2$]; 68.2[$(CH_3O\text{-}C_6H_3\text{-}C_6H_3\text{-}(CH_3)_2\text{-}N)\text{-}CH_2\text{-}(CH_2)_5\text{-}CH_2O\text{-}C_6H_3\text{-}(OCOCH_3)_2$]; 56.3[$(CH_3O\text{-}C_6H_3\text{-}C_6H_3\text{-}(CH_3)_2\text{-}N)\text{-}CH_2\text{-}(CH_2)_5\text{-}CH_2O\text{-}C_6H_3\text{-}(OCOCH_3)_2$]; 52.4[$(CH_3O\text{-}C_6H_3\text{-}C_6H_3\text{-}(CH_3)_2\text{-}N)\text{-}CH_2\text{-}(CH_2)_5\text{-}CH_2O\text{-}C_6H_3\text{-}(OCOCH_3)_2$]; 44.8[$(CH_3O\text{-}C_6H_3\text{-}C_6H_3\text{-}(CH_3)_2\text{-}N)\text{-}CH_2\text{-}(CH_2)_5\text{-}CH_2O\text{-}C_6H_3\text{-}(OCOCH_3)_2$]; 30.7, 29.2, 29.1, 27.2, 26.1[$(CH_3O\text{-}C_6H_3\text{-}C_6H_3\text{-}(CH_3)_2\text{-}N)\text{-}CH_2\text{-}(CH_2)_5\text{-}CH_2O\text{-}C_6H_3\text{-}(OCOCH_3)_2$]; 20.3[$(CH_3O\text{-}C_6H_3\text{-}C_6H_3\text{-}(CH_3)_2\text{-}N)\text{-}CH_2\text{-}(CH_2)_5\text{-}CH_2O\text{-}C_6H_3\text{-}(OCOCH_3)_2$]; 20.4[$(CH_3O\text{-}C_6H_3\text{-}C_6H_3\text{-}(CH_3)_2\text{-}N)\text{-}CH_2\text{-}(CH_2)_5\text{-}CH_2O\text{-}C_6H_3\text{-}(OCOCH_3)_2$].

Mass spectrum: 531.64 [$(CH_3O\text{-}C_6H_3\text{-}C_6H_3\text{-}(CH_3)_2\text{-}N)\text{-}CH_2\text{-}(CH_2)_5\text{-}CH_2O\text{-}C_6H_3\text{-}(OCOCH_3)_2$].

Elemental analysis of 9c: calcd. for $C_{32}H_{37}NO_6$ (%): C 72.29, H 7.01, N 2.63. Found (%): C 72.14, H 7.18, N 2.75.

4.2.4 General procedures for the synthesis ofn compounds 5,6 and 8a-c

Methyl salicylate (l.35 mmol) and Cs2CO3 (2.7 mmol) were dissolved in DMF (10 ml). A solution of N-bromoalkyl-substituted carbazole (1.35 mmol) in DMF was added at room temperature. The mixture was stirred for 20 h. After the reaction, the solvent was evaporated, poured into water and extracted with chloroform (5 50 ml). The organic layer was dried over anhydrous MgSO4, filtered and the solvent removed by evaporation. Final product was an orange/brown solid (80% yield).

4.2.4.1 Methyl-2-(6-(2-hydroxy-6-methoxy-9H-carbazol-9-yl) hexyloxy)benzoate (5)

^{1}H NMR (d ppm, $CDCl_3$): 4.25 [(OH-$C_{12}H_7N$)-CH_2-$(CH_2)_4$-CH_2O-C_6H_3-$OCOCH_3$, 1H, s]; 4.18 [(OH-$C_{12}H_7N$)-CH_2-$(CH_2)_4$-CH_2O-C_6H_3-$OCOCH_3$, 2H, t]; 4.09 [(OH-$C_{12}H_7N$)-CH_2-$(CH_2)_4$-CH_2O-C_6H_3-$OCOCH_3$, 2H, t]; 3.89 [(OH-$C_{12}H_7N$)-CH_2-$(CH_2)_4$-CH_2O-C_6H_3-$OCOCH_3$, 3H, s]; 1.21-1.97 [(OH-$C_{12}H_7N$)-CH_2-$(CH_2)_4$-CH_2O-C_6H_3-$OCOCH_3$, 8H, m]; 6.70-8.10 [(OH-$C_{12}H_7N$)-CH_2-$(CH_2)_4$-CH_2O-C_6H_3-$OCOCH_3$, 11H, m].
Mass spectrum: 417.5 [(OH-$C_{12}H_7N$)-CH_2-$(CH_2)_4$-CH_2O-C_6H_3-$OCOCH_3$].
Elemental analysis of 5: calcd. for $C_{26}H_{27}NO_4$ (%): C 74.80, H 6.52, N 3.35. Found (%): C 74.59, H 6.64, N 3.44.

4.2.4.2 Methyl-2-(6-(5-hydroxy-3-methoxy-9H-carbazol-9-yl) hexyloxy)benzoate (6)

^{1}H NMR (d ppm, $CDCl_3$): 4.32 [(OH-$C_{12}H_7N$)-CH_2-$(CH_2)_4$-CH_2O-C_6H_3-$OCOCH_3$, 1H, s]; 4.09 [(OH-$C_{12}H_7N$)-CH_2-$(CH_2)_4$-CH_2O-C_6H_3-$OCOCH_3$, 2H, t]; 3.99 [(OH-$C_{12}H_7N$)-CH_2-$(CH_2)_4$-CH_2O-C_6H_3-$OCOCH_3$, 2H, t]; 3.90 [(OH-$C_{12}H_7N$)-CH_2-$(CH_2)_4$-CH_2O-C_6H_3-$OCOCH_3$,3H, s]; 1.26-2.19 [(OH-$C_{12}H_7N$)-CH_2-$(CH_2)_4$-CH_2O-C_6H_3-$OCOCH_3$, 8H, m]; 6.54-8.50 [(OH-$C_{12}H_7N$)-CH_2-$(CH_2)_4$-CH_2O-C_6H_3-$OCOCH_3$, 11H, m].

Mass spectrum: 417.5 [(OH-$C_{12}H_7N$)-CH_2-$(CH_2)_4$-CH_2O-C_6H_3-$OCOCH_3$].
Elemental analysis of 6: calcd. for $C_{26}H_{27}NO_4$ (%): C 74.80, H 6.52, N 3.35. Found (%): C 74.69, H 6.70, N 3.46.

4.2.4.3 Methyl 2-(5-(6-methoxy-1,4-dimethyl-9H-carbazol-9-yl) pentyloxy) benzoate (8a)

^{1}H NMR (d ppm $CDCl_3$): 3.89 [(CH_3O-C_6H_3-C_6H_3-$(CH_3)_2$-N)-CH_2-$(CH_2)_3$-CH_2O-C_6H_3-$OCOCH_3$, 3H, s]; 4.52 [(CH_3O-C_6H_3-C_6H_3-$(CH_3)_2$-N)-CH_2-$(CH_2)_3$-CH_2O-C_6H_3-$OCOCH_3$, 2H, t]; 4.00 [(CH_3O-C_6H_3-C_6H_3-$(CH_3)_2$-N)-CH_2-$(CH_2)_3$-CH_2O-C_6H_3-OCOC H_3, 2H, t]; 3.86 [(CH_3O-C_6H_3-C_6H_3-$(CH_3)_2$-N)-CH_2-$(CH_2)_3$-CH_2O-C_6H_3-$OCOCH_3$, 3H, s]; 2.80 [(CH_3O-C_6H_3-C_6H_3-$(CH_3)_2$-N)-CH_2-$(CH_2)_3$-CH_2O-C_6H_3-$OCOCH_3$, 3H, s]; 2.83 [(CH_3O-C_6H_3-C_6H_3-$(CH_3)_2$-N)-CH_2-$(CH_2)_3$-CH_2O-C_6H_3-$OCOCH_3$, 3H, s]; 1.10-2.00 [(CH_3O-C_6H_3-C_6H_3-$(CH_3)_2$-N)-CH_2-$(CH_2)_3$-CH_2O-C_6H_3-$OCOCH_3$, 6H, m]; 6.60-8.40 [(CH_3O-C_6H_3-C_6H_3-$(CH_3)_2$-N)-CH_2-$(CH_2)_3$-CH_2O-C_6H_3-$OCOCH_3$, 9H, m].
Mass spectrum: 445.55 [(CH_3O-C_6H_3-C_6H_3-$(CH_3)_2$-N)-CH_2-$(CH_2)_3$-CH_2O-C_6H_3-$OCOCH_3$].
Elemental analysis of 8a: calcd. for $C_{28}H_{31}NO_4$ (%): C 75.48, H 7.01, N 3.14. Found (%): C 75.35, H 7.12, N 3.26.

4.2.4.4 Methyl-2-(6-(6-methoxy-1,4-dimethyl-9H-carbazol-9-yl) hexyloxy)benzoate (8b)

^{1}H NMR (d ppm CDCl3): 3.99 [(CH_3O-C_6H_3-C_6H_3-$(CH_3)_2$-N)-CH_2-$(CH_2)_4$-CH_2O-C_6H_3-$OCOCH_3$, 3H, s]; 4.53 [(CH_3O-C_6H_3-C_6H_3-$(CH_3)_2$-N)-CH_2-$(CH_2)_4$-CH_2O-C_6H_3-$OCOCH_3$, 2H, t]; 4.04 [(CH_3O-C_6H_3-C_6H_3-$(CH_3)_2$-N)-CH_2-$(CH_2)_4$-CH_2O-C_6H_3-OCOC H_3, 2H, t]; 3.94 [(CH_3O-C_6H_3-C_6H_3-$(CH_3)_2$-N)-CH_2-$(CH_2)_4$-CH_2O-C_6H_3-$OCOCH_3$, 3H, s]; 2.82 [(CH_3O-C_6H_3-C_6H_3-$(CH_3)_2$-N)-CH_2-$(CH_2)_4$-CH_2O-C_6H_3-$OCOCH_3$, 3H, s]; 2.84 [(CH_3O-C_6H_3-C_6H_3-$(CH_3)_2$-N)-CH_2-$(CH_2)_4$-CH_2O-C_6H_3-$OCOCH_3$, 3H, s]; 1.30-1.90 [(CH_3O-C_6H_3-C_6H_3-$(CH_3)_2$-N)-CH_2-(CH2)4-

CH_2O-C_6H_3-$OCOCH_3$, 8H, m]; 6.60-8.00 [(CH_3O-C_6H_3-C_6H_3-$(CH_3)_2$-N)-CH_2-$(CH_2)_4$-CH_2O-C_6H_3-$OCOCH_3$, 9H, m].
Mass spectrum: 459.58 [(CH_3O-C_6H_3-C_6H_3-$(CH_3)_2$-N)-CH_2-$(CH_2)_4$-CH_2O-C_6H_3-$OCOCH_3$].
Elemental analysis of 8b: calcd. for $C_{29}H_{33}NO_4$ (%): C 75.79, H 7.24, N 3.05. Found (%): C 75.62, H 7.38, N 3.14.

4.2.4.5 Methyl-2-(7-(6-methoxy-1,4-dimethyl-9H-carbazol-9-yl) heptyloxy)benzoate (8c)

^{1}H NMR (d ppm CDCl3): 3.95 [(CH_3O-C_6H_3-C_6H_3-$(CH_3)_2$-N)-CH_2-$(CH_2)_5$-CH_2O-C_6H_3-$OCOCH_3$, 3H, s]; 4.50 [(CH_3O-C_6H_3-C_6H_3-$(CH_3)_2$-N)-CH_2-$(CH_2)_5$-CH_2O-C_6H_3-$OCOCH_3$, 2H, t]; 3.95 [(CH_3O-C_6H_3-C_6H_3-$(CH_3)_2$-N)-CH_2-$(CH_2)_5$-CH_2O-C_6H_3-$OCOCH_3$, 2H, t]; 3.85 [(CH_3O-C_6H_3-C_6H_3-$(CH_3)_2$-N)-CH_2-$(CH_2)_5$-CH_2O-C_6H_3-$OCOCH_3$, 3H, s]; 2.87 [(CH_3O-C_6H_3-C_6H_3-$(CH_3)_2$-N)-CH_2-$(CH_2)_5$-CH_2O-C_6H_3-$OCOCH_3$, 3H, s]; 2.95 [(CH_3O-C_6H_3-C_6H_3-$(CH_3)_2$-N)-CH_2-$(CH_2)_5$-CH_2O-C_6H_3-$OCOCH_3$, 3H, s]; 1.20-1.90 [(CH_3O-C_6H_3-C_6H_3-$(CH_3)_2$-N)-CH_2-$(CH_2)_5$-CH_2O-C_6H_3-$OCOCH_3$, 10H, m]; 6.76-8.12 [(CH_3O-C_6H_3-C_6H_3-$(CH_3)_2$-N)-CH_2-$(CH_2)_5$-CH_2O-C_6H_3-$OCOCH_3$, 9H, m].

Mass spectrum: 473.60 [(CH_3O-C_6H_3-C_6H_3-$(CH_3)_2$-N)-CH_2-$(CH_2)_5$-CH_2O-C_6H_3-$OCOCH_3$].

Elemental analysis of 8c: calcd. for $C_{30}H_{35}NO_4$ (%): C 76.08, H 7.45, N 2.96. Found (%): C 75.96, H 7.52, N 3.02.

4.2.5 Synthesis of 5,8-dimethyl-9H-carbazole-3-sulfonyl chloride (18)

1,4-dimethyl-9H-carbazole (**10**) (2.56 mmol) was dissolved in chloroform (20 mL). The solution was cooled to 0 °C. To this solution chlorosulfonic acid (9.76) was added and the mixture was stirred at room temperature for 30 min. After the reaction the solution was cooled, poured into water and extracted with chloroform (3 x 30 mL). The organic layer was dried over

anhydrous $MgSO_4$, filtered and the solvent removed by evaporation to give a white solid.

^{1}H NMR (δ_{ppm} $CDCl_3$ 250 MHz): 2.57 [(ClOOS-C_6H_3-C_6H_2-(CH_3)$_2$-NH 3H,s]; 2.89 [(ClOOS-C_6H_3-C_6H_2-(CH_3)$_2$-NH 3H,s]; 6.96-7.42 [(ClOOS-C_6H_3-C_6H_2-(CH_3)$_2$-NH 5H,m]; 8.01 [(ClOOS-C_6H_3-C_6H_2-(CH_3)$_2$-*NH* 1H,s].

^{13}C NMR (δ_{ppm} THF-d_8 689 MHz): 16.55 [(ClOOS-C_6H_3-C_6H_2-(CH_3)$_2$-NH]; 20.46 [(ClOOS-C_6H_3-C_6H_2-(CH_3)$_2$-NH]; 110.37-137.28 [(ClOOS-C_6H_3-C_6H_2-(CH_3)$_2$-NH].

Elemental analysis: calcd. for $C_{14}H_{12}ClNO_2S$ (%): C, 57.24; H, 4.12; N, 4.77. Found (%): C, 57.81; H, 4.15; N, 4.81.

4.2.6 Synthesis of 5,8-dimethyl-9H-carbazole-3-sulfonamide (19)

5,8-dimethyl-9H-carbazole-3-sulfonyl chloride (**18**) (4.68 mmol) was dissolved in 15 mL of tetrahydrofuran. To this solutions 0.08 mL of a 2M ammonia solution in ethanol was added. The mixture was stirred at room temperature for 2 h. After the reaction the solution was evaporated and purified on a silica gel column chromatography in hexane/ethyl acetate (8:2).

^{1}H NMR (δ_{ppm} THF-d_8 250 MHz): 2.51 [(NH_2OOS-C_6H_3-C_6H_2-(CH_3)$_2$-NH 3H,s]; 2.79 [(NH_2OOS-C_6H_3-C_6H_2-(CH_3)$_2$-NH 3H,s]; 6.80-7.44 [(NH_2OOS-C_6H_3-C_6H_2-(CH_3)$_2$-NH 5H,m]; 8.12 [(*NH_2*OOS-C_6H_3-C_6H_2-(CH_3)$_2$-NH 1H,s]; 10.18 [(NH_2OOS-C_6H_3-C_6H_2-(CH_3)$_2$-*NH* 1H,s].

^{13}C NMR (δ_{ppm} THF-d_8 689 MHz): 16.55 [(NH_2OOS-C_6H_3-C_6H_2-(CH_3)$_2$-NH]; 20.46 [(NH_2OOS-C_6H_3-C_6H_2-(CH_3)$_2$-NH]; 110.37-139.58 [(NH_2OOS-C_6H_3-C_6H_2-(CH_3)$_2$-NH].

IR (KBr) (cm^{-1}): 3482 [(NH_2OOS-C_6H_3-C_6H_2-$(CH_3)_2$-NH];

Elemental analysis: calcd. for $C_{14}H_{14}N_2O_2S$ (%): C, 61.29; H, 5.14; N, 10.21. Found (%): C, 61.90; H, 5.19; N, 10.29.

4.2.7 Synthesis of 6-methoxy-1,4,9-trimethyl-carbazole (20)

1,4-dimethyl-9H-carbazole (**10**) (1.82 mmol) was dissolved in anhydrous dimethylformamide and stirred at room temperature for 10 min. To the solution at 0 °C sodium hydride (60% dispersion in mineral oil) (2.72 mmol) was added. The solution was warmed up to room temperature and 0.37 mL of iodomethane (5.47 mmol) were added and stirred at room temperature for 1 h. Then the mixture was poured into water and extracted with ethyl acetate (3 x 30 mL). The organic layer was dried over anhydrous $MgSO_4$, filtered and the solvent removed by evaporation to give a white solid.

^{1}H NMR (δ_{ppm} $CDCl_3$ 250 MHz): 2.51 [(CH_3O-C_6H_3-C_6H_2-$(CH_3)_2$-N-CH_3 3H,s]; 2.79 [(CH_3O-C_6H_3-C_6H_2-$(CH_3)_2$-N-CH_3 3H,s]; 3.83 [(CH_3O-C_6H_3-C_6H_2-$(CH_3)_2$-N-CH_3 3H,s]; 4.1 [(CH_3O-C_6H_3-C_6H_2-$(CH_3)_2$-N-CH_3 3H,s]; 6.86-7.34 [(CH_3O-C_6H_3-C_6H_2-$(CH_3)_2$-N-CH_3 5H,m].

^{13}C NMR (δ_{ppm} $CDCl_3$ 689 MHz): 16.55 [(CH_3O-C_6H_3-C_6H_2-$(CH_3)_2$-N-CH_3]; 20.47 [(CH_3O-C_6H_3-C_6H_2-$(CH_3)_2$-N-CH_3]; 55.34 [(CH_3O-C_6H_3-C_6H_2-$(CH_3)_2$-N-CH_3]; 44.3 [(CH_3O-C_6H_3-C_6H_2-$(CH_3)_2$-N-CH_3]; 105.44-153.65 [(CH_3O-C_6H_3-C_6H_2-$(CH_3)_2$-N-CH_3].

Elemental analysis: calcd. for $C_{16}H_{17}NO$ (%): C, 80.30; H, 7.16; N, 5.85. Found (%): C, 81.02; H, 7.23; N, 5.91.

4.2.8 Synthesis of 6-methoxy-1,4-dimethyl-9-ethyl-carbazole (21)

The synthesis of **21** was carried out with the same procedure used for **20**.

^{1}H NMR (δ_{ppm} $CDCl_3$ 250 MHz): 2.51 [(CH_3O-C_6H_3-C_6H_2-(CH_3)$_2$-N-CH_2-CH_3 3H,s]; 2.79 [(CH_3O-C_6H_3-C_6H_2-(CH_3)$_2$- N-CH_2-CH_3 3H,s]; 3.83 [(CH_3O-C_6H_3-C_6H_2-(CH_3)$_2$- N-CH_2-CH_3 3H,s]; 4.4 [(CH_3O-C_6H_3-C_6H_2-(CH_3)$_2$- N-CH_2-CH_3 3H,s]; 2.3 [(CH_3O-C_6H_3-C_6H_2-(CH_3)$_2$- N-CH_2-CH_3 3H,s] 6.86-7.34 [(CH_3O-C_6H_3-C_6H_2-(CH_3)$_2$- N-CH_2-CH_3 5H,m].

^{13}C NMR (δ_{ppm} $CDCl_3$ 689 MHz): 14.7 [(CH_3O-C_6H_3-C_6H_2-(CH_3)$_2$-N-CH_2-CH_3]; 20.47 [(CH_3O-C_6H_3-C_6H_2-(CH_3)$_2$-N-CH_2-CH_3];16.55 [(CH_3O-C_6H_3-C_6H_2-(CH_3)$_2$-N-CH_2-CH_3]; 20.47 [(CH_3O-C_6H_3-C_6H_2-(CH_3)$_2$-N-CH_2-CH_3]; 55.34 [(CH_3O-C_6H_3-C_6H_2-(CH_3)$_2$-N-CH_2-CH_3]; 44.3 [(CH_3O-C_6H_3-C_6H_2-(CH_3)$_2$-N-CH_2-CH_3]; 105.44-153.65 [(CH_3O-C_6H_3-C_6H_2-(CH_3)$_2$-N-CH_2-CH_3].

Elemental analysis: calcd. for $C_{17}H_{19}NO$ (%): C, 80.60; H, 7.56; N, 5.53. Found (%): C, 80.68; H, 7.63; N, 5.58.

4.2.9 Synthesis of 6-methoxy-1,4-dimethyl-3-nitro-9H-carbazole (22)

1,4-dimethyl-9H-carbazole (**10**) (2.22 mmol) was dissolved in 20 mL of acetic anhydride and then cooled to 0-5 °C. To this solution fuming HNO_3 100% (2.22 mmol) was added dropwise to give a dark solution. The reaction mixture was stirred at room temperature overnight. Then the mixture was filtered and dried in vacuum and then washed with diethyl ether (3 x 10 mL) to give an orange solid.

^{1}H NMR (δ_{ppm} $CDCl_3$ 250 MHz): 2.57 [(CH_3O-C_6H_3-C_6H_2-(CH_3)$_2$-NO_2-NH, 3H, s]; 3.05 [(CH_3O-C_6H_3-C_6H_2-(CH_3)$_2$-NO_2-NH, 3H, s]; 4.01 [(CH_3O-C_6H_3-C_6H_2-(CH_3)$_2$-NO_2-NH, 3H, s]; 7.89-8.18 [(CH_3O-C_6H_3-C_6H_2-(CH_3)$_2$-NO_2-NH, 4H, m]; 9.97 2.57 [(CH_3O-C_6H_3-C_6H_2-(CH_3)$_2$-NO_2-NH, 1H, s].

^{13}C NMR(δ_{ppm} $CDCl_3$ 689 MHz): 14.5 [(CH_3O-C_6H_3-C_6H_2-(CH_3)$_2$-NO_2-NH]; 15.3 [(CH_3O-C_6H_3-C_6H_2-(CH_3)$_2$-NO_2-NH]; 55.8 [(CH_3O-C_6H_3-C_6H_2-(CH_3)$_2$-NO_2-NH]; 103.0-162.3 [(CH_3O-C_6H_3-C_6H_2-(CH_3)$_2$-NO_2-NH].

Elemental analysis: calcd. for $C_{15}H_{14}N_2O_3$ (%): C, 66.66; H, 5.22; N, 10.36. Found (%): C, 67.32; H, 5.27; N, 10.46.

4.2.10 Synthesis of ethyl-5,8-dimethyl-9H-carbazole-3-nitro-carboxylate (23)

The synthesis of **23** was carried out with the same procedure used for **22** by reacting ethyl-5,8-dimethyl-9H-carbazole-3-carboxylate with fuming HNO_3 in stoichiometric amount.

^{1}H NMR (δ_{ppm} $CDCl_3$ 250 MHz): 2.57 [(CH3-CH_2-OOC-C_6H_3-C_6H_2-(CH_3)$_2$-NO_2-NH, 3H, s]; 3.05 [(CH_3O-C_6H_3-C_6H_2-(CH_3)$_2$-NO_2-NH, 3H, s]; 4.01 [(CH_3O-C_6H_3-C_6H_2-(CH_3)$_2$-NO_2-NH, 3H, s]; 7.89-8.18 [(CH_3O-C_6H_3-C_6H_2-(CH_3)$_2$-NO_2-NH, 4H, m]; 9.97 2.57 [(CH_3O-C_6H_3-C_6H_2-(CH_3)$_2$-NO_2-*NH*, 1H, s].

^{13}C NMR(δ_{ppm} $CDCl_3$ 689 MHz): 14.5 [(CH_3-CH_2-OOC-C_6H_3-C_6H_2-(CH_3)$_2$-NO_2-NH]; 15.3 [(CH_3-CH_2-OOC-C_6H_3-C_6H_2-(CH_3)$_2$-NO_2-NH]; 18.2 [(CH_3-CH_2-OOC-C_6H_3-C_6H_2-(CH_3)$_2$-NO_2-NH]; 60.9 [(CH_3-CH_2-OOC-C_6H_3-C_6H_2-(CH_3)$_2$-NO_2-NH]; 103.0-169.5 [(CH_3-CH_2-OOC-C_6H_3-C_6H_2-(CH_3)$_2$-NO_2-NH].

Elemental analysis: calcd. for $C_{18}H_{19}N_2O_4$ (%): C, 66.04; H, 5.85; N, 8.56. Found (%): C, 66.56; H, 5.90; N, 8.64.

4.2.11 Synthesis of 2-chlorodibenzofuran (24)

In the first step 2,4-dichloro-phenol (5.98 mmol) was dissolved in acetonitrile (30 mL) and stirred at room temperature; after completely dissolution silylaryl triflate (8.38 mmol) and cesium fluoride (23.44

mmol) were added. The mixture was stirred for 48 h at room temperature under nitrogen. Then the mixture was poured into water and extracted with diethyl ether (3 x 30 mL); the organic layer was dried over anhydrous $MgSO_4$, filtered and the solvent removed by evaporation to give the pure product in good yield. In the second step the intermediate, previously obtained, was added to a solution of K_2CO_3, tricyclohexylphosphine (added as the air-stable HBF_4 salts) (0.48 mmol) and $Pd(OAc)_2$ (0.05 mmol) in 10 mL of dimethylacetamide.
The mixture was stirred al 130 °C for 16 h under nitrogen. After the reaction the mixture was poured into water and extracted with diethyl ether (3 x 30 mL); the organic layer was dried over anhydrous $MgSO_4$, filtered and the solvent removed by evaporation to give the pure product as a brown oil in good yield.

^{1}H NMR (δ_{ppm} $CDCl_3$ 250 MHz): 6.92-7.41 [Cl-C_6H_3-C_6H_4-O, 7H, m].

^{13}C NMR(δ_{ppm} $CDCl_3$ 689 MHz): 112.25-156.30 [Cl-C_6H_3-C_6H_4-O].

Elemental analysis: calcd. for $C_{12}H_7ClO$ (%): C, 71.13; H, 3.48. Found (%): C, 71.84; H, 3.51.

4.2.12 Synthesis of 2-methoxydibenzofuran (25)

The synthesis of **25** was carried out with the same procedure used for **24** using 2-chloro-4-methoxy-phenol instead of phenol used for **24**.

^{1}H NMR (δ_{ppm} $CDCl_3$ 250 MHz): 3.93 [CH_3O-C_6H_3-C_6H_4-O, 3H, s]; 6.91-7.95 [CH_3O-C_6H_3-C_6H_4-O, 7H, m].

^{13}C NMR(δ_{ppm} $CDCl_3$ 689 MHz): 55.92 [CH_3O-C_6H_3-C_6H_4-O]; 103.60-151.78 [CH_3O-C_6H_3-C_6H_4-O].

Elemental analysis: calcd. for $C_{13}H_{10}O_2$ (%): C, 78.77; H, 5.09. Found (%): C, 79.55; H, 5.14.

4.3 Pharmacology

Human epithelial lung adenocarcinoma (A549), human melanoma (A375) and human epithelial cervix adenocarcinoma (HeLa) cell lines (3.5 x 10^4 cells/well) were plated on 96-well microtiter plates and allowed to adhere at 37 °C in a 5 % CO_2 atmosphere for 2 h.

Thereafter, the medium was replaced with 50 μL of fresh medium and a 75 μL aliquot of serial dilution of each test compound was added and then the cells incubated for 72 h. In some experiments, serial dilutions of cis-platin were added. Mitochondrial respiration, an indicator of cell viability, was assessed by the mitochondrial-dependent reduction of [3-(4,5-dimethylthiazol-2-yl)-2,5-phenyl-2H-tetrazolium bromide] (MTT) to formazan and cells viability was assessed accordingly to the method previously described (JPP).

Briefly 25 μL of MTT (5 mg/mL) were added and the cells were incubated for an additional 3 h. Thereafter, cells were lysed and the dark blue crystals solubilised with 100 μL of a solution containing 50% (v:v) N, N-dimethylformamide, 20% (w:v) SDS with an adjusted pH of 4.5. The optical density (OD) of each well was measured with a microplate spectrophotometer (Titertek Multiskan MCC/340) equipped with a 620 nm filter. The viability of each cell line in response to treatment with tested compounds and Doxorubicin, used as positive control drug, was calculated as: % dead cells=100-(OD treated/OD control) x 100.

4.3.1 Cell culture

Human monocytic leukemia THP-1 cells (American Type Culture Collection, Manassas, VA) were cultured in RPMI 1640 supplemented with 10% FBS, 100 UI/ml penicillin, 100 mg/ml streptomycin and 40 mg/ml gentamycin in a 5% CO2 atmosphere at 37 C.

4.3.2 Electrophoretic mobility shift assay e EMSA

Nuclear extracts of THP-1 cells were prepared according to Osborn et al. [19] in presence of 10 mg/ml leupeptin, 5 mg/ml anti- pain, 5 mg/ml pepstatin, and 1 mM phenylmethylsulfonyl fluoride. Eight micrograms of nuclear extract were incubated with 2e 5 104 cpm of 32P-labeled double-stranded oligonucleotides, the consensus STAT1/3 DNA binding site (sis-inducible factor-binding recognition element, SIE/m67) from the c-fos promoter (50-gtcga- CATTTCCCGTAAATCg-30), in a 15 ml reaction mixture containing 20 mM Hepes, pH 7.9, 50 mM KCl, 0.5 mM dithiothreitol, 0.1 mM EDTA, 2 mg of poly(dI-dC), 1 mg of salmon sperm DNA, and 10% glycerol. Products were fractionated on a non-denaturing 5% polyacrylamide gel. The gels were dried and autoradiographed and the intensity of hybridization was quantified using the public domain NIH Image 1.61 program (developed at the U.S. National Institutes of Health and available on http://rsb.info.nih.gov/nih-image/). Supershift assay was performed by incubating the nuclear extracts in a binding buffer for 1 h at 4 _C with 1 ml of antibody before addition of labeled oligonucleotide. Polyclonal antibodies against STAT3 and STAT1 were purchased from Santa Cruz Biotecnology (Santa Cruz, CA).

4.3.3 Western blot analysis

Cells were homogenized at 4 _C in 20 mM HEPES, pH 7.4, containing 420 mM NaCl, 1 mM EDTA, 1 mM EGTA, 1% Nonidet-P40 (NP-40), 20% glycerol, protease cocktail inhibitors (GE Healthcare, Amersham Place, UK) and phosphatase cocktail inhibitors. Aliquots of the cell lysate (40 mg total protein/lane) were loaded on 7.5% SDS- polyacrylamide gels. Electrophoresis was performed at 100 V with a running buffer containing 0.25 M Tris HCl, pH 8.3, 1.92 M glycine, and 1% SDS. The resolved protein were electroblotted onto a PVDF membrane (Immobilon P, Millipore, Bedford MA) and incubated overnight at 4 _C with rabbit anti-phospho-Tyr705Stat3 (Cell Signaling Technology, Beverly, MA). After washing, membranes were developed using anti-rabbit IgG peroxidase-

conjugated anti- body (Cell Signaling Technology) and chemiluminescent detection system (Immun-Star! WesternC! Kit, Bio-Rad, Hercules, CA). Blotted proteins were detected and quantified using the ChemiDoc XRS Imaging System (Bio Rad). After stripping, membranes were re-hybridized with rabbit anti-STAT3 antibodies (Santa Cruz Biotechnology)

Chapter V

Bioorganometallic chemistry is an emerging field which exploits the biological potential of organometallic compounds. Medicinal inorganic chemistry offers additional opportunities for the design of therapeutic agents not accessible to organic compounds. The wide range of coordination numbers and geometries, available redox states, thermodynamic and kinetic characteristics, and intrinsic properties of the cationic metal ion and ligand itself offer the medicinal chemist a large variety of reactivities to be exploited.

Organometallic moieties that have been studied most intensively include among others metallocenes, metal arenes or metal carbonyl complexes.

Over the last few years *N-heterocyclic carbenes* (NHCs) have entered the field as new ligands for bioactive coordination compounds.

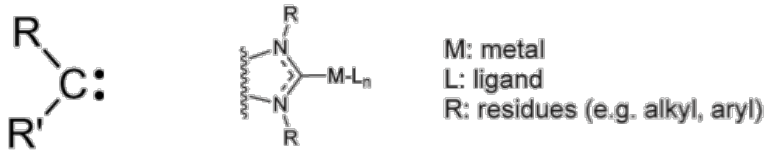

5 Carbenes

Carbenes have played an important role in organic chemistry since the first firm evidence of their existence.

Carbenes are uncharged compounds with a divalent carbon atom and two unshared electrons (the general formula is R-(C:)-R' or R=C:), which can be assigned to two nonbonding orbitals in different ways. For this reason, the chemistry of carbenes, nitrenes, and arynes is similar in many respects. Depending on spin multiplicity and ground state, the (electronic) structure of a given carbene varies as follows: if the carbene has a nonlinear structure with an sp2-hybridized carbon atom, the structures of the singlet ground state and the triplet state compare to that of carbenium ions (CR,)'

and free radicals 'CR, respectively. For the triplet state and excited singlet states linear structures with sp-hybridized carbon atoms also need to be considered. A nonlinear triplet ground state is experimentally established for the majority of carbenes; singlet-state dihalocarbenes and carbenes with oxygen, sulfur, or nitrogen substituents are exceptions.

N-Heterocyclic carbenes can be stabilized by two neighbouring nitrogens and form stable transition metal complexes. Knowledge in this area goes back to early works by Öfele and Wanzlick et al. in 1968 and to the breakthrough result of the isolation of stable carbenes by Arduengo et al. in 1991 [128,129,130,131]

The first assumption of a carbene species was made in 1855 by Geuther and Hermann .

They suggested that the alkaline hydrolysis of chloroform proceeds though the formation of a reaction intermediate with a divalent carbon called dichlorocarbene. In 1897, Nef proposed the same reaction intermediate for the Reimer–Tiemann reaction and the transformation of pyrrol to α-chloropyridine in chloroform. Indeed, it was only 3 years later that Gomberg characterized the first example of a free radical, triphenylchloromethylene, through elemental analysis and chemical reactivity.

In 1951, Lennard-Jones and Pople used quantum mechanics to determine the geometric structures and properties of small molecules [132]. They assumed the existence of two different ground states for the methylene carbene, but could not determine which one was of lowest energy.

One of the ground states they proposed was a singlet state with triangular geometry possessing three orbitals filled with two paired electrons and an empty orbital. The other proposed ground state was a triplet state with a linear geometry possessing two orbitals filled with paired electrons and two orbitals filled with unpaired electrons [132].

In 1968, Hoffmann et al. accurately determined the minimum splitting energy required between both ground states to have a methylene with a singlet state [133]. They also suggested that the singlet state could be favored by π-overlap between the p-orbitals of the carbene and the α-substituents (Scheme 9).

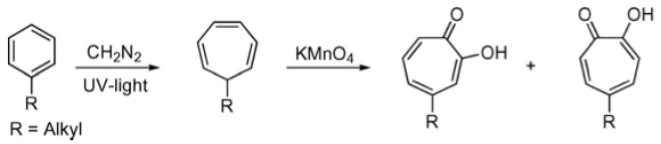

Scheme 9

During the 1970s and 1980s, numerous theoretical works using *ab initio* quantum calculations were published to rationalize the electronic structures and the geometries of methylene moieties such as :CH2, :CHF, :CHBr, :CF2, and :CCl2 [134].

It became more and more obvious that inductive and mesomeric effects act synergistically to determine the energy gap between both ground states [135]. In 1992, Goddard et al. were able to predict accurately the ground state configuration of a series of carbenes :CXY (X, Y = H, F, Cl, Br, I, SiH3), with a method using only low accuracy level calculations and which is applicable to other arbitrary carbenes [136]. It should be noted that it is important to predict the ground states of carbenes as it will directly affect their stability and reactivity [137].

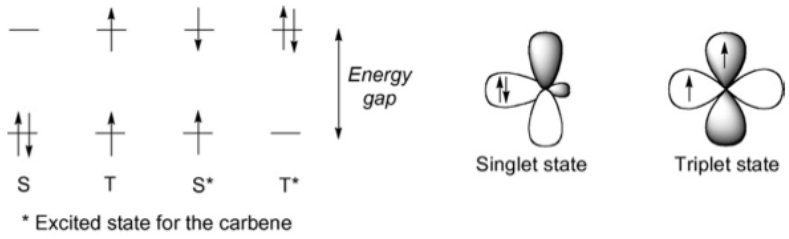

The formation of the C–M bond of a carbene–metal complex by orbitals overlapping requires a narrowing of the valence angle (XCY) at the carbene center [138]. Carbenes stabilized by donation from α-groups, such as diaminocarbenes or dialkoxycarbenes, adopt a bent geometry with a small valence angle at the central carbon. They have the required geometry to strongly and easily bind a metal fragment. In contrast push–pull carbenes, alkylidenes, and triplet carbenes adopt a widened valence angle and tend to be linear. They do not have the adequate geometry to bind the metal fragment and any changes of conformation to narrow their valence angle are energetically unfavorable [138]. Consequently, they are very reluctant to form a metal complex and give a weaker metal–carbon bond.

Well-stabilized heteroatom-containing singlet carbenes, such aminocarbenes and alkoxycarbenes have a significant gap between their singlet and triplet ground states. They form a metal–carbon bond constituted by mutual donor–acceptor interaction of two closed-shell (singlet) fragments. The dominant bonding arises from carbene–metal α-donation and simultaneously from metal–carbene π-back donation (Scheme 10) [139]. The π-electrons are usually polarized toward the metal and the carbon–metal bond has a partial double bond character, which diminishes with the stabilization of the carbene by its α-groups [139]. For instance, in diaminocarbenes, including NHCs, the metal–carbon bond is seen as a simple bond; the π-back donation is usually weak because the carbenic carbon is already well stabilized by π - donation from its amino-groups [140,141]. Fisher carbene complexes are electrophilic at the carbon–metal bond and are prone to nucleophilic attack at the carbene center (OMe/NMe2 exchange for instance) [139,140]. They are associated with low oxidation state metals [140,141].

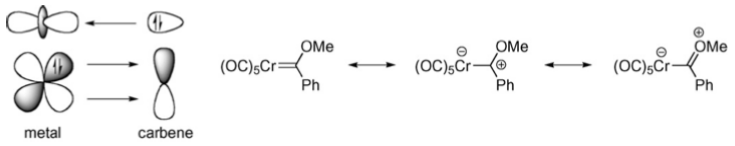

Scheme 10

5.1 Carbenes and organometallic chemistry

A carbene-containing structure was first proposed in 1970 [142], based on previous related observations [143], and triggered further studies on the generation of carbene–metal complexes from isocyanide and hydrazine [144]. The definitive structure was later resolved in 1973 by NMR and X-ray single crystal diffraction [145]. During the 1960s, Fischer and Öfele were working on alkene–metal–carbonyl (Mn, Re) complexes [146]. In 1964, while carbenes were in vogue in organic chemistry, Fischer reported and characterized unambiguously the first metal–carbene complex [147] : methoxyphenylmethylene tungsten(0) pentacarbonyl (Scheme 11).

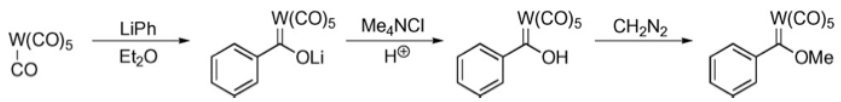

Scheme 11

During the same period, Wanzlick was interested in isolating carbenes and believed that diaminocarbenes would be stable. He proposed the synthesis of the 1,3-diphenyl-2-imidazolidinylidene via 1,3-diphenyl-2-trichloromethylimidazolidine [148]. The carbene was not isolated and only the corresponding enetetramine was recovered. He also reported different carbene adducts by using thiophosgene, thionylchloride, cyclopentanone or benzaldehyde [149]. In 1968, Wanzlick and Öfele separately reported two different NHC–metal complexes (Scheme 12) more than 20 years before the first isolation of a NHC.

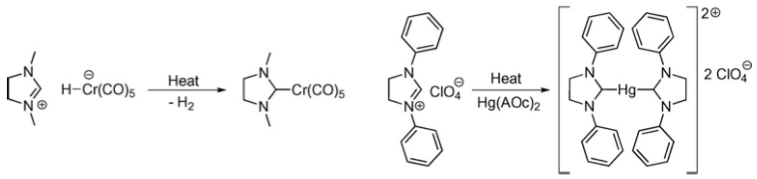

Scheme 12

The same year, Öfele also reported the first complex bearing a non-stabilized carbene without any α -heteroatoms (Scheme 13) [150].

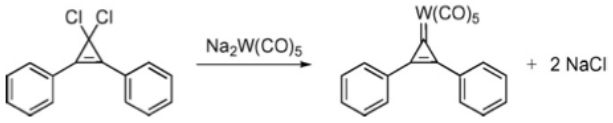

Scheme 13

5.2 NHCs (N-heterocyclic carbenes)

NHCs, also called Arduengo carbenes, are diaminocarbenes and form Fischer-type complexes with transition metals. Since the first work of Wanzlick during the 1960s, NHC–metal complexes have been synthesized following the route to Fischer complexes without the involvement of any free carbene ligand. The real breakthrough came in 1991, when Arduengo et al. synthesized and isolated the first stable NHC, 1,3-bis(adamantyl)imidazol-2-ylidene [151]. Since then, a great variety of NHCs bearing different scaffolds have been synthesized (Figure 19) and reacted with transition metals leading to well-defined complexes [152]. Today, these carbenes are recognized as an exciting alternative to the limitations of phosphine ligands in the field of organometallic chemistry and its related catalysis [153,154].

Slight changes to the NHC architectures have a dramatic change on the electronic donor properties of the carbene moieties and impose geometric constraints on the *N*-substituents, influencing their steric impact [155]. These *N*-substituents allow for a modulation of the steric pressure on both the carbene and the coordinated metal [156,157,158]. Nevertheless, five-membered ring, imidazolylidenes and imidazolidinylidenes are widely used to generate NHC-complexes, while the other frameworks are rarely employed.

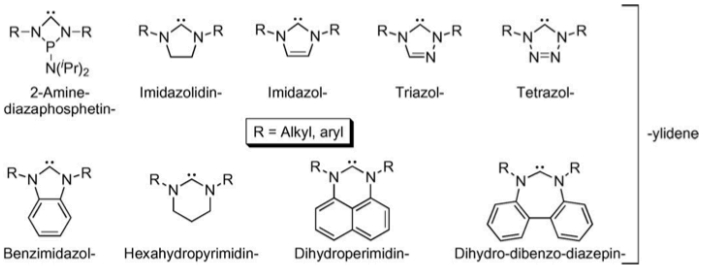

Figure 19

5.2.1 Imidazolium salts and imidazolylidenes

Various reliable routes are available to prepare imidazolium precursors [159]. One of the most straightforward is a one-pot synthesis, using, a primary amine, and formaldehyde [160]. Under acidic conditions the reaction proceeds through a coupling between the amine and the glyoxal, which forms the corresponding Schiff base. Condensation with formaldehyde leads to the imidazolium salt (Scheme 14).

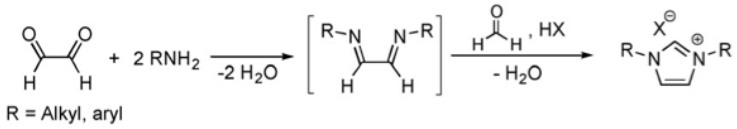

Scheme 14

The reaction can be split in two distinct steps, with the isolation of the Schiff base (diimine). It allows for the synthesis of symmetrically *N*,*N*′ - substituted imidazolium salts with various aryl- and alkyl-groups such as the 1,3-bis(2,6- diisopropylphenyl)imidazolium (IPr·HX), 1,3-bis(2,4,6-trimethyl- phenyl)imidazolium (IMes·HX), 1,3-bis(cyclohexyl)imidazolium (ICy·HX), 1,3-bis(adamantyl)imidazolium (IAd·HX), 1,3-bis(*tert*- butyl)imidazolium (ItBu·HX) and 1,3-bis(dodecyl)imidazolium (IDD·HX) (Figure 20) [161].

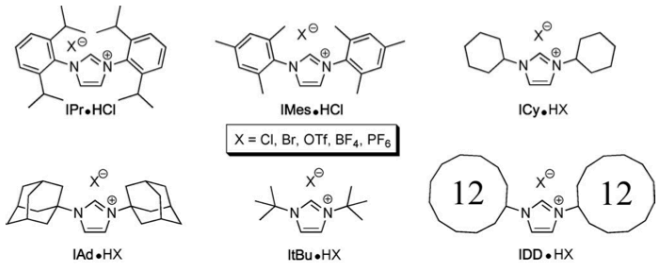

Figure 20

Recently, Glorius et al. proposed an alternative approach for the synthesis of sterically hindered imidazolium salts. The reaction of silver triflate

with chloromethyl pivalate generates, in situ, an alkylating reagent, which efficiently cyclizes hindered and non-hindered diimines (Scheme 15) [162].

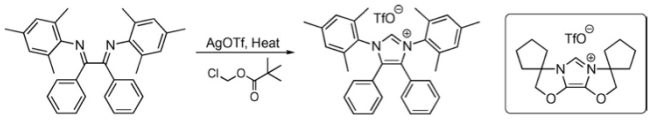

Scheme 15

The one-pot reaction between glyoxal, ammonium chloride, paraformaldehyde, and only one equivalent of primary amine leads to the mono *N*-substituted imidazole. It can be further *N*-alkylated by reaction with an alkyl halide to form an unsymmetrically *N*,*N*′- substituted imidazolium salt (Scheme 16) [163].

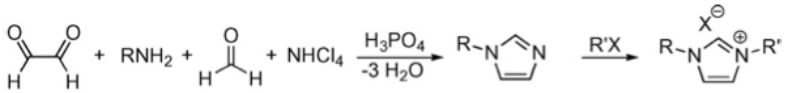

Scheme 16

Another route to synthesize unsymmetrical imidazolium salts is the stepwise alkylation of an imidazolide anion generated from the reaction of imidazole with potassium (Scheme 17).

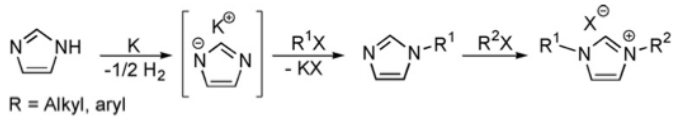

Scheme 17

Imidazolium salts lead to imidazolylidenes by deprotonation. The reaction can be carried out in ammonia or in non-protic solvents such as THF or ethers. The deprotonation requires anhydrous conditions and the use of strong bases, with pKa values above 14. Usually, potassium or sodium hydride with a catalytic amount of tert-butoxide is employed, but tert-butoxide itself, lithium aluminum hydride, n-butyllithium, potassium hexamethyldisilazide (KHMDS) and 1,8-diazabicyclo[5.4.0]undec-7-ene (DBU) are also efficient alternatives (Scheme 18) [164,165,166].

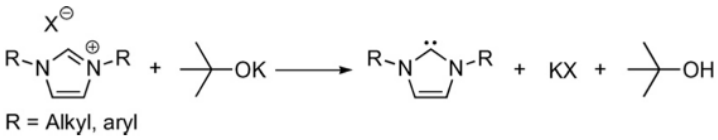

Scheme 18

5.2.2 Reactivity of NHCs

Imidazolylidenes and sterically stabilized imidazolidinylidenes are thermodynamically stable. They do not react with triplet dioxygen for kinetic reasons, even if the formation of ketones appears to be very exothermic [167,168]. They are inert toward carbon monoxide and oxidating agents such as CuO and HgO. They react slowly with dihydrogen to form aminals by 1,1-addition in the presence of a catalytic amount of palladium or platinum [168]. On the other hand, they are extremely sensitive to moisture and have to be handled under dry atmosphere [169]. They hydrolyze through the insertion of the carbene into H2O, or by nucleophilic attack of OH. Both pathways lead to a formamide by ring opening of a cyclic α-diaminomethanol intermediate (Scheme 19) [168].
NHCs react with acids and form iminium salts quantitatively due to their high p*K*a values, ranging from 20 to 30 (in water) [170]. They are among the most powerful neutral organic bases.

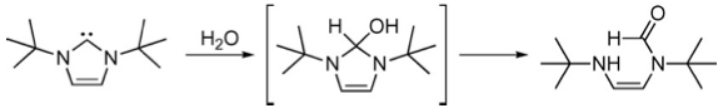

Scheme 19

The distance between the carbenic carbon and the metal in organometallic complexes gives an insight on the ability of the carbene to accept any transfer of electron density from the metal (π-back donation). A short distance accounts for a partially metal–carbon double bond due to a π-back donation. Studies of different types of carbenes show that the π-accepting ability decreases from Schrock to Fischer-type (non-diaminocarbenes) to NHCs [171].
It is well accepted that NHCs bind strongly to metals by π-bonding while the π-back bonding can be considered negligible [172]. Nevertheless, the bonding between a metal center and a NHC always presents a π-back bonding component which, while marginal in most cases, becomes

significant for Group 11 metals, copper, silver and gold [173]. Furthermore, it has been shown that π-back donation is favored in saturated imidazolidinylidenes when compared to unsaturated imidazolylidenes [174]. It is important to add that the 6 π-delocalization in NHCs, such as imidazolylidenes, only provides a marginal effect in the bonding nature of NHCs.
In metal complexes, NHCs share with phosphines the characteristics of being monodendate two-electron donor ligands [175]. Carbonyl–metal complexes bearing a CO group placed in trans position to an NHC or a phosphine ligand are of special interest in infrared spectroscopy. The vibrational frequency of C–O stretching is known to be proportional to the π-back donating ability of the NHC or phosphine ligand. In a totally symmetric vibrational mode, more basic ligands (σ-donors) induce lower vibrational frequencies. Studies of different complexes of nickel(0) have shown that NHCs appear to be more electron-donating than most basic phosphines [176]. They bind more firmly the metal center than phosphines ligands. Finally, contrary to the phosphines, NHCs bind with alkaline, lanthanides and high oxidation state metals in which π-back donation is not possible [177].

5.3 NHCs in medicinal chemistry

Metal-NHCs have become a well-known system to the organometallic chemists as they found several applications due to their strong and stable metal-ligand bond, compared to phosphines. The synthesis of stable metal-N heterocyclic carbenes have lunched them as catalysts at the expense of phosphines and applied for olefin metathesis among other reactions; the same feature has recently allowed therapeutics investigations, at the first as antimicrobials [178] and more recently as anti-cancer agents. In fact it has been demonstrated that metal NHC complexes can be used to develop highly efficient metal based drugs with possible applications in the treatment of cancer or infectious diseases. Complexes of silver and gold have been biologically evaluated most frequently but also platinum or other transition metals have demonstrated promising biological properties.

5.3.1 Silver NHC complexes

Silver NHC complexes are currently the most widely studied type of metal NHC as anti-infectives and anticancer. Silver Metal NHC complexes have been studied as potential antibacterial and antimicrobial agents. Silver has been since antiquity used as antimicrobial agent, it was earlier employed in the purification of drinking water, wine and vinegar, and also Hippocrates remarked its therapeutic properties [179]. Still today silver salts are used particularly in the treatment of chronic ulcers, extensive burns and to prevent conjunctivitis into newborn's eyes as well as other bacterial infections [180].

The activity of silver against Gram-positive and Gram-negative bacteria, fungi and yeast is due to Ag cations, which can interact with the cell membrane, interfere with the electron transport system of the cell and interact with thiol groups of the vital enzymes of bacteria [181].

The efficacy of a silver-drug as antibacterial agent is, of course, linked to its bioavailability which must be slow and continues for an appropriate time in the affected area [182]. In fact, silver nitrate and silver sulfadiazine, commonly used topical antibacterials, have very quick bactericidal action, but rapidly lose their effectiveness by exposing the wound-site to a possible re-infection.

Thus, the search for a silver-compound that slowly releases silver cations into the wound, maintaining a constant source of antibacterial agents to prevent infection, is a topic of great interest in the medical community.

The slow release of Ag cation at the wound-site is closely related to the choice of ancillary ligands to silver, which can play an important role stabilizing the complexes, thus retaining the anti- bacterial effect over a longer period of time.

N-heterocyclic carbenes (NHC), due to their excellent σ-donating properties and, as theoretical and structural studies suggest, p-backbonding ability [183,184], are widely used as ancillary ligands to stabilize both main group and transition metals [185].

In recent years many N-heterocyclic silver compounds have been synthesized, mainly for use in transmetalation of N-heterocyclic carbenes from silver to other metals, making it the most important synthetic method to give other metal NHC compounds [186,187].

Silver-N-heterocyclic carbene complexes can slowly release silver ions into the wound, enabling better prevention of infection and promoting healing [188,189].

In the report by Youngs et al. [190] the synthesis of two pyridine-linked pincer silver NHC complexes **1** and **2** (Figure 21) is presented. These two compounds were active against Escherichia coli (E. coli), Staphylococcus aureus (S. aureus) and Pseudomonas aeruginosa (P. aeruginosa), showing a MIC value much lower than that of $AgNO_3$, which is the appropriate reference for this type of study. The efficiency was interpreted as the result of the slow release of Ag^+ into the culture medium from the stabilized pincer type ligands. An interesting delivery method for silver NHC complexes is the encapsulation of these molecules in nanoparticles or nanofibres [191,192] One example for this is provided by the dinuclear complex **3**, which was tested in the same three bacterial cultures as mentioned above. Comparing **3** and AgNO3, there was no difference in potency after 24 hours but after 48 hours $AgNO_3$ triggered a better anti-microbial activity. However, after encapsulating complex **3** in Tecophilic, which is a family of hydrophilic polyether-based thermoplastic aliphatic polyurethanes, and tests on the Gram- positive and Gram-negative prokaryotes (E. coli, S. aureus and P. aeruginosa) it showed a faster bactericidal activity with lower concentrations of silver ([Ag+] = 140 μg mL−1 or 424 μg mL−1) compared with 0.5% silver nitrate ([Ag^+] = 3176 μg mL−1) and silver sulfadiazine ([Ag^+] = 3020 μg mL−1). In both cases the encapsulated compounds showed a sustained release of active Ag^+ ions into solution resulting in a constant antibacterial activity over a period of several days.

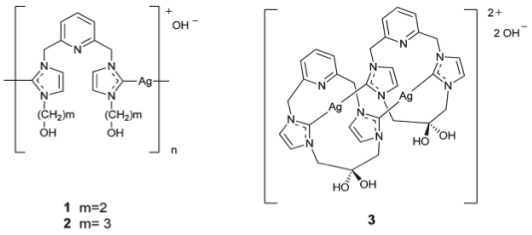

Figure 21

Other silver(I) NHC complexes, which contain a NHC and an acetate ligand coordinated to the metal center (Figure 22), were synthesized by Youngs et al. (**4**–**7**) [193,194] and by Tacke et al. (**8**–**27**) [195,196,197,198]

Symmetric and non-symmetric acetate silver(I) NHC complexes were synthesized and tested against the Gram-positive bacteria S. aureus and the Gram-negative bacteria E. coli. From these experiments it was concluded that by increasing the lipophilicity, the complexes were able to penetrate the cell membrane more effectively leading to the observed antibacterial activities. However, the increase in lipophilicity may also lead to a lower solubility of the complexes under the assay conditions. Independent of the magnitude of the inhibitory activity for most of the complexes a selectivity against S. aureus compared to E. coli was observed.

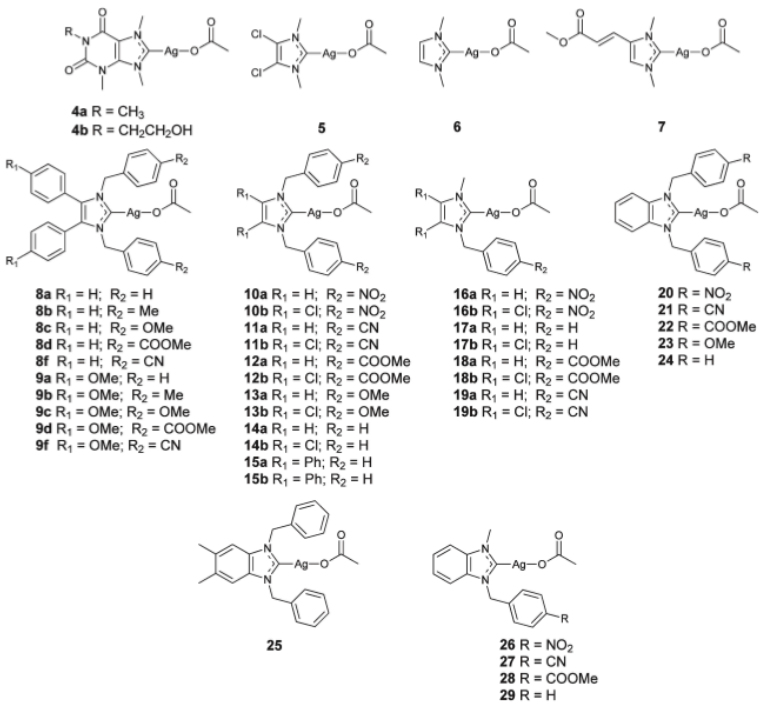

Figure 22

Roland and Jolivalt et al. reported a study on 14 halido Ag(I)–NHC complexes (**30**–**43**, Figure 23) tested as antibacterial agents against E. coli, S. aureus and the resistant strains S. aureus NorA (a ciprofloxacin resistant strain that overexpresses the multidrug efflux pump NorA), and S. aureus MsrA, which contains the plasmid pUL5054 with constitutive resistance to erythromycin [199]. Complexes **30**–**32** and **35**–**41** showed significant activity against E. coli and S. aureus in the range of 4–16 μg mL−1 (MIC value of 30 against S. aureus = 32 μg mL−1). On the other hand, complexes **33**, **34**, **42** and **43** showed low inhibitory activity against E. coli, but the highest antibacterial efficacy against S. aureus. With the exception of **42** all complexes were active against the resistant strains

with MIC values in the range of 1–32 μg mL−1. Complexes **33** and **43** exhibited the highest potencies.

Synergistic effects against S. aureus NorA were noted in combination of silver NHC complexes with the antibiotic drug ciprofloxacin administered in subinhibitory concentration. The most significant antibacterial effects against S. aureus NorA were observed with complexes **32**, **42** and **43** in combination with ciprofloxacin [199] Of these, **42** triggered the most advanced synergistic effects.

Complex **44** was studied against Bacillus subtilis (B. subtilis) and E. coli and was active only against first one of the strains, with a MIC value of 3.2 μM. No considerable morphological changes were observed in the cells after incubation with 10 μM of the compound [200]. For the complexes **45** and **46** reported by Gust et al. antibacterial properties were observed against E. coli DH5α, E. amylovora EA273, B. subtilis 168 and Bacillus megaterium. In particular promising activity was noted against B. subtilis 168 and Bacillus megaterium [201].

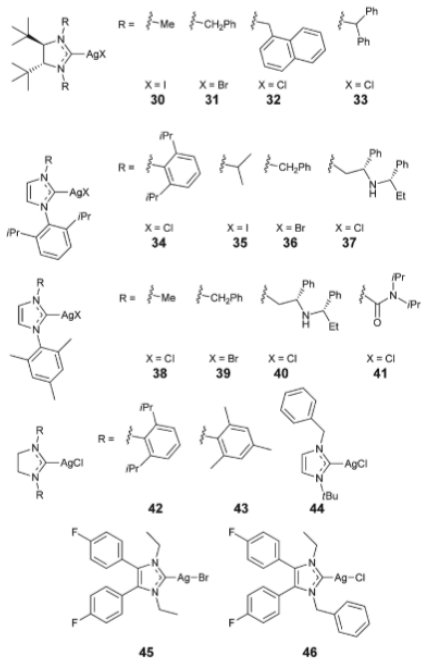

Figure 23

In their series of papers dedicated to the biological activities of Ag-NHCs, Youngs *et al.* Have reported the cancer activities of silver acetate NHCs. Some of them bear chlorine atoms, on the imidazol-2-ylidene skeleton, that enhances the stability of complexes due to their electron-withdrawing effect. In D_2O an increase of the Complex **47** half life was observed from 2h than 17 weeks for **48**.

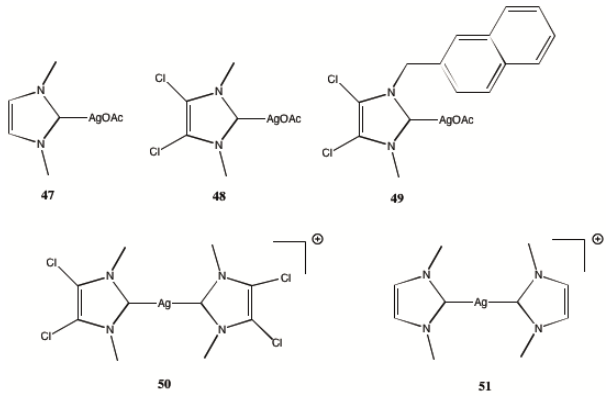

Figure 24

IC_{50}s were determined and compared with those of DDP. Complexes **48** and **49** proved efficiency similar to that of DPP on OVCAR-3 and MB157. In contrast complexes **50** and **51** are 10 fold less active than DDP on H460.

Still in the silver acetate series, Tacke group published several papers demonstrating the cytotoxic effect of symmetrical and asymmetrical complexes on Caki-1 cell line. The majority of the acetate complexes are active but in less extent than DDP, with few exceptions.

A. Gautier *et al.* [202] reported IC_{50} values for heteroleptic silver chlorine NHCs complexes on MCF-7. The same complexes were are been tested by Roland *et al.* on both MCR5 (a non cancerous cell line in rapid proliferation) and EPC, a quiescent one.

In all cases , a 35-fold increased cytotoxicity is observed for complexes **55** compared to that of DDP. Complex **55** is until today the most active silver-NHC.

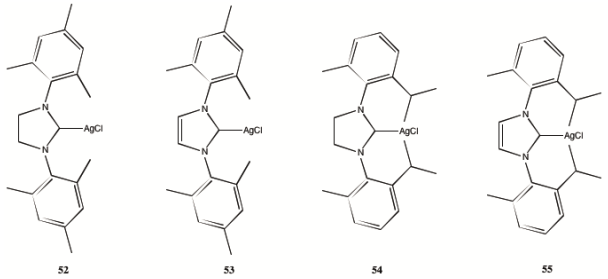

Figure 25

5.3.2 Copper NHC complexes

Copper-based complexes have been investigated on the assumption that endogenous metals may be less toxic for normal cells with respect to cancer cells. However, copper can also be toxic due to its redox activity and affinity for binding sites that should be occupied by other metals. The altered metabolism of cancer cells and differential response between normal and tumor cells to copper are the basis for development of copper complexes endowed with antineoplastic characteristics.
Copper forms a rich variety of coordination complexes with oxidation states Cu(II) and Cu(I). The coordination chemistry of copper is dominated by Cu(II) derivatives with little but important examples of Cu(I) compounds. Since copper(I/II) complexes are (i) redox active, (ii) frequently labile, and (iii) atypical in their preference for distorted coordination geometries, they are much less structurally predictable than other first-row transition metal complexes. Copper(I) strongly prefers ligands having soft donor atoms such as P, C, thioether S, and aromatic amines. Although two- coordinated linear and three-coordinated trigonal arrangements are known, Cu(I) complexes are mostly four-coordinated species adopting a tetrahedral geometry. In Cu(II) complexes the coordination number varies from four to six, including four- coordinate square-planar (sp), five-coordinate trigonal bipyramidal (tbp), and six-coordinate octahedral (oc) geometries. The variety of accessible arrays

allows for a great assortment in the choice of the ligands (from mono- to hexadentate chelates) and of the donor atoms (N, O, S, and halides) [203]. Detailed molecular mechanisms for tumor-associated copper elevation are not completely elucidated. Links among copper homeostasis/metabolism regulation and the X-linked inhibitor of apoptosis (XIAP) protein have recently emerged [204] XIAP promotes ubiquitination and degradation of COMMD1 (copper metabolism gene MURR1 domain containing 1), a protein that stimulates the efflux of copper from the cell, thus regulating copper export from the cell and, potentially, acting as an additional intracellular sensor for copper levels. Biochemical studies demonstrated that XIAP can directly bind copper ions through cysteine domains (CxxC motifs) that are distributed across the whole protein. The interaction between XIAP and copper results in a marked conformational change of XIAP, determining the inability of this potent antiapoptotic protein to inhibit caspases and leading to activation of caspase-dependent cell death cascades. Hence, intracellular copper accumulation and generation of the copper- bound form of XIAP increase the susceptibility of cells to apoptotic stimuli.

Most of the reports regarding copper complexes as anti-cancer agents [205] have focused on copper(II) precursors in the presence of reducing agents that yield a copper(I) active species which acts as a chemical nuclease [206,207].

Despite that Cu(II) complexes are active via the generation of Cu(I), few investigations were conducted on stable copper(I) complexes.32 An hypothesis is that copper(I)–NHCs would be able to reach biological targets inside the cell. Subsequently, Cu(I)–NHC complexes could react with intracellular oxygen or hydrogen peroxide, producing in situ Reactive Oxygen Species (ROS) ultimately leading to cellular damages [208]. A. Gautier *et al*. first evaluated the effect of the well-known copper(I)–NHCs (**1**-**4**, Figure 26) on the MCF-7 cell line [209].

All candidates exhibited submicromolar IC50s significantly lower than that of the reference drug cisplatin. The biological action of [CuCl(SIMes)] **1** was studied from the point of view of the effect on the cell cycle arrest. A G1-phase stop was induced at concentrations at least ten times lower than those of DDP. Furthermore, an in vitro comparative evaluation with silver and palladium of genotoxicity was performed using supercoiled plasmids. As expected, the copper(I)–NHCs are unique in

being able to act as chemical nucleases. The mechanism of **1** is believed to imply the metal as a direct dioxygen activator in the presence of DNA as the reaction is inhibited by $^1O_2$ scavengers.

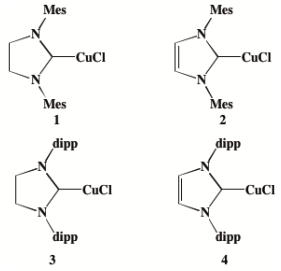

Figure 26

5.3.3 Gold NHC complexes

The application of gold in medicine is traceable for several thousand years and gold complexes have been evaluated for many different pharmaceutical purposes, notably cancer and arthritis. The spectrum of gold complexes with described cell growth inhibiting properties comprises a large variety of different ligands attached to gold in the oxidation states +I or +III. Based on the great structural variety of the used ligands, a unique mode of action or pharmacological profile is unlikely to exist. In particular, direct DNA damage, modification of the cell cycle, mitochondrial damage including thioredoxin reductase (TrxR) inhibition, proteasome inhibition, modulation of specific kinases, and other cellular processes affected by gold compounds, which eventually trigger apoptosis, seem to play a major role in the mechanism of action of gold compounds [208-215].
Two lead structures for antitumor active gold complexes are auranofin and its chloride analogue Et3PAuCl Figure 27. Both complexes exhibit their antitumor activities mainly due to the inhibition of the enzyme TrxR [210,211]. The mammalian TrxR is a family of selenocysteine containing pyridine nucleotide-disulfide oxido-reductases and its major cytosolic

forms are known as TrxR1 (cytosolic), TrxR2 (mitochondrial), and TrxR3 (testis specific) [212,210,213]. Since this enzyme is relevant for the control of mitochondrial function and the intracellular redox state, it is associated with many cellular processes, such as antioxidant defense and redox homeostasis [214]. Moreover, it is found at elevated levels in human tumor cell lines. Gold complexes are in general good inhibitors of this enzyme [215]. They demonstrated strong affinity for TrxR leading to inactivation due to the formation of a covalent bond at the Se-center of the enzyme.

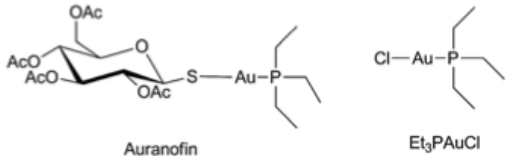

Figure 27

Previous structure–activity relationship (SAR) studies on auranofin and Et3PAuCl indicated that the phosphine ligand is more important for the biological potency than the halide or the thioglucose. Exchange of the carbohydrate ligand of auranofin (or the chlorine ligand of Et3PAuCl) does not lead to a loss of antitumor activity in vitro [216]. Of late, there has been considerable interest in NHCs as alternatives to phosphines as ligands for the soft Au(I) ion. NHC ligands have similar donor properties to phosphines, but they are usually more easily synthesized.

The application of Au(I)–NHC complexes for targeting mitochondrial cell death pathways was widely studied. Following the successful application of gold phosphine complexes as antitumor agents, Berners-Price et al. reported the induction of mitochondrial permeability transition in isolated rat liver mitochondria by dinuclear Au(I)–bis(NHC) complexes [215-219]. The wingtip groups were modified in order to adjust the lipophilic character of the complexes, a critical factor for targeting malignant cells. Antimitochondrial effects (induction of Ca2+sensitive mitochondrial swelling) were also observed for a series of mononuclear, linear, cationic Au–NHC complexes which was synthesized by the same group. In

accordance with previous studies on Au(I) species, which demonstrated that the bioactivity can be influenced by fine-tuning of the lipophilicity, the onset of mitochondrial swelling was most rapidly induced by the complexes with the highest lipophilicity. A complex (1, Figure 28) with significant antimitochondrial property and intermediate lipophilicity was selected for further studies. It was found that 1 could selectively induce apoptosis via the activation of caspase 9 and caspase 3 in cancer cells, but not in normal cells. Furthermore, 1 selectively inhibited TrxR activity but not glutathione reductase (GR) activity in MDA-MB 231 cells and was accumulated in mitochondria [217].

1

Figure 28

With the same purpose of targeting mitochondria, Rauben- heimer et al. designed a bis-ferrocenylcarbene Au(I) complex **2** (Figure 29), which exhibited higher growth inhibition potency at lower concentrations than cisplatin against two of the three tested cancer cell lines. It is possible that the antitumor activity of the complex was enhanced by the presence of the ferrocene fragment.

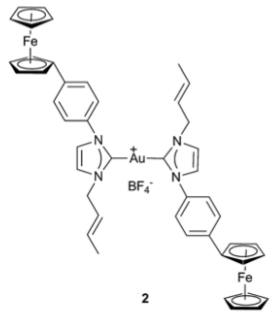

Figure 29

Taking advantage of their developments in the synthesis of novel Au(I)–NHC complexes and the associate synthetic routes facilitated by a versatile Au(I)–NHC synthon, two different series (neutral and cationic) gold complexes were prepared and screened against LNCaP (prostate carcinoma) and MDA-MB 231 cell lines by Nolan and his coworkers [218]. The cationic complexes were more effective than the neutral complexes, possible because they could cause cell death by an apoptotic pathway in cancer cell lines, which may reflect the importance of the mitochondrial apoptotic pathway in the action of the effective compounds.108 Among the neutral complexes, **3a** and **3b** (Figure 30) are the most effective and were more potent than cisplatin. In addition, both complexes exhibited similar cytotoxic effects on normal prostate, breast epithelial cells and tumor cells from the same tissue.

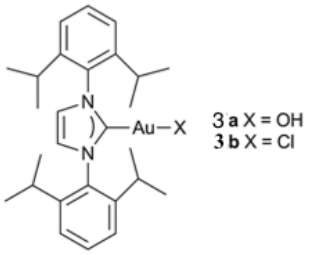

Figure 30

More recently, a series of Au(I)–NHC complexes was rational designed by Ott et al. based on available crystal structure data of the gold phosphole complex chloro[1-phenyl- 2,5-di(2-pyridyl)-phosphole]gold(I) (GoPI) in the active site of GR.150 The target complexes were based on a benzimidazol-2- ylidene core and demonstrated a good stability against the thiol glutathione.151 TrxR was selectively inhibited by these complexes in comparison to the closely related enzyme GR, and all complexes triggered significant antiproliferative effects in cultured tumor cells. Unfortunately, the expected enhanced activity with increasing the lipophilicity/surface volume of the residues at the benzimidazol-2-ylidene nitrogens could not be observed. The tumor selective behavior was not observed in these complexes as comparative experiments in nontumorigenic cell lines (HEK-293 human embryonic kidney cells and HFF human foreskin fibroblasts) afforded similar activities.

More detailed experiments on chloro[1,3-diethylbenzimidazol- 2-ylidene]gold(I) **4** (Figure 31) revealed a distinct pharmacodynamic profile including the high increase of ROS formation, apoptosis induction, strong effects on cellular metabolism (related to cell surface properties, respiration, and glycolysis), inhibition of mitochondrial respiration and activity against resistant cell lines. In addition, the described bioactivities depended on the presence of the Au(I) center (the corresponding free ligand was ineffective in all comparative experiments).

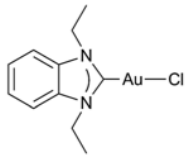

4

Figure 31

Next, to modify the pharmacodynamic properties of **4**, an additional NHC ligand and a triphenylphosphine were chosen by the same group, respectively.152 The coordination with these neutral ligands led to the formation of cationic species. The introduction of a positive charge turned out to be a key feature to increase the cellular uptake, induce mitochondrial accumulation, and improve general cytotoxic properties. This could be related to effects commonly known for delocalized lipophilic cations. The modulation of the stability of the coordinative bonds of the complexes affected the reactivity toward the target enzyme TrxR. These two cationic complexes might provide a useful compromise between good inhibitory effects against TrxR and strong anti-proliferative/antimitochondrial properties.

Similar to the structure of **4**, two Au(I)–NHC complexes (**5** and **6**, Figure 32) bearing benzimidazolin-2-ylidene ligands were synthesized and characterized by Dinda et al. [219]. However, the IC50 values of the tested complex **5** were nearly thrice higher than those of cisplatin on B16F10 (mouse melanoma), HepG2 (human hepatocarcinoma) and HeLa (human cervical carcinoma) cell lines. Prominent morphological changes (such as cell rounding and shrinkage and nuclear fragmentation), were observed when treated with the complex **5** for 24 h at 25 mM on these three cell lines, which indicate that complex **5** induced cell death is mostly via apoptosis. Interestingly, this complexes did not show any significant cytotoxic effects on normal human peripheral blood mono nuclear cells at 100 mM, whereas cisplatin showed 75% cytotoxicity at 10 mM.

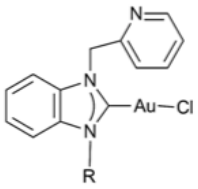

5 R = Me
6 R = CH_2Ph

Figure 32

Three new benzyl- or 4-cyanobenzyl-substituted Au(I)– NHC complexes (**7a–c**, Figure 33) were prepared by Tacke et al. [220]. Compared to the corresponding Ag(I)–NHC complexes, the gold complexes showed superior cytotoxic activities because of their solubility factor. However, they were less active than cisplatin against Caki-1 cells.

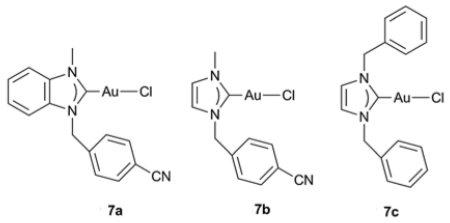

Figure 33

Li et al. also developed an Au(I)–NHC complex (**8**, Fig. 6) bearing an amino-NHC ligand, which exhibited selective cytotoxicity against U-87 MG cells [221]. However, this complex did not inhibit human TrxR indicating that it might trigger apoptosis through a DNA dependent mechanism. Further experiments indicated that this complex mediated S-phase arrest via down-regulation of cyclin A, cyclin B1, and cdk2. Apoptosis was induced by this substance in U-87 MG cells through a p53-bak pathway. Moreover, the complex participated in an important molecular event that mediated negative regulation of p21. Consequently,

it had therapeutic potential in the treatment of glioblastoma in the case of p21-dependent resistance of p53-induced apoptosis.

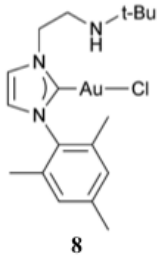

8 **Figure 34**

Five Au(I)–NHC complexes **9 a-e** (Figure 35) derived from N-methyl-4,5-diarylimidazolium salts were prepared by Schobert's group [222]. All complexes showed cytotoxic activity with IC50 in the micromolar range and distinct selectivity for certain cell lines. In addition, they were generally more cytotoxic than their respective silver precursors. In contrast to related metal free 1-methyl-4,5-diarylimidazoles, the complexes did not noticeably inhibit the polymerisation of tubulin to give microtubules. The cellular uptake of complexes **9 a–d** occurred mainly via the copper transporter (Ctr1) and the organic cation transporters (OCT-1/2). In addition, complex **9**e was accumulated preferentially via the organic cation transporters and by Na+ /K+ -dependent endocytosis. These gold complexes seem to operate a mechanism different from that of the parent 1-methylimidazolium ligands.

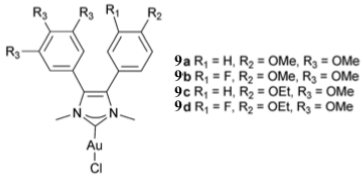

9a R_1 = H, R_2 = OMe, R_3 = OMe
9b R_1 = F, R_2 = OMe, R_3 = OMe
9c R_1 = H, R_2 = OEt, R_3 = OMe
9d R_1 = F, R_2 = OEt, R_3 = OMe

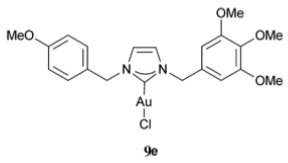

9e

Figure 35

A series of Au(I)–NHC (NHC = 1,3-substituted imidazole- 2-ylidene or benzimidazole-2-ylidene) complexes with chloro and 2-pyrimidinethiolato ligands was prepared by the groups of Mohr and Casini [223]. The compounds were screened for their antiproliferative effects on cisplatin-sensitive and resistant human ovarian cancer cells (A2780S/R), as well in the non- tumorigenic human embryonic kidney cell line (HEK-293T), and were found to be potent cytotoxic agents. Four cytotoxic Au(I)–NHC complexes (**10a–d**, Figure 36) were selected to be screened for their TrxR inhibition properties both on the purified enzyme and on cell extracts in vitro. These complexes inhibited cytosolic TrxR1 better than mitochondrial TrxR2 and even to a much lesser extent GR. Unlike auranofin, the inhibition of TrxR by the complexes appears to be relevant in cancer cell lines but not in non-tumorigenics cells. Interestingly, a correlation between cytotoxicity and thioredoxin oxidation via TrxR inhibition in the presence of gold complexes in cancer cells was observed. Further biochemical assays about complexes on glutathione systems and ROS formation evidenced great differences compared to auranofin.

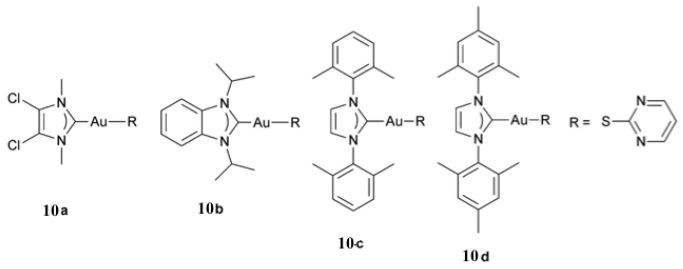

Figure 36

Inspired by the scarcity of Au(I) complexes containing ylideneamine ligands and together with the biological activity displayed by ylideneamine metal complexes, Cronje et al. reported on the preparation and extensive characterization of a series of pentafluorophenyl-, phosphine- and NHC-containing ylideneamine Au(I) complexes. These complexes were evaluated for their potential as antitumor and antimalarial agents [224]. All complexes including Au(I)–NHC complex **11** (Figure 37) exhibited a significant increase in growth inhibition with respect to the free ligands against cervical carcinoma cells and the 3D7 strain of Plasmodium falciparum. However, they were less active than cisplatin in the antitumor test and chloroquine in the antimalarial test, respectively.

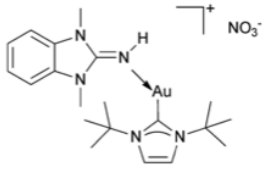

11

Figure 37

In continuation of the SAR study with their Ag–NHC complexes derived from 4,5-diarylimidazoles, R. Gust group focused their attention on the design of analogous Au–NHC complexes (**12a–m**, Figure 38) [225]. They supposed that the replacement of the phosphine in Et3PAuCl by an NHC ligand with pharmacological activity (e.g. hormonal activity, cyclooxygenase (COX) inhibitory properties) could lead to new multi-target antitumor agents including the TrxR.

The novel Au–NHC complexes (**12a–k**) caused growth inhibitory effects against tumor cell lines. There are at least six Au–NHC complexes (**12a–d**, **12f**, and **12g**) among thirteen complexes which were more active than cisplatin and Et3PAuCl and as active as auranofin against the used breast (MCF-7 and MDA-MB 231) and colon (HT-29) cancer cell lines.

Especially, the most active complex **12d** exhibited distinctly higher antiproliferative potency than cisplatin.

High growth inhibitory effects depended on the presence of the C4,C5-standing aromatic rings. Methoxy groups and fluorine substituents only marginally changed the cytotoxicity against the used cell lines, while 4-hydroxy groups nearly terminated the activity. The substituents at the nitrogens and the oxidation state of the metal played a subordinate role. In addition, the growth inhibitory effects of the complexes depended on the presence of a metal center (the imidazoles were inactive).

All complexes inhibited the TrxR, which led to the conclusion that this enzyme might be the main target of these complexes. The missing SAR and the missing correlation with cytotoxic properties indicated the involvement of further targets. Based on the investigations on cellular and

nuclear uptake, as well as the binding to the ER, DNA binding and interference in the hormonal system could be excluded. The selective inhibition of the COX-1 enzyme by complex **12f** opens a new perspective for use Au–NHC complexes in medicinal chemistry.

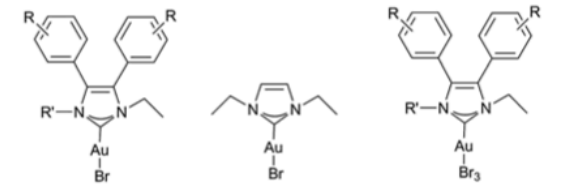

12a-j **12k** **12l,m**

Comp.	R	R'	Comp.	R	R'
a	2-MeO	Et	f, m	4-F	Et
b	3-MeO	Et	g	H	Et
c, l	4-MeO	Et	h	4-OH	Et
d	2-F	Et	i	4-MeO	$PhCH_2$
e	3-F	Et	j	4-F	$PhCH_2$

Figure 38

Besides, they decided to investigate the influence of the halide exchange at the Au–NHC complexes on their pharmacological properties [226]. They selected the 4-F and 4-OCH3 (4-OH) substituted bromo[1,3-diethyl-4,5-diarylimidazol-2-ylidene]gold(I) complexes and exchanged the bromide by a second NHC ligand (Au– bis(NHC): **13a–i**, Figure 39) to realize the concept of bivalent drugs or in relation to auranofin by 20,30,40,60-tetra-O-acetyl- b-D-glucopyranosyl-1-thiolate (**14a,b**, Figure 39) as well as a phosphine ligand (triphenylphosphine) (**14c,d**, Figure 39). Compared to Au–NHC complexes, the growth inhibitory effects of the Au–bis(NHC) complexes against breast (MCF-7 and MDA- MB 231) and colon (HT-29) cancer cells strongly increased.

This effect, which is more than 10-fold higher than that of cisplatin, is independent of the oxidation state of the metal and the anionic counter ion. Besides, the gold core seems to be responsible for the high cytotoxic

activity of cationic Au–bis(NHC) complexes, thus, the exchange of the gold center by a methylene group decreased the growth inhibitory effects.
Next, exchange of the Br ligand in bromo[1,3-diethyl-4,5-diarylimidazol-2-ylidene]gold(I) complexes by 20,30,40,60-tetra- O-acetyl-b-D-glucopyranosyl-1-thiolate almost did not increased the growth inhibitory effects against the tumor cells while the use of triphenylphosphine ligand led to a 5-fold higher activity despite the building of cationic species.
All these results indicated that the attempt to increase the antitumor potency of Au–NHC complexes was successful if the bromide ligand was exchanged by PPh3 or a further NHC ligand. The resulting complexes were more active than cisplatin with an IC50 in the low nanomolar range. In this SAR study they could demonstrated that gold complexes bearing two 1,3-diethyl- 4,5-diarylimidazol-2-ylidene ligands represented effective cytostatics with growth inhibitory effects at MCF-7, MDA-MB 231 and HT-29 cells up to 10-fold higher than cisplatin. Further investigations with selected complexes demonstrated that they were effectively accumulated in the tumor cells and located in high amounts in the nuclei.

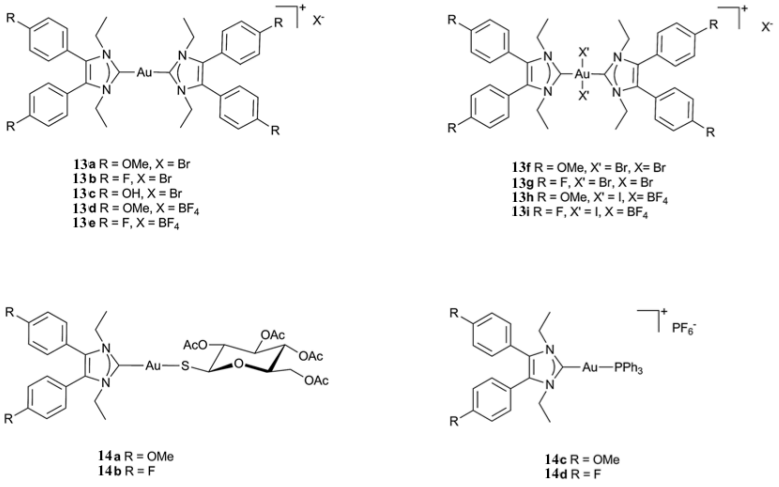

Figure 39

Chapter VI

6 Aims of the project

The increasing interest in the fields of bioorganometallic chemistry and the notable results achieved, have encouraged many groups to aim for the synthesis of new complexes with biological properties.
Over the last few years N-heterocyclic carbenes (NHCs) have entered the field as new ligands for bioactive coordination compounds.
The aim of this work is to contribute in discovering stable complexes, bearing NHC ligands and evaluate their biological properties.
For this pourpose we decided to synthesize, characterize by nuclear magnetic resonance (NMR), mass spectroscopy and elemental analysis, the NHC-ligands (Figure 40) and their respective Ag(I), Cu(I) and Au(I) complexes showed in Figure 41.
All ligands and complexes presented are racemic mixture.

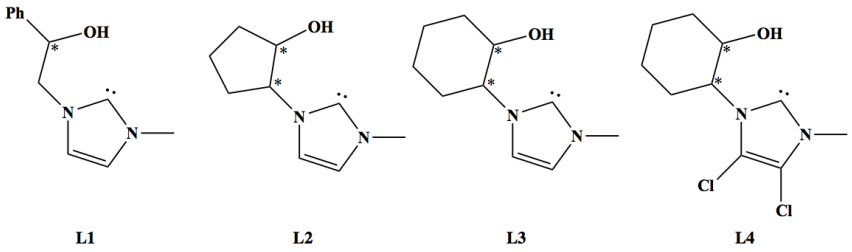

Figure 40 *Structures of synthesized proligands*

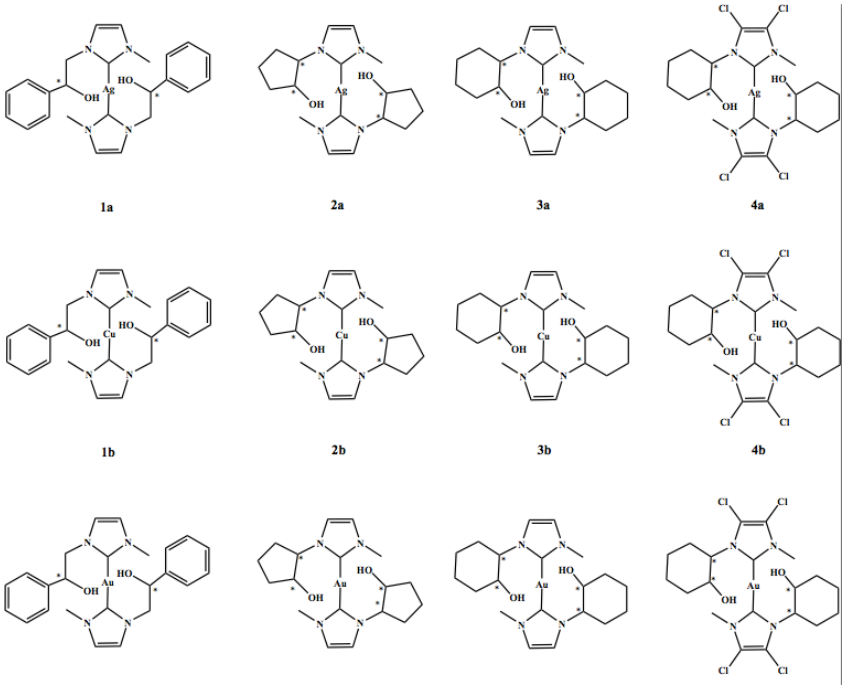

Figure 41 *Structures of synthesized complexes*

The success of metallodrugs is, however, closely interlinked with the proper choice of the ancillary ligands, as they play a crucial role in modifying reactivity and lipophilicity, in stabilizing specific oxidation states, in imparting substitution inertness, and in suppressing the adverse effect of the metal ion in order to facilitate positive impacts in the areas of diagnosis and therapy. All synthesized complexes contain different substituents on N_1 and N_2.The wingtip groups were modified in order to adjust the lipophilic character of the complexes, a critical factor for targeting malignant cells which demonstrated that the bioactivity can be influenced by fine-tuning of the lipophilicity.

Chapter VII

7 Results and discussion

7.1 Chemistry

We report the preparation and characterization of some iodide silver, copper and gold complexes stabilized by N-heterocyclic carbene ligands having an alcohol group on alkyl substituent of one of the two nitrogen atoms of the heterocycle (NHC-OH).
The three proligand are unsaturated imidazolium-N-substituted. They present the same substiuent on the N_1 and a different one on N_2. **L1** is an imidazolium-*N*-methyl-*N'*-benzyl-2-hydroxy-iodide in which there is a –benzyl-2-hydroxy group in N_2; the **L2** is a imidazolium-N-methyl- N'-cyclopentenyl-2-hydroxy-iodide in which there is a cyclopentyl-2-hydroxy group in N2 and L3 is a imidazolium-N-methyl- N'- cyclohexyl-2-hydroxy-iodide in which the N2 is functionalized with a cyclohexyl-2-hydroxy group, **L4** is a 4,5-imidazolium-*N*-methyl- *N'*- cyclohexyl-2-hydroxy-iodide in which the N_2 is functionalized with a cyclohexyl-2-hydroxy group

7.1.1 Synthesis of imidazolium salts

The synthesis of the iodide salts was carried out in the same way as reported by some of us [227], by reacting phenylethylenoxide, cyclohexene or cyclopentene oxide with imidazole, followed by addition of iodomethane in acetonitrile (Scheme 20). After distillation of the solvent, the products were purified by crystallization in acetone, obtaining the imidazolium salts as a white solid in high yield. [NHC-O] ligand L1 have one stereogenic center but L2, L3 and L4 presents two stereogenic centers that can be SS or RR, due to the nonselective trans ring opening of the epoxide produced during the synthesis. All ligands are made and used as racemates.

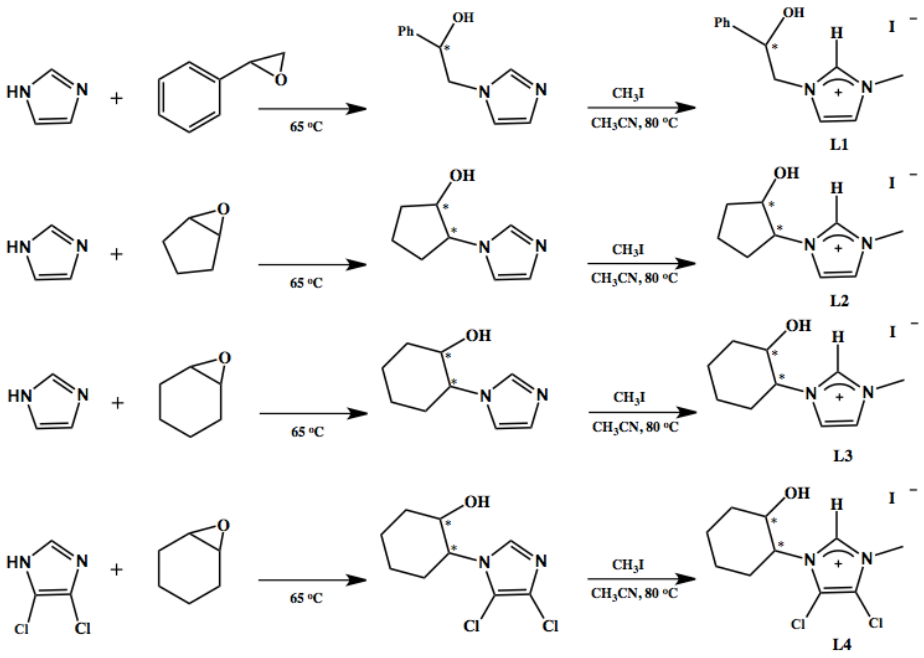

Scheme 20 *Synthetic routes for the preparation of ligands*

All imidazolium salts were characterized by H^1 and ^{13}C NMR.
As an example ^1H NMR spectrum of **L3** is reported

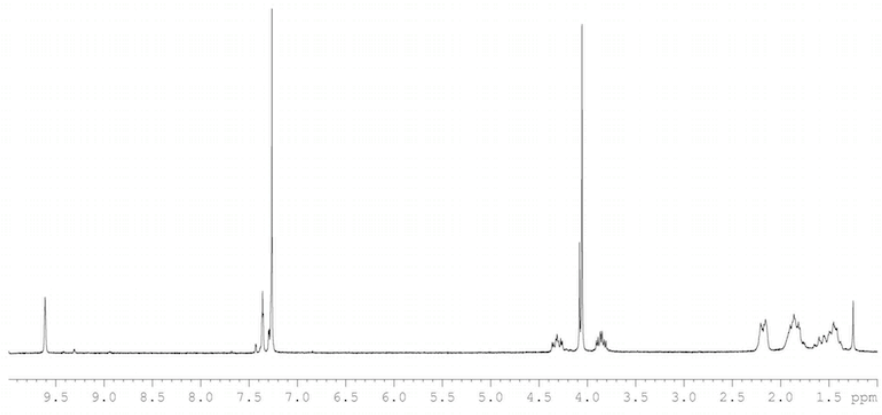

Figure 42 *^1H NMR spectrum of compound **L3***

7.1.2 Synthesis of Ag(I)-NHC complexes

Complexes **1a**, **2a** and **3a** and **4a** were synthesized by reacting the imidazolium salt with a stoichiometric amount of Ag_2O in methylene chloride and molecular sieves in darkness. Silver oxide act also as a base for the deprotonation of the imidazolium salt to the imidazolin-2-ylidene which was then stabilized by coordination to the metal center.

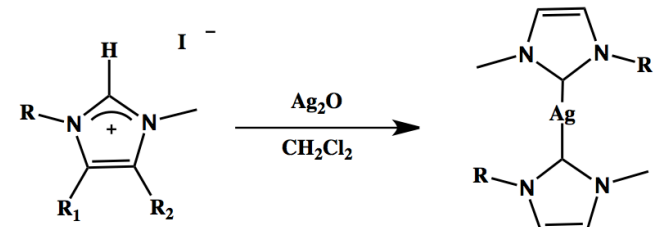

L1: R=-CH_2-CH-OH; R_1=H; R_2=H
C_6H_5
L2: R=-C_5H_9-OH; R_1=H; R_2=H
L3: R=-C_6H_{11}-OH; R_1=H; R_2=H
L4: R=-C_6H_{11}-OH; R_1=Cl; R_2=Cl

Figure 43 *Syntehtic route for the preparation of silver complexes*

All silver complexes were characterized by H^1 and ^{13}C NMR.
As an example ^1H NMR and 13C NMR spectra of **3a** are reported

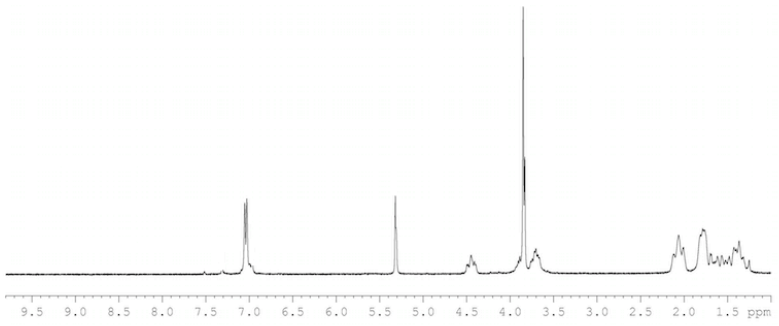

Figure 44 *^1H NMR spectrum of compound **3a***

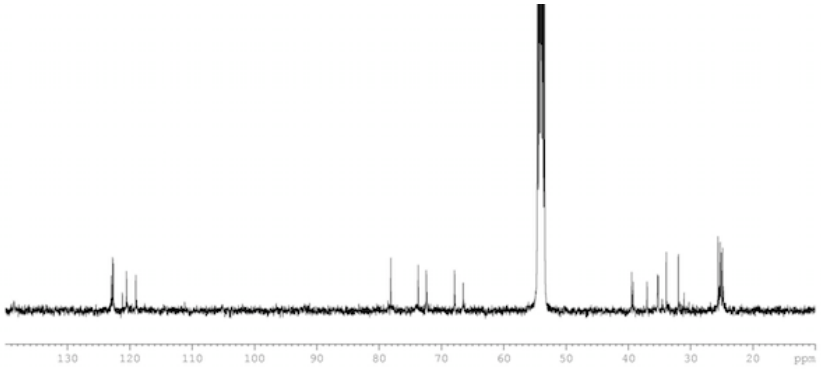

Figure 45 *^{13}C NMR spectrum of compound **3a***

7.1.3 Synthesis of Cu(I)-NHC complexes

Complexes **1b**, **2b**, **3b** and **4b** were synthesized by reacting the imidazolium salt with an excess of base (Lithium HexaMethylDiSilazide) in tetrahydrofurane. After stirring for 1 hour a solution of CuCl in acetonitrile was added. After stirring at room temperature over night was filtered through celite and the solvent removed by distillation to afford the complexes as a violet solid in high yelds.

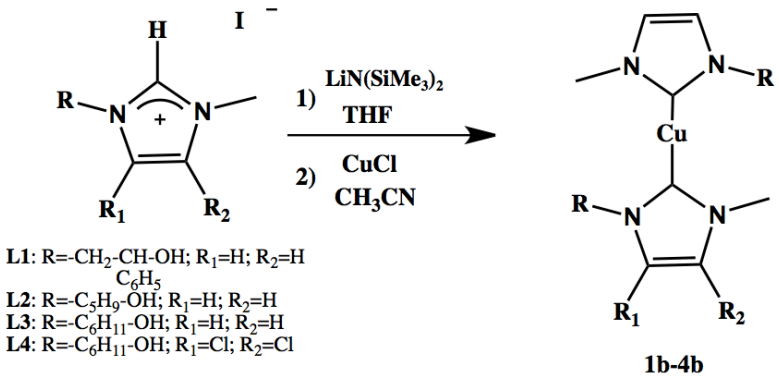

L1: R=-CH_2-CH-OH; R_1=H; R_2=H
C_6H_5
L2: R=-C_5H_9-OH; R_1=H; R_2=H
L3: R=-C_6H_{11}-OH; R_1=H; R_2=H
L4: R=-C_6H_{11}-OH; R_1=Cl; R_2=Cl

Figure 46 *Synthetic route for the preparation of copper complexes*

All copper complexes were characterized by H^1 and ^{13}C NMR.
As an example ^1H NMR and 13C NMR spectra of **3b** are reported.

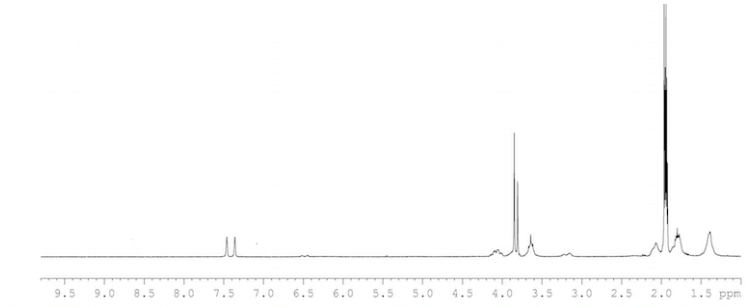

Figure 47 *^{1}H NMR spectrum of compound **3b***

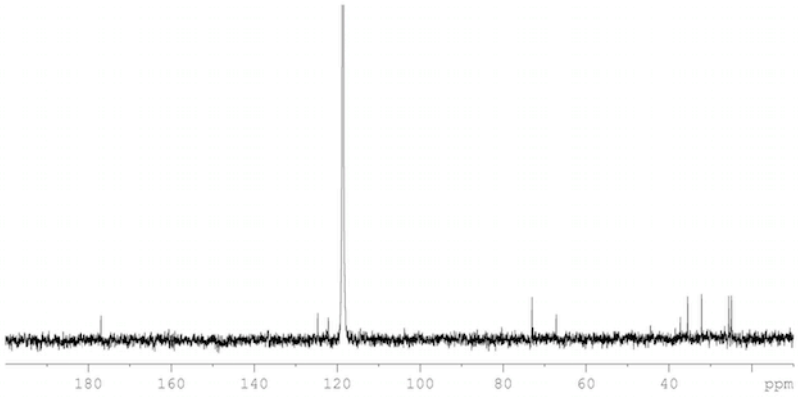

Figure 48 *^{13}C NMR spectrum of compound **3b***

7.1.4 Synthesis of Gold(I)-NHC complexes

Complexes **1c**, **2c, 3c** and **4c** were synthesized through a trasmetallation of the each silver complexes and Me_2SAuCl. In a solution containing an equimolar amount of silver complexes was added Me_2SauCl. The resulting mixture was stirred in methylene chloride at room temperature for 4 hours. The suspension thus obtained was filtered, the filtered was

dried in vacuo and washed in hexane. A yellow solid was obtained in good yields.

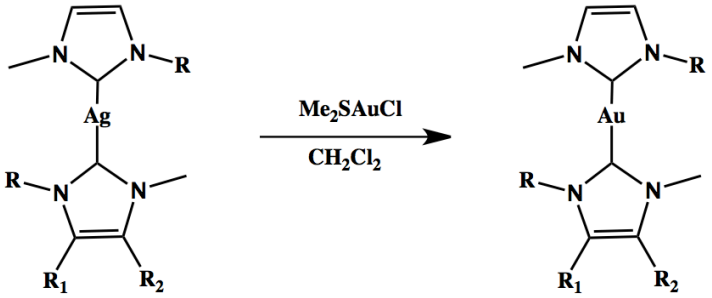

1c-4c

Figure 49 Synthetic route for the preparation of gold complexes

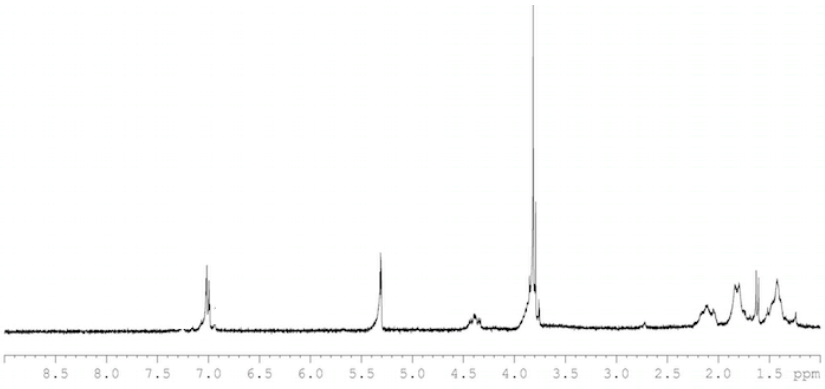

Figure 50 *^{1}H NMR spectrum of compound **3c***

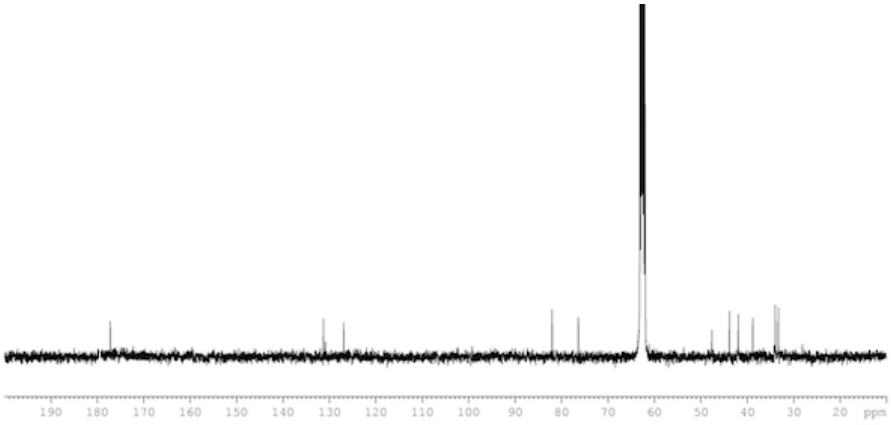

Figure 51 *^{13}C NMR spectrum of compound **3c***

Chapter VIII

8 Experimental section

8.1 Chemistry

All reagents and solvents were purchased from Sigma-Aldrich s.r.l. (Milan, Italy).
^{1}H NMR and ^{13}C NMR spectra were recorded at 298 K on a Bruker Avance 300 Spectrometer operating at 300 MHz (^{1}H) and 75 MHz (^{13}C) and referred to internal tetramethylsilane.

8.2 Synthesis of imidazolium-N-methyl-N'-benzyl-2-hydroxy-iodide (L1)

Imidazole (6 g, 0,088 mol.) was added to a stoichiometric amount of phenylethylenoxide (10,59 g, 0,088 mol.) and left stirring overnight at 65°C. After this time a solution of iodomethane (12,50g, 0,088 mol.) in acetonitrile (25 ml) was added and the suspension stirred for additional 5h at 80°C. After removing the solvent in vacuo, the crude product was obtained as a yellow oil.
The pure product was precipitated as white solid by adding cool acetone and isolated in good yield.

Yield: 70%.

^{1}H NMR (d ppm, DMSO): 8.23 (s, 1H, NC*H*N); 6.84 (d, 1H, NC*H*CHN); 6.82 (d, 1H, NCHC*H*N); 6.60-6.40 (m, 5H, Ph ring); 5.10 (d, 1H, OH); 4.11 (dd, 1H, OCH); 3.60-3.10 (m, 2H, NCH_2); 3.01 (s, 3H, NCH_3).

^{13}C NMR (d ppm, DMSO): 136.9 (N*C*HN), 123.0 (N*C*HCHN), 123.0 (NCH*C*HN), 128.3, 141.2, 128.3, 127.8, 125.9 (Carbons of Ph ring); 70.6 (O*C*H), 55.6(N*C*H_2), 35.8 (N*C*H_3).

8.3 Synthesis of imidazolium-N-methyl-N'-cyclopentyl-2-hydroxy-iodide (L2)

Imidazole (6,8 g, 0,099 mol.) was added to a stoichiometric amount of cyclopentane oxide (8,40 g, 0,099 mol.) and left stirring overnight at 65°C. After this time a solution of iodomethane (14,16g, 0,099 mol.) in acetonitrile (25 ml) was added and the suspension stirred for additional 5h at 80°C. After removing the solvent in vacuo, the crude product was obtained as a yellow oil.
The pure product was precipitated as white solid by adding cool acetone and isolated in good yield.

Yield: 76%.

^{1}H NMR (d ppm CD_3CN): 8.68 (s, 1H, NC*H*N), 7.40 (s,1H, NC*H*CH), 7.32 (s, 1H, NCHC*H*), 4.37 (m, 1H, OC*H*), 4.34 (m, 1H, NC*H*), 3.78 (s, 3H, NCH_3), 2.25 (m, 2H, $OCHCH_2$), 2.01 (m, 2H, $NCHCH_2$), 1.64 (m, 2H, $CH_2CH_2CH_2$)
^{13}C NMR (d ppm CD_3CN): 136.6 (N*C*HN), 125.6 (N*C*HCH,) 121.7 (NCH*C*H), 77.4 (O*C*H), 67.3 (N*C*H), 46.3 (NCH_3),32.0 ($OCHCH_2$), 26.8 ($NCHCH_2$), 19.3 ($CH_2CH_2CH_2$).

8.4 Synthesis of imidazolium-N-methyl-N'-cyclohexenyl-2-hydroxy-iodide (L3)

Imidazole (6 g, 0,088 mol.) was added to a stoichiometric amount of cyclohexene oxide (8,64 g, 0,088 mol.) and left stirring overnight at 65°C. After this time a solution of iodomethane (12,50g, 0,088 mol.) in acetonitrile (25 ml) was added and the suspension stirred for additional 5h at 80°C. After removing the solvent in vacuo, the crude product was obtained as a yellow oil.
The pure product was precipitated as white solid by adding cool acetone and isolated in good yield.

Yield: 60%.

^{1}H NMR (d ppm $CDCl_3$): 9.60 (s, 1H, NC*H*N), 7.40 (s,1H, NC*H*CH), 7.32 (s, 1H, NCHC*H*), 4.31 (m, 1H, OC*H*), 4.34 (m, 1H, NC*H*), 3.84 (s, 3H, NCH_3), 2.25 (m, 2H, $OCHCH_2$), 2.01 (m, 2H, $NCHCH_2$), 1.64 (m, 2H, $OCHCH_2CH_2$), 1.24 (m, 2H, $NCHCH_2CH_2$).

^{13}C NMR (d ppm $CDCl_3$): 136.6 (N*C*HN), 125.6 (N*C*HCH,) 121.7 (NCH*C*H), 77.4 (O*C*H), 67.3 (N*C*H), 46.3 (NCH_3), 32.0 ($OCHCH_2$), 30.0 ($NCHCH_2CH_2$), 26.8 ($NCHCH_2$), 22.3 ($OCHCH_2CH_2$).

8.5 Synthesis of imidazolium 4,5-dichloro-N-methyl-N'-cyclohexenyl-2-hydroxy- iodide (L4)

4,5-dichloro-imidazole (5 g, 0,0365 mol.) was added to a stoichiometric amount of cyclohexene oxide (3,58 g, 0,0365 mol.) and left stirring overnight at 65°C. After this time a solution of iodomethane (5,18 g 0,0365 mol.) in acetonitrile (25 ml) was added and the suspension stirred for additional 5h at 80°C. After removing the solvent in vacuo, the crude product was obtained as a yellow oil.
The pure product was precipitated as white solid by adding cool acetone and isolated in good yield.

Yield: 60%.

^{1}H NMR (d ppm $CDCl_3$): 9.60 (s, 1H, NC*H*N), 4.31 (m, 1H, OC*H*), 4.34 (m, 1H, NC*H*), 3.84 (s, 3H, NCH_3), 2.25 (m, 2H, $OCHCH_2$), 2.01 (m, 2H, $NCHCH_2$), 1.64 (m, 2H, $OCHCH_2CH_2$), 1.24 (m, 2H, $NCHCH_2CH_2$).

^{13}C NMR (d ppm $CDCl_3$): 136.6 (N*C*HN), 125.6 (N*C*HCH,) 121.7 (NCH*C*H), 77.4 (O*C*H), 67.3 (N*C*H), 46.3 (NCH_3), 32.0 ($OCHCH_2$), 30.0 ($NCHCH_2CH_2$), 26.8 ($NCHCH_2$), 22.3 ($OCHCH_2CH_2$).

8.6 Synthesis of Silver complex 1a

To a suspension of imidazolium salt (L1 $1{,}51*10^{-3}$* mol) in CH_2Cl_2 and molecular sieves, an excess of solid silver(I) oxide ($2{,}27*10^{-3}$ mmol) was added under N_2 atmosphere and stirred for 2 hours at 45°C under

protection from light. After this time the mixture was filtered through celite and the solvent removed in vacuo. The pure product was recovered as a white powder.

Yield: 53,30 %
^{1}H NMR (ppm CD_2Cl_2): 7.25-7.40 (m, 5H, Ph ring); 6.90 (d, 1H, NC*H*CHN); 6.84 (d, 1H, NCHC*H*N); 5.19 (t, 1H, C*H*OH); 4.39 (d, 2H, NCH_2); 3.86 (s, 3H, NCH_3).

^{13}C NMR (ppm CD_2Cl_2): 185.3 (N*C*N); 141.8, 129.2, 128.6, 126.6 (Ph ring); 122.9 (N*C*HCHN), 122.0 (NCH*C*HN), 73.7 (O*C*H_2), 59.3 (N*C*H_2), 39.2 (N*C*H_3).

Mass spectrum: 513 $[Ag(L1)_2]^+$

8.7 Synthesis of Silver complex 2a

To a suspension of imidazolium salt (L2 5,48*10^{-3} mol) in CH_2Cl_2 and molecular sieves, an excess of solid silver(I) oxide (8,23*10^{-3} mmol) was added under N_2 atmosphere and stirred for 2 hours at 45°C under protection from light. After this time the mixture was filtered through celite and the solvent removed in vacuo. The pure product was recovered as a white powder.

Yield: 43,30 %
^{1}H NMR (d ppm CD_2Cl_2): 6.99 (s,1H, NC*H*CH), 7.05 (s, 1H, NCHC*H*), 4.41 (m, 1H, OC*H*), 4.34 (m, 1H, NC*H*), 3.80 (s, 3H, NCH_3), 2.11 (m, 2H, OCHCH_2), 2.08 (m, 2H, NCHCH_2), 1.36 (m, 2H, $CH_2CH_2CH_2$)
^{13}C NMR (d ppm CD_2Cl_2): 182.0 (N*C*N), 121.1 (NCHCH,) 119.0 (NCHCH), 78.1 (OCH), 67.5 (NCH), 39.4 (NCH3),36.9 (OCH*C*H_2), 31.0 (NCH*C*H_2), 26.3 ($CH_2CH_2CH_2$).
Mass spectrum: 441 $[Ag(L2)_2]^+$

8.8 Synthesis of Silver complex 3a

To a suspension of imidazolium salt (L3 6,778*10-3 mol) in CH_2Cl_2 and molecular sieves, an excess of solid silver(I) oxide (10,16*10^{-3} mmol) was added under N_2 atmosphere and stirred for 2 hours at 45°C under protection from light. After this time the mixture was filtered through celite and the solvent removed in vacuo. The pure product was recovered as a white powder.

Yield: 49,70 %
^{1}H NMR (d ppm CD_2Cl_2): 7.39 (s,1H, NC*H*CH), 7.13 (s, 1H, NCHC*H*), 5.43 (m, 1H, OC*H*), 5.12 (m, 1H, NC*H*), 4.00 (s, 3H, NCH_3), 2.49 (m, 2H, OCHCH_2), 2.24 (m, 2H, NCHCH_2), 2.01 (m, 2H, OCHCH$_2$CH_2), 1.96 (m, 2H, NCHCH$_2$CH_2).

^{13}C NMR (d ppm $CDCl_3$): 178.9 (N*C*N), 122.6 (N*C*HCH,) 120.7 (NCH*C*H), 71.4 (O*C*H), 67.0 (N*C*H), 40.0 (N*C*H$_3$), 35.0 (OCH*C*H$_2$), 33.0 (NCHCH$_2$CH_2), 24.8 (NCH*C*H$_2$), 23.9 (OCHCH$_2$CH_2).

Mass spectrum: 469 $[Ag(L3)_2]^+$

8.9 Synthesis of Silver complex 4a

To a suspension of imidazolium salt (L4 6,778*10-3 mol) in CH_2Cl_2 and molecular sieves, an excess of solid silver(I) oxide (10,16*10^{-3} mmol) was added under N_2 atmosphere and stirred for 2 hours at 45°C under protection from light. After this time the mixture was filtered through celite and the solvent removed in vacuo. The pure product was recovered as a white powder.

Yield: 60 %
^{1}H NMR (d ppm CD_2Cl_2): 5.43 (m, 1H, OC*H*), 5.12 (m, 1H, NC*H*), 4.00 (s, 3H, NCH_3), 2.49 (m, 2H, OCHCH_2), 2.24 (m, 2H, NCHCH_2), 2.01 (m, 2H, OCHCH$_2$CH_2), 1.96 (m, 2H, NCHCH$_2$CH_2).

^{13}C NMR (d ppm $CDCl_3$): 178.9 (N*C*N), 122.6 (N*C*HCH,) 120.7 (NCH*C*H), 71.4 (O*C*H), 67.0 (N*C*H), 40.0 (N*C*H_3), 35.0 (OCH*C*H_2), 33.0 (NCHCH$_2$C*H*$_2$), 24.8 (NCH*C*H_2), 23.9 (OCHCH$_2$C*H*$_2$).

Mass spectrum: 605 $[Ag(L3)_2]^+$

8.10 Synthesis of Copper complex 1b

LiHMDS (557 mg, $3{,}33*10^{-3}$ mol) was added to a solution of the imidazolium salt (L1 $3{,}02*10^{-3}$ mol) in THF. After the resulting mixture was stirred for 1 hour a solution of CuCl ($3{,}02*10^{-3}$ mol) in CH_3CN was added and the suspension stirred for additional 12 hours. Then the mixture was filtered through celite and the solvent removed in vacuo. The crude product was washed with hexane and recovered as a violet powder.

Yield: 43%

^{1}H NMR (ppm CD_2Cl_2): 7.35-7.52 (m, 5H, Ph ring); 6.93 (d, 1H, NC*H*CHN); 6.84 (d, 1H, NCHC*H*N); 5.19 (t, 1H, C*H*OH); 4.49 (d, 2H, NCH_2); 3.90 (s, 3H, NCH_3).

^{13}C NMR (ppm CD_2Cl_2): 185.0 (N*C*N); 141.8, 129.2, 127.5, 126.6 (Ph ring); 122.9 (N*C*HCHN), 122.0 (NCH*C*HN), 75.2 (O*C*H_2), 59.3 (N*C*H_2), 41.0 (N*C*H_3).

Mass spectrum: 469 $[Cu(L1)_2]^+$

8.11 Synthesis of Copper complex 2b

LiHMDS (594 mg, $3{,}55*10^{-3}$ mol) was added to a solution of the imidazolium salt (L2 $3{,}23*10^{-3}$ mol) in THF. After the resulting mixture was stirred for 1 hour a solution of CuCl ($3{,}23*10^{-3}$ mol) in CH_3CN was added and the suspension stirred for additional 12 hours. Then the mixture was filtered through celite and the solvent removed in vacuo. The crude product was washed with hexane and recovered as a violet powder.

Yield: 59,63%

^{1}H NMR (d ppm CD_2Cl_2): 7.08 (s,1H, NC*H*CH), 7.45 (s, 1H, NCHC*H*), 4.41 (m, 1H, OC*H*), 4.09 (m, 1H, NC*H*), 3.80 (s, 3H, NCH_3), 2.11 (m, 2H, OCHCH_2), 2.06 (m, 2H, NCHCH_2), 1.38 (m, 2H, $CH_2CH_2CH_2$)
^{13}C NMR (d ppm CD_2Cl_2): 182.0 (N*C*N), 124.5 (N*C*HCH,) 122.0 (NCH*C*H), 72.9 (O*C*H), 67.5 (N*C*H), 38.6 (NCH_3), 36.9 (OCH*C*H_2), 31.0 (NCH*C*H_2), 26.3 ($CH_2CH_2CH_2$).
Mass spectrum: 397 $[Cu(L2)_2]^+$

8.12 Synthesis of Copper complex 3b

LiHMDS (621 mg, $3{,}71*10^{-3}$ mol) was added to a solution of the imidazolium salt (L3 $3{,}39*10^{-3}$ mol) in THF. After the resulting mixture was stirred for 1 hour a solution of CuCl ($3{,}39*10^{-3}$ mol) in CH_3CN was added and the suspension stirred for additional 12 hours. Then the mixture was filtered through celite and the solvent removed in vacuo. The crude product was washed with hexane and recovered as a violet powder.

Yield: 40%

^{1}H NMR (d ppm CD_2Cl_2): 7.45 (s,1H, NC*H*CH), 7.35 (s, 1H, NCHC*H*), 4.15 (m, 1H, OC*H*), 3.62 (m, 1H, NC*H*), 3.79 (s, 3H, NCH_3), 2.49 (m, 2H, OCHCH_2), 2.16 (m, 2H, NCHCH_2), 2.01 (m, 2H, $OCHCH_2CH_2$), 1.54 (m, 2H, $NCHCH_2CH_2$).

^{13}C NMR (d ppm $CDCl_3$): 178.9 (N*C*N), 124.5 (N*C*HCH,) 122.4 (NCH*C*H), 72.9 (O*C*H), 67.4 (N*C*H), 40.0 (NCH_3), 35.6 (OCH*C*H_2), 32.1 ($NCHCH_2CH_2$), 25.6 (NCH*C*H_2), 24.9 ($OCHCH_2CH_2$).

Mass spectrum: 425 $[Cu(L3)_2]^+$

8.13 Synthesis of Copper complex 4b

LiHMDS (470 mg, $2{,}91*10^{-3}$ mol) was added to a solution of the imidazolium salt (L4 $2{,}65*10^{-3}$ mol) in THF. After the resulting mixture

was stirred for 1 hour a solution of CuCl ($2{,}65*10^{-3}$ mol) in CH_3CN was added and the suspension stirred for additional 12 hours. Then the mixture was filtered through celite and the solvent removed in vacuo. The crude product was washed with hexane and recovered as a violet powder.

Yield: 40%

^{1}H NMR (d ppm CD_2Cl_2): 5.75 (m, 1H, OC*H*), 4.58 (m, 1H, NC*H*), 3.79 (s, 3H, NCH_3), 2.49 (m, 2H, OCHCH_2), 2.16 (m, 2H, NCHCH_2), 2.01 (m, 2H, OCHCH$_2$CH_2), 1.54 (m, 2H, NCHCH$_2$CH_2).

^{13}C NMR (d ppm $CDCl_3$): 178.9 (N*C*N), 124.5 (N*C*HCH,) 122.4 (NCH*C*H), 72.9 (O*C*H), 67.4 (N*C*H), 40.0 (NCH_3), 35.6 (OCHCH_2), 32.1 (NCHCH$_2$CH_2), 25.6 (NCHCH_2), 24.9 (OCHCH$_2$CH_2).

Mass spectrum: 561 $[Cu(L3)_2]^+$

8.14 Synthesis of Gold complex 1c

To a solution of the silver complex **1a** ($5{,}32*10^{-4}$ mol) in CH_2Cl_2 a stoichiometric ammount of $AuCl(SMe_2)$ was added. The mixture was left to stirr for 4 hours at room temperature. After this time was filtered through celite and the solvent was removed in vacuo. The crude product was washed in hexane to obtain a yellow powder.

Yield: 71,81%
^{1}H NMR (ppm CD_2Cl_2): 7.31-7.41 (m, 5H, Ph ring); 7.05 (d, 1H, NC*H*CHN); 6.99 (d, 1H, NCHC*H*N); 4.31 (t, 1H, C*H*OH); 3.94 (d, 2H, NCH_2); 3.71 (s, 3H, NCH_3).
^{13}C NMR (ppm CD_2Cl_2): 185.0 (N*C*N); 141.8, 129.2, 127.5, 126.6 (Ph ring); 122.9 (N*C*HCHN), 122.0 (NCH*C*HN), 75.2 (O*C*H$_2$), 59.3 (N*C*H$_2$), 41.0 (N*C*H$_3$).

Mass spectrum: 603 $[Au(L1)_2]^+$

8.15 Synthesis of Gold complex 2c

To a solution of the silver complex **2a** ($7{,}21*10^{-4}$ mol) in CH_2Cl_2 a stoichiometric ammount of $AuCl(SMe_2)$ was added. The mixture was left to stirr for 4 hours at room temperature. After this time was filtered through celite and the solvent was removed in vacuo. The crude product was washed in hexane to obtain a yellow oil.

Yield: 46,68%

^{1}H NMR (d ppm CD_2Cl_2): 6.94 (s,1H, NC*H*CH), 7.01 (s, 1H, NCHC*H*), 4.81 (m, 1H, OC*H*), 4.47 (m, 1H, NC*H*), 3.83 (s, 3H, NCH_3), 2.56 (m, 2H, $OCHCH_2$), 2.24 (m, 2H, $NCHCH_2$), 1.75 (m, 2H, $CH_2CH_2CH_2$)

^{13}C NMR (d ppm CD_2Cl_2): 169.5 (N*C*N), 124.5 (N*C*HCH,) 122.0 (NCH*C*H), 78.4 (O*C*H), 69.5 (N*C*H), 45.6 (NCH_3), 39.9 ($OCHCH_2$), 34.0 ($NCHCH_2$), 28.2 ($CH_2CH_2CH_2$).
Mass spectrum: 531 $[Au(L2)_2]^+$

8.16 Synthesis of Gold complex 3c

To a solution of the silver complex **3a** ($1{,}25*10^{-3}$ mol) in CH_2Cl_2 a stoichiometric amount of $AuCl(SMe_2)$ was added. The mixture was left to stir for 4 hours at room temperature. After this time was filtered through celite and the solvent was removed in vacuo. The crude product was washed in hexane to obtain a yellow powder.
Yield: 49,85%

^{1}H NMR (d ppm CD_2Cl_2): 6.99 (s,1H, NC*H*CH), 7.01 (s, 1H, NCHC*H*), 5,48 (s, 1H, O*H*CH) 4.48 (m, 1H, OC*H*), 3.62 (m, 1H, NC*H*), 3.69 (s, 3H, NCH_3), 2.29 (m, 2H, $OCHCH_2$), 2.00 (m, 2H, $NCHCH_2$), 1.57 (m, 2H, $OCHCH_2CH_2$), 1.40 (m, 2H, $NCHCH_2CH_2$).

^{13}C NMR (d ppm $CDCl_3$): 178.9 (N*C*N), 131.5 (N*C*HCH,) 126.9 (NCH*C*H), 72.9 (O*C*H), 67.4 (N*C*H), 43.8 (NCH_3), 41.9 ($OCHCH_2$), 35.1 ($NCHCH_2CH_2$), 33.2 ($NCHCH_2$), 26.8 ($OCHCH_2CH_2$).
Mass spectrum: 559 $[Au(L3)_2]^+$

8.17 Synthesis of Gold complex 4c

To a solution of the silver complex **4a** ($1{,}25*10^{-3}$ mol) in CH_2Cl_2 a stoichiometric amount of $AuCl(SMe_2)$ was added. The mixture was left to stir for 4 hours at room temperature. After this time was filtered through celite and the solvent was removed in vacuo. The crude product was washed in hexane to obtain a yellow powder.

Yield: 65,76%
^{1}H NMR (d ppm CD_2Cl_2): 4.70 (m, 1H, OC*H*), 4.48 (m, 1H, NCH), 3.79 (s, 3H, NCH3), 2.49 (m, 2H, OCHCH2), 2.11 (m, 2H, NCHCH2), 2.01 (m, 2H, $OCHCH_2CH_2$), 1.43 (m, 2H, $NCHCH_2CH_2$).

^{13}C NMR (d ppm $CDCl_3$): 178.9 (N*C*N), 131.5 (N*C*HCH,) 126.9 (NCH*C*H), 72.9 (O*C*H), 67.4 (N*C*H), 43.8 (NCH_3), 41.9 ($OCHCH_2$), 35.1 ($NCHCH_2CH_2$), 33.2 ($NCHCH_2$), 26.8 ($OCHCH_2CH_2$).
Mass spectrum: 695 $[Au(L4)_2]^+$

Conclusions (2)

In this second section, synthesis and characterization of some iodide silver, copper and gold complexes stabilized by N-heterocyclic carbene ligands having an alcohol group on alkyl substituent of one of the two nitrogen atoms of the heterocycle (NHC-OH) are reported.
All synthesized ligands and their silver, copper and gold complexes were characterized by NMR analysis and the mass spectroscopy.
Biological studies, such as antimicrobial and cytotoxicity assays, are ongoing.

References

[1] Y.W., M.J. Balunas, H.B. Chai and A.D. Kinghorn, Chin, *Drug Discovery From Natural Sources.* , vol. 8, no. 2, pp. 239-253 , 2006.

[2] G.A., M.L. Quinn-Beattie and N.R. Farnsworth, Cordell, "The potential of alkaloids in drug discovery ," *Phytother Res.* , vol. 15, no. 3, pp. 183-205 , 2001.

[3] E.H. and J.V. Shanks, Hughes, "Metabolic engineering of plants for alkaloid production ," *Metab. Eng.* , vol. 4, no. 1, pp. 41-48 , 2002.

[4] J.A. and K. Mills Joule, "Heterocyclic Chemistry, 4th Ed. ," *Blackwell Publishing* , p. 369 , 2000.

[5] F.E. and G.T. Carter, Koehn, "The evolving role of natural products in drug discovery.," *Nat. Rev. Drug Discov.*, vol. 4, pp. 206-209, 2005.

[6] A. Mittal, "Synthetic Nitroimidazoles: Biological Activities and Mutagenicity Relationships ," *Sci. Pharm.*, vol. 77, pp. 497-520 , 2009.

[7] G. Nagalakshmi, "Synthesis, Antimicrobial and Antiinflammatory Activity of 2,5 Disubstituted-1,3,4- oxadiazoles," *Indian J. Pharm. Sci.*, vol. 70, pp. 49-55, 2008.

[8] D.D. Nekrasov, "Biological Activity of 5- and 6- Membered Azaheterocycles and Their Synthesis from 5-Aryl-2, 3-Dihydrofuran-2,3-diones ," vol. 37, pp. 263-275 , 2001.

[9] J.B. and D.L. Wright Sperry, "Furans, thiophenes and related heterocycles in drug discovery ," *Current Opinion in Drug Discovery and Development*, vol. 8, pp. 723-740 , 2005.

[10] K. A. Brameld, J. Graton, J.-Y. Le Questel, and E. Renault C. Laurence, *J. Med. Chem* , vol. 52, p. 4073 , 2009.

[11] Hans-Joachim Kno¨lker and Kethiri R. Reddy, *Chem. Rev.* , vol. 102, p. 4303−4427 , 2002.

[12] V. Peciuraite, S. Grigalevicius, J. Simokaitiene, and J. V. J. Photoch Grazulevicius, *Photobio* , vol. 182 , p. 38, 2006.

[13] O. D. Is, F. B. Koyuncu, S. Koyuncu, and E. Ozdemir, *Polymer* , vol. 51, p. 1663, 2010.

[14] K. Srinivas et al., *Synth. Met.* , vol. 161, p. 96, 2011.

[15] K. S. Lee et al., "Mater. Sci.," vol. 46, p. 1239, 2011.

[16] L. Wang et al., *Polymer*, vol. 52, p. 1748, 2011.

[17] R. M. Adhikari, D. C. Neckers, and B. K. J. Shah, *Org. Chem.*, vol. 74, p. 3341, 2009.

[18] D. Tsvelikhovsky and S. L. J. Am Buch- wald, "Chem. Soc.," vol. 133, p. 14228 , 2011.

[19] Amit Kumar Jana, Dipakranjan Mal Joyeeta Roy, *Tetrahedron* , vol. 68, pp. 6099-6121 , 2012.

[20] H. J. Knolker, *Chem. Lett.*, vol. 38, p. 8, 2009.

[21] H. J. Knolker and K. R. Reddy, *Chem. Rev.*, vol. 102, p. 4303, 2002.

[22] P. Bhattacharyya and D. P Chakraborty, *In Progress in the Chemistry of Organic Natural Products* , vol. 52, p. 159, 1987.

[23] B. K. Chowdhury, A. Mustafa, M. Graba, and P Bhattacharyya, *Phytochemistry* , vol. 26, p. 2138, 1988.

[24] D. P. Chakraborty, *In Progress in the Chemistry of Organic Natural Products* , vol. 34, p. 299, 1977.

[25] S. Roy, P. Bhattacharyya, and D. P. Chakraborty, *Phytochemistry* , vol. 13, p. 1071, 1974.

[26] B. S. Joshi, V. N. Kamat, D. H. Gawad, and T. R. Govindachari, *Phytochemistry* , vol. 11, p. 2065, 1974.

[27] S. Ray and D. P. Chakraborty, *Phytochemistry* , vol. 15, p. 356, 1976.

[28] S. P. Kureel, R. S. Kapil, and S. P Popli, *Chemm. Commun.*, p. 1120, 1969.

[29] P. Bhattacharyya and B.K. Chowdhury, *ndian J.Chem* , vol. 24, p. 452, 1985.

[30] P. Bhattacharyya and A. Chakraborty, *Phytochemistry* , vol. 23, p. 471, 1984.

[31] D.P. Chakraborty, S. Roy, and R Guha, *J.IndianChem.Soc.* , vol.

75, p. 1114, 1978.

[32] J. L. et al Arbiser, *J. Invest. Dermatol.* , vol. 126, pp. 1396–1402 , 2006.

[33] Chiara Palladino , Mariagrazia Napoli , Maria Stefania Sinicropi , Antonio Botta , Marina Sala , Alessandra Carcereri de Prati , Ettore Novellino , Hisanori Suzuki Carmela Saturnino, *Eur. J. Med. Chem.* , vol. 60c, pp. 112-119, 2012.

[34] Darnell Jr JE, *Science*, vol. 1997, pp. 1630-1635 , 277.

[35] Horvath CM and Darnell Jr JE., *Curr. Opin. Cell. Biol* , vol. 9, pp. 233-239, 1997.

[36] Kerr I, Williams B, Silverman R and Schreiber R Stark G, *Annu. Rev. Biochem.*, vol. 67, pp. 227-264 , 1998.

[37] Akira S., *Oncogene*, vol. 2000, pp. 2607-2611 , 19.

[38] Briggs SD, Schreiner S, Lerner EC, Cheng H and Wilson MB. Smithgall TE, *Oncogene*, vol. 19, pp. 2612-2618 , 2000.

[39] J. & Darnell, J. E. Jr. Bromberg, *Oncogene* , vol. 19, pp. 2468–2473 , 2000.

[40] L., Souckova, K. & Kovarik, J. Adamkova, *Folia Biol.* , vol. 53, pp. 1-7, 2007.

[41] S. J. et al. Szabo, *Annu. Rev. Immunol.* , vol. 21, pp. 713–758 , 2003.

[42] M. A. et al. Meraz, *Cell.*, vol. 84, pp. 431-442, 1996.

[43] S. et al. Agrawal, *Circulation*, vol. 115, pp. 2939–2947 , 2007.

[44] L. et al Liu, *J. Exp. Med* , vol. 208, pp. 1635-1648, 2011.

[45] A. M. et al Gamero, *Cancer Prev. Res.* , vol. 3, pp. 495-504, 2010.

[46] K. et al. Takeda, *Proc. Natl Acad. Sci. USA* , vol. 94, pp. 3801-3804, 1997.

[47] S. Akira, *Stem. Cells*, vol. 17, pp. 138-146, 1999.

[48] K. et al. Takeda, *J. Immunol.*, vol. 161, pp. 4652–4660 , 1998.

[49] S. et al. Sano, *EMBO J.*, vol. 18, pp. 4657–4668 , 1999.

[50] E., Rao, D. & Digiovanni, J. Macias, *J. Skin Cancer* , 2013.

[51] T. et al Bowman, *Oncogene*, vol. 19, pp. 2474–2488 , 2000.

[52] J. E. Darnell, *Nature Med.*, vol. 11, pp. 595–596 , 2005.

[53] N. & Tweardy, D. J. Jing, *Anticancer Drugs*, vol. 16, pp. 601-607, 2005.

[54] H. & R. Jove, Yu, *Nature Rev. Cancer*, vol. 6, pp. 97-105, 2004.

[55] R., Mora, L. B. & Jove, R. Buettner, *Clin. Cancer Res.*, vol. 8, pp. 945-954, 2002.

[56] M. et al Kortylewski, *Nature Med* , vol. 11, pp. 1314–1321 , 2005.

[57] T. et al. Wang, *Nature Med.*, vol. 10, pp. 48-54, 2004.

[58] K. et al. Siddiquee, *Proc. Natl Acad. Sci* , vol. 104, pp. 7391–7396 , 2007.

[59] M. et al. Sen, *Cancer Chemother. Pharmacol.* , vol. 63, pp. 983–995 , 2009.

[60] H. L. et al. Koskela, *N. Engl. J. Med* , vol. 366, pp. 1905-1913, 2012.

[61] T. H., Jakobsen, M. A. & Larsen, C. S. Mogensen, *Scand. J. Infect. Dis.* , vol. 45, pp. 235-238, 2013.

[62] A. E., Yang, Y. & Racke, M. K. Lovett-Racke, *Biochim. Biophys. Acta* , vol. 1812, pp. 246-251, 2011.

[63] J. et al. Menke, *Kidney Int.*, vol. 79, pp. 452-463, 2011.

[64] J. X. & Leonard, W. J Lin, *Oncogene*, vol. 17, pp. 2566–2576 , 2000.

[65] M. et al. Buitenhuis, *Blood*, vol. 2003, pp. 134-142, 101.

[66] G. B. et al Udy, *Proc. Natl Acad. Sci.* , vol. 94, pp. 7239–7244 , 1997.

[67] K. et al. Imada, *J. Exp. Med* , vol. 188, pp. 2067-2074, 1998.

[68] E. A. et al. Nelson, *Blood*, vol. 117, pp. 3421–3429 , 2011.

[69] I. et al. Cotarla, *Int. J. Cancer* , vol. 108, pp. 665-671, 2004.

[70] M., Baumann, H. & Wetzler, M. Benekli, *J. Clin. Oncol* , vol. 27, pp. 4422-4432, 2009.

[71] E. A. et al. Nelson, *Oncotarget*, vol. 2, pp. 518–524 , 2011.

[72] J. et al. Hou, *Science*, vol. 265, pp. 1701-1707, 1994.

[73] S. et al. Sehra, *J. Immunol.* , vol. 184, pp. 3186–3190 , 2010.

[74] S. P. et al. Chapoval, *J. Immunol.*, vol. 186, pp. 2571–2583 , 2011.

[75] D. A. & Schleimer, R. P. Kuperman, *Curr. Mol. Med* , vol. 8, pp. 384–392 , 2008.

[76] Y. et al Chiba, *Am. J. Respir. Cell. Mol. Biol* , vol. 40, pp. 159–167 , 2009.

[77] Y. et al. Chiba, *Am. J. Respir. Cell. Mol. Biol.* , vol. 41, pp. 516–524 , 2009.

[78] W. T. et al. Khaled, *Development* , vol. 134, pp. 2739–2750 , 2007.

[79] Tay A, Guy GR and Tan YH. Cao X, *Mol. Cell. Biol.* , vol. 16, pp. 1595 -1603 , 1996.

[80] Meyer DJ, Campbell GS, Larner AC, Carter-Su C, Schwartz J and Jove R. Yu CL, *Science*, vol. 1995, pp. 81-83, 269.

[81] Horvath CM, Besser D, Lathem WW and Darnell Jr JE. Bromberg JF, *Mol. Cell. Biol* , vol. 18, pp. 2553-2558 , 1998.

[82] Bowman T, Garcia R, Caldenhoven E, De Groot RP and Jove R. Turkson J, *Mol. Cell. Biol.* , vol. 18, pp. 2545-2552 , 1998.

[83] Wrzeszczynska MH, Devgan G, Zhao Y, Pestell RG, Albanese C and Darnell Jr JE. Bromberg JF, *Cell.*, vol. 98, pp. 295-303 , 1999.

[84] Bromberg JF, Darnell Jr JE and Hanafusa H. Besser D, *Mol. Cell. Biol.* , vol. 19, pp. 1401-1409 , 1999.

[85] Zeng L, Jiang Y, Sadowski HB and Wang LH. Zong CS, *J. Biol. Chem* , vol. 273, pp. 28065-28072 , 1998.

[86] Yu CL, Hudnall A, Catlett R, Nelson KL, Smithgall T, Fujita DJ, Ethier SP and Jove R. Garcia R, *Cell Growth Diff.*, vol. 8, pp. 1267-1276 , 1997.

[87] Lin HH, Shih HM, Kung HJ and Ann DK. Wen X, *Biol. Chem.*, vol. 274, pp. 38204-38210 , 1999.

[88] Medveczky MM and Medveczky PG. Lund T, *J. Virol.* , vol. 71, pp. 378-382 , 1997.

[89] Lin JX, Cereseto A, Mulloy JC, O'Shea JJ, Franchini G and Leonard WJ. Migone TS, *Science*, vol. 269, pp. 79-81, 1995.

[90] Egen C, Wehinger J, Ludwig W, Gouilleux-Gruart V, Mertelsmann R and Finke J. Weber-Nordt RM, *Blood*, vol. 88, pp. 809-816 ,

1996.

[91] Danial NN and Rothman P., *Oncogene*, vol. 19, pp. 2523-2531 , 2000.

[92] Frank DA and Gri□n JD. Carlesso N, *J. Exp. Med.* , vol. 183, pp. 811-820, 1996.

[93] Raaijmakers JA, Lammers JW, Jove R and Koenderman L. de Groot RP, *Blood*, vol. 94, pp. 1108-1112, 1999.

[94] Gesbert F, Frank DA, Sattler M and Grin JD. Sillaber C, *Blood*, vol. 95, pp. 2118-2125 , 2000.

[95] Ariyoshi K, Nosaka T, Yamada K, Onishi M, Oka Y, Miyajima A and Kitamura T. Yamada K, *Int. J. Hematol.* , vol. 71, pp. 46-54, 2000.

[96] E. et al Caldenhoven, *J. Biol. Chem.* , vol. 271, pp. 13221–13227 , 1996.

[97] T.S., Sanders, L.K. & Nathans, D. Schaefer, *Proc. Natl. Acad. Sci.* , vol. 92, pp. 9097–9101 , 1995.

[98] J.Y., Huso, D.L., Nathans, D. & Desiderio, S Yoo, *Cell*, vol. 108, pp. 331–344 , 2002.

[99] Michelle L Sugrue, Silvia Tininini, Sarah Dewilde, Birgit Strobl, XinPing Fu, Victoria Murray-Tait, Roberto Chiarle,Valeria Poli Diego Maritano, *Nature Immunol.*, vol. 5, pp. 401-409, 2004.

[100] Drenning SD, Zeng Q, Watkins SC, Melhem MF, Endo S, Johnson DE, Huang L, He Y and Kim JD. Grandis JR, *Proc. Natl. Acad. Sci.* , vol. 97, pp. 4227-4232 , 2000.

[101] Kaltoft K, Nordahl M, Ropke C, Geisler C, Mustelin T, Dobson P, Svejgaard A and Odum N. Nielsen M, *Proc. Natl. Acad. Sci.* , vol. 94, pp. 6764-6769 , 1997.

[102] J. & Jove, R Turkson, *Oncogene*, vol. 19, pp. 6613–6626 , 2000.

[103] J. Turkson, *Expert Opin. Ther. Targets* , vol. 8, pp. 409-422, 2004.

[104] J. et al. Turkson, *J. Biol. Chem* , vol. 276, pp. 45443–45455 , 2001.

[105] Z. et al. Ren, "Bioorg. Med. Chem. Lett. ," vol. 13, pp. 633-636, 2003.

[106] J. S. McMurray, *Biopolymers* , vol. 90, pp. 69-79, 2008.

[107] P. T. et al. Gunning, *Bioorg. Med. Chem. Lett* , vol. 17, pp. 1875-1878, 2007.

[108] W. Jaganathan, S. & Turkson, J Zhao, *J. Biol. Chem* , vol. 285, pp. 35855–35865 , 2010.

[109] H. et al. Song, *Proc. Natl Acad. Sci* , vol. 102, pp. 4700-4705, 2005.

[110] B. et al Fuh, *Br. J. Cancer* , vol. 100, pp. 106-112, 2009.

[111] W. et al Hao, *Bioorg. Med. Chem. Lett.* , vol. 18, pp. 4988–4992 , 2008.

[112] J. et al. Schust, *Chem. Bio*, vol. 13, pp. 1235–1242 , 2006.

[113] K. et al Matsuno, *ACS Med. Chem. Lett.* , vol. 1, pp. 3751–3755 , 2010.

[114] H. et al. Chen, *Eur. J. Med. Chem* , vol. 62c, pp. 498-507, 2013.

[115] M. J. et al. Kim, *Cancer Lett* , vol. 335, pp. 145–152 , 2013.

[116] Cheng-Liang Yang et al., *PLoS ONE* , vol. 7, p. e37960 , 2012.

[117] S. L. et al. Fossey, *BMC cancer*, vol. 11, p. 112, 2011.

[118] K. et al. Selvendiran, *Cancer Biol. Ther.* , vol. 12, pp. 837–845 , 2011.

[119] B. J. et al. ierney, *Cancer Biol. Ther.* , vol. 13, pp. 766-775, 2012.

[120] G. I. et al. Onimoe, *Invest. New Drugs* , vol. 30, pp. 916-926, 2012.

[121] H. K. et al. Bid, *PLoS ONE* , vol. 7, p. e35513 , 2012.

[122] M., Harikumar, K. B. & Aggarwal,B. B. Shakibaei, *Mol. Nutr. Food Res.* , vol. 53, pp. 115-128, 2009.

[123] J. E. et al. Kim, *Exp. Mol. Med* , vol. 40, pp. 514-522, 2008.

[124] J,E. Saxton, P.A. Cranwell, *J. Chem. Soc.*, p. 3482, 1967.

[125] B.Letois, S.Rault, N.H.Dung, C.Saturnino, M.Robba, J.C.Lancelot, *Gazz. Chim. Ital.*, vol. 121, pp. 301-307, 1991.

[126] M. Parisien, A. Jean, K. Fagnou L.C. Campeau, *J. Am. Chem. Soc.*, vol. 128, pp. 581-590, 2006.

[127] Z. Wen, J.E. Darnell Z. Zhong, *Science*, vol. 264, pp. 95-98, 1994.

[128] K. Öfele, *J. Organomet. Chem* , vol. 12, p. p42, 1968.

[129] H.-W. Wanzlick and H.-J. Schönherr, *Angew. Chem., Int. Ed. Engl.* , vol. 7, pp. 141-142, 1968.

[130] R. L. Harlow and M. Kline A. J. Arduengo, *J. Am. Chem. Soc.*, vol. 113, pp. 361-363, 1991.

[131] M. Kline, J. C. Calabrese and F. Davidson A. J. Arduengo, *J. Am. Chem. Soc* , vol. 113, pp. 9704–9705 , 1991.

[132] J.A. Pople J. Lennard-Jones, *Discus. Faraday. Soc.*, vol. 10, p. 9, 1951.

[133] G.D. Zeiss, G.W. Van Dine R. Hoffmann, *J. Am. Chem. Soc.* , vol. 90, p. 1485, 1968.

[134] K. Raghavachari, M.J. Frisch, J.S. Binkley, P.v.R. Schleyer, A. Pople, *J. Am. Chem. Soc.*, vol. 105, p. 6389, 1983.

[135] J. L. Pauling, *Chem. Soc., Chem. Commun.* , p. 688, 1980.

[136] W.A. Goddard III, J.L. Beauchamp K.K. Irikura, *J. Am. Chem. Soc.* , vol. 144, p. 48, 1992.

[137] G.B. Schuster, *Adv. Phys. Org. Chem* , vol. 22, p. 311, 1986.

[138] M. Soleilhavoup, S. Conejero, G. Bertrand Y. Canac, *Organomet. Chem.*, vol. 689, p. 3857, 2004.

[139] M.B. Hall, T.E. Taylor, *J. Am. Chem. Soc.* , vol. 106, p. 1576, 1984.

[140] M.F. Lappert, *J. Organomet. Chem* , vol. 358, p. 185, 1988.

[141] M. Solà, S.F. Vyboishchikov G. Frenking, *J. Organomet. Chem* , vol. 690, p. 6178, 2005.

[142] B.L. Shaw G. Rouschias, *J. Chem. Soc., Chem. Commun.* , vol. 183, 1970.

[143] J. Chatt, R.L. Richards, G.A. Sim E.M. Badley, *J. Chem. Soc. D* , p. 1322, 1969.

[144] A.L. Balch, *J. Organomet. Chem.* , vol. 37, p. c19, 1972.

[145] J.H. Enemark, J. Parks, A.L. Balch W.M. Butler, *Inorg. Chem.*, vol. 12, p. 451, 1973.

[146] K. Fichtel, K. Öfele E.O. Fischer, *Chem. Ber.* , vol. 85, p. 249, 1962.

[147] A. Maasböl E.O. Fischer, *Angew. Chem., Int. Ed. Engl.* , vol. 3, p. 580, 1964.

[148] E. Fjedor, K.H. Jerg H.W. Wanzlick, *Chem. Ber* , vol. 96, p. 1208, 1963.

[149] H.J. Schoenherr H.W. Wanzlick, *Angew. Chem., Int. Ed. Engl* , vol. 7, p. 141, 1968.

[150] K. Öfele, *Angew. Chem., Int. Ed. Engl* , vol. 7, p. 950, 1968.

[151] R.L. Harlow, M. Kline A.J. Arduengo III, *J. Am. Chem. Soc* , vol. 113, p. 3611, 1991.

[152] T.-G. Ong, J.S. O'Brien, N. Lavoie, E. Bell, G.P.A. Yap, I. Korobkov, D.S. Richerson P. Bazinet, *Organometallics* , vol. 26, p. 2885, 2007.

[153] M. Elison, J. Fischer, C. Köcher, G.R.J. Artus W.A. Herrmann, *Angew. Chem., Int. Ed. Engl* , vol. 34, p. 2371, 1995.

[154] S.P. Nolan S. Díez-González, *Annu. Rep. Prog. Chem.*, vol. 101, p. 171, 2005.

[155] R.H. Grubbs E. Despagnet-Ayoub, *J. Am. Chem. Soc.* , vol. 126, p. 10198, 2004.

[156] M.C. Jahnke F.E. Hahn, *Angew. Chem., Int. Ed.*, vol. 47, p. 3122, 2008.

[157] S. Pearson P.L. Arnold, *Coord. Chem. Rev* , vol. 251, p. 596 , 2007.

[158] A.A. Danopoulos D. Pugh, *Coord. Chem. Rev.* , vol. 251, p. 610, 2007.

[159] W.A. Herrmann, *Angew. Chem., Int. Ed* , vol. 41, p. 1290, 2002.

[160] I.M. Mihaltseva A.A. Gridnev, *Synth. Commun* , vol. 24, p. 1547, 1994.

[161] N.M. Scott, E.D. Stevens, T. Ramnial, O.C. Lightbody, C.L.B. Mac- Donald, J.A.C. Clyburne, S.P. Nolan P. de Frémont, *Organometallics* , vol. 24, p. 6301, 2005.

[162] G. Altenhoff, R. Goddard, C.W. Lehmann F. Glorius, *Chem. Commun.* , p. 2704, 2002.

[163] W.A. Herrmann, *Angew. Chem., Int. Ed* , vol. 41, p. 1290, 2002.

[164] R. Krafczyk, R. Schmutzler A.J. Arduengo III, *Tetrahedron* , vol. 55, p. 14523, 1999.

[165] E.D. Stevens, S.P. Nolan L. Jafarpour, *J. Organomet. Chem* , vol. 606, p. 49, 2000.

[166] Beilstein L. Hintermann, *J. Org. Chem* , vol. 3, p. 22, 2007.

[167] J.P. Donahue R.H. Holm, *Polyhedron* , vol. 93, p. 571, 2012.

[168] J.M. Rodezno, S. Gupta, A.J. Lough M.K. Denk, *J. Organomet. Chem.* , vol. 617, p. 242, 2001.

[169] J.M. Rodezno M.K. Denk, *J. Organomet Chem* , vol. 617, p. 737, 2001.

[170] K.J. Cavell, B.F. Yates A.M. Magill, *J. Am. Chem. Soc.* , vol. 126, p. 8717, 2004.

[171] C.-H. Hu M.-T. Lee, *Organometallics* , vol. 23, p. 976, 2004.

[172] G. Frenking C. Boehme, *Organometallics* , vol. 17, p. 5801, 1998.

[173] I. Castro-Rodriguez, K. Olsen, K. Meyer X. Hu, *Organometallics* , vol. 23, p. 755, 2004.

[174] J.L. Petersen, H. Jacobsen, L. Cavallo, S.P. Nolan S. Fantasia, *Organometallics* , vol. 26, p. 5880, 2007.

[175] R.H. Crabtree, *J. Organomet. Chem* , vol. 690, p. 5451, 2005.

[176] E.D. Stevens, N.M. Scott, C. Costabile, L. Cavallo, C.D. Hoff, S.P. Nolan R. Dorta, *J. Am. Chem. Soc* , vol. 127, p. 2485, 2005.

[177] S.P. Nolan S. Díez-González, *Coord. Chem. Rev.* , vol. 251, p. 874, 2007.

[178] E. Cetinkaya, H. Kucukbay and R. Durmaz B. Cetinkaya, *Arzneim. Forsch.*, vol. 46, pp. 821-823, 1996.

[179] F.R. Path, W.B. Hugo A.D. Russel, *Prog. Med. Chem* , vol. 31, pp. 351-370, 1994.

[180] J.T. Grayston, M.A. Krohn, R.A. Kronmal T.A. Bell, *Pediatrics* , vol. 92, pp. 755-760, 1993.

[181] A. Sugie, K. Nomiya N.C. Kasuga, *Dalton Trans* , pp. 3732-3740 , 2004.

[182] A. Falabella, R.S. Kirsner A. Drousou, *Wounds*, vol. 15, pp. 149-166 , 2003.

[183] B.J. Herbert, J. J.C. Green, *Chem. Soc. Dalton Trans.* , vol. 7, pp. 1214-1220, 2005.

[184] W.H. Guo, M.T. Lee, C.H. Hu C.L. Lai, *J. Organomet. Chem.* , vol. 690, pp. 5867-5875 , 2005.

[185] O. Kühl, *Chem. Soc. Rev.* , vol. 36, pp. 592-607 , 2007.

[186] L.B. Munro, C.E. Strasser, A.F. Samin V.J. Catalano, *Inorg. Chem.*, vol. 50, pp. 8465-8476 , 2011.

[187] W. Chen, S. Jin B. Liu, *Organometallics* , vol. 26, pp. 3660-3667, 2007.

[188] R. Mohan, J.K. Singh, M.K. Samantaray, M.M. Shaikh, D. Panda, P. Ghosh S. Ray, *J. Am. Chem. Soc.* , vol. 129, pp. 15042-15053 , 2007.

[189] T.J. Siciliano, S. Durmus, M.J. Panzner, D.A. Medvetz, D.V. Reddy, L.A. Hogue, C.E. Hovis, J.K. Hilliard, R.J. Mallet, C.A. Tessier, C.L. Cannon, W.J. Youngs K.M. Hindi, *J. Med. Chem.* , vol. 51, pp. 1577-1583 , 2008.

[190] R. S. Simons, A. Milsted, F. Pingitore, C. Wesdemiotis, C. A. Tessier and W. J. Youngs A. Melaiye, *J. Med. Chem.* , vol. 47, pp. 973-977, 2004.

[191] A. M. Al-Enizi, E. A. Elsayed, R. R. Butorac, S. S. Al-Deyab, M. A. Wadaan and A. H. Cowley A. A. Elzatahry, *Int. J. Nanomed* , vol. 7, pp. 2829–2832 , 2012.

[192] A. J. Ditto, A. Knapp, P. N. Shah, B. D. Wright, R. Blust, L. Christensen, C. B. Clemons, J. P. Wilber, G. W. Young, A. G. Kang, M. J. Panzner, C. L. Cannon, Y. H. Yun, W. J. Youngs, N. M. Seckinger and E. K. Cope J. G. Leid, *J. Antimicrob. Chemother* , vol. 67, pp. 138-148, 2012.

[193] A. Melaiye, K. Hindi, S. Durmus, M. J. Panzner, L. A. Hogue, R. J. Mallett, C. E. Hovis, M. Coughenour, S. D. Crosby, A. Milsted, D. L. Ely, C. A. Tessier, C. L. Cannon and W. J. Youngs A. Kascatan-Nebioglu, *J. Med. Chem*, vol. 49, pp. 6811–6818, 2006.

[194] T. J. Siciliano, S. Durmus, M. J. Panzner, D. A. Medvetz, D. V. Reddy, L. A. Hogue, C. E. Hovis, J. K. Hilliard, R. J. Mallet, C. A. Tessier, C. L. Cannon and W. J. Youngs K. M. Hindi, *J. Med. Chem.*, vol. 51, pp. 1577–1583, 2008.

[195] K. Dietrich, A. Deally, B. Gleeson, H. Müller-Bunz, F. Paradisi and M. Tacke S. Patil, *Helv. Chim. Acta*, vol. 93, pp. 2347– 2364, 2010.

[196] J. Claffey, A. Deally, M. Hogan, B. Gleeson, L. M. M. Méndez, H. Müller-Bunz, F. Paradisi and M. Tacke S. Patil, *Eur. J. Inorg. Chem*, pp. 1020-1031, 2010.

[197] A. Deally, B. Gleeson, H. Müller-Bunz, F. Paradisi and M. Tacke S. Patil, *Appl. Organomet. Chem*, vol. 11, pp. 781-793, 2010.

[198] G. Lally, H. Müller-Bunz, F. Paradisi, D. Quaglia, W. Streciwilk and M. Tacke F. Hackenberg, *J. Organomet. Chem.*, vol. 717, pp. 123-134, 2012.

[199] C. Jolivalt, T. Cresteil, L. Eloy, P. Bouhours, A. Hequet, V. Mansuy, C. Vanucci and J.-M. Paris S. Roland, *Chem.–Eur. J*, vol. 17, pp. 1442–1446, 2011.

[200] R. Mohan, J. K. Singh, M. K. Samantaray, M. M. Shaikh, D. Panda and P. Ghosh S. Ray, *J. Am. Chem. Soc.* , vol. 129, pp. 15042–15053., 2007.

[201] K. Bensdorf, M. Proetto, U. Abram, A. Hagenbach and R. Gust W. Liu, *J. Med. Chem* , vol. 54, pp. 8605–8615 , 2011.

[202] A.-S. Jarrousse, M. Manin, A. Chevry, S. Roche, F. Norre, C. Beaudoin, L. Morel, D. Boyer, R. Mahiou and A. Gautier M.-L. Teyssot, *Dalton Trans.*, pp. 6894–6902 , 2009.

[203] R.,McCleverty, J. A., Meyer, T. J. Mukherjee, *In Comprehensive Coordination Chemistry II-From Biology to Nanotechnology*, vol. 6, 2004.

[204] A. R. Mufti, E. Burstein, and C. S. Duckett, *Arch. Biochem. Biophys.* , vol. 463, p. 168, 2007.

[205] M. Pellei, F. Tisato and C. Santini C. Marzano, *Anti-Cancer Agents Med. Chem* , vol. 9, pp. 185–211 , 2009.

[206] A´. Garcı´a-Raso, A´. Terro´n, E. Molins, M. J. Prieto, V. Moreno, J. Martı´nez, V. Llado´, I. Lo´pez, A.Gutie´rrezandP.V.Escriba´ M. Barcelo´-Oliver, *J.Inorg.Biochem* , vol. 101, pp. 649–659 , 2007.

[207] B. Donnadieu and B. Meunier M. Pitie´, *Inorg. Chem.* , vol. 37, pp. 3486–3489 , 1998.

[208] J. B. Shipley, D. C. Heimbrook, H. Sugiyama, E. C. Long, B. J. H. Van, d. M. G. A. Van, N. J. Oppenheimer and S. M. Hecht G. M. Ehrenfeld, *Biochemistry* , vol. 26, pp. 931–942 , 1987.

[209] A.-S. Jarrousse, A. Chevry, H. A. De, C. Beaudoin, M. Manin, S. P. Nolan, S. Diez-Gonzalez, L. Morel and A. Gautier M.-L. Teyssot, *Chem.–Eur. J.*, vol. 15, pp. 314-318, 2009.

[210] C. Gabbiani, G. Mastrobuoni, F. Sorrentino, B. Dani, M. P. Rigobello, A. Bindoli, M. A. Cinellu, G. Pieraccini and L. Messori A. Casini, *Medchemcomm* , vol. 2, pp. 50-54, 2011.

[211] Y. You and I. Ott H. Scheffler, *Polyhedron* , vol. 29, pp. 66-69, 2010.

[212] P. J. Barnard and S. J. Berners-Price, *Coord. Chem. Rev.*, vol. 251, pp. 1889–1902 , 2007.

[213] A. M. Shearwood, R. Thyer, E. McNamara, S. M. Davies, B. A. Callus, A. Miranda-Vizuete, S. J. Berners- Price, Q. Cheng, E. S. Arner and A. Filipovska O. Rackham, *Free Radical. Biol. Med.* , vol. 50, pp. 689–699 , 2011.

[214] B. J. Bhuyan and G. Mugesh K. P. Bhabak, *Dalton Trans.* , vol. 40, pp. 2099–2111 , 2011.

[215] C. P. Bagowski, M. Kokoschka, M. Stefanopoulou, H. Alborzinia, S. Can, D. H. Vlecken, W. S. Sheldrick, S. Wo¨ lfl and I. Ott A. Meyer, *Angew. Chem., Int. Ed.* , vol. 51, pp. 8895–8899 , 2012.

[216] R. K. Johnson, D. T. Hill, L. F. Faucette, G. R. Girard, G. Y. Kuo, C. M. Sung and S. T. Crooke C. K. Mirabelli, *J. Med. Chem.*, vol. 29, pp. 218–223 , 1986.

[217] R. A. Ruhayel, P. J. Barnard, M. V. Baker, S. J. Berners-Price and A. Filipovska J. L. Hickey, *J. Am. Chem. Soc.*, vol. 130, pp. 12570–12571 , 2008.

[218] S., Gaillard, C. Toye, S. Macpherson, S. P. Nolan and A. Riches J. Weaver, *Chem.–Eur. J.*, vol. 17, pp. 6620–6624 , 2011.

[219] D. Bose, P. Mitra, K. Das Saha, V. Bertolasi and J. Dinda S. Das Adhikary, *New J. Chem.*, vol. 36, pp. 759–767 , 2012.

[220] A. Deally, F. Hackenberg, L. Kaps, H. Mu¨ ller-Bunz, R. Schobert and M. Tacke S. Patil, *Helv. Chim. Acta* , vol. 94, pp. 1551–1562 , 2011.

[221] W. C. Shih, H. C. Chang, Y. Y. Kuo, W. C. Hung, T. G. Ong and W. S. Li C. H. Wang, *J. Med. Chem.* , vol. 54, pp. 5245–5249 , 2011.

[222] B. Biersack, H. Mu¨ ller-Bunz, K. Mahal, J. Munzner, M. Tacke, T. Mueller and R. Schobert L. Kaps, *J. Inorg. Biochem.* , vol. 106, pp.

52-58, 2012.

[223] C. Pfluger, A. Citta, A. Folda, M. P. Rigobello, A. Bindoli, A. Casini and F. Mohr E. Schuh, *J. Med. Chem.*, vol. 55, pp. 5518-5528, 2012.

[224] S. Cronje, L. Dobrzanska, H. G. Raubenheimer, G. Joone, M. J. Nell and H. C. Hoppe J. Coetzee, *Dalton Trans.*, vol. 40, pp. 1471–1483 , 2011.

[225] K. Bensdorf, M. Proetto, U. Abram, A. Hagenbach and R. Gust W. Liu, *J. Med. Chem.* , vol. 54, pp. 8605-8615, 2011.

[226] K. Bensdorf, M. Proetto, A. Hagenbach, U. Abram and R. Gust W. Liu, *J. Med. Chem.*, vol. 55, pp. 3713–3724 , 2012.

[227] M. Napoli, C. Costabile, P. Longo C. Bocchino, *Polym. Sci. A Polym. Chem.*, vol. 49, pp. 862-870 , 2011.

[228] M. J. Chmielewski, M. Charon, and J. Jurczak, "Org. Letters," vol. 6, p. 3501, 2004.

[229] M. P. Rigobello, G. Scutari, C. Gabbiani, A. Casini and L. Messori A. Bindoli, *Coord. Chem. Rev.* , vol. 253, pp. 1692–1707 , 2009.

[230] V. Milacic and Q. P. Dou, *Coord. Chem. Rev* , vol. 253, pp. 1649–1660 , 2009.

[231] A. Molter and F. Mohr, *Coord. Chem. Rev.* , vol. 254, pp. 19-45, 2010.

[232] I. Ott, *Coord. Chem. Rev* , vol. 253, pp. 1670–1681 , 2009.

[233] M. R. Kilburn, J. B. Cliff, L. Filgueira, M. Saunders and S. J. Berners-Price L. E. Wedlock, *Metallomics* , vol. 3, pp. 917–925 , 2011.

[234] C. M. Che and R. W. Sun, *Chem. Commun* , vol. 47, pp. 9554–9560 , 2011.

[235] M. Navarro, *Coord. Chem. Rev.* , vol. 253, pp. 1619–1626 , 2009.

[236] M. V. Baker, S. J. Berners-Price and D. A. Day P. J. Barnard, *J. Inorg. Biochem.*, vol. 98, pp. 1642–1647 , 2004.

[237] M. V. Baker, S. J. Berners-Price, B. W. Skelton and A. H. White P. J. Barnard, *Dalton Trans.* , pp. 1038–1047 , 2004.

[238] P. J. Barnard, S. J. Berners-Price, S. K. Brayshaw, J. L. Hickey, B.

W. Skelton and A. H. White M. V. Baker, *J. Organomet. Chem.*, vol. 690, pp. 5625–5635 , 2005.

[239] R. A. Ruhayel, P. J. Barnard, M. V. Baker, S. J. Berners-Price and A. Filipovska J. L. Hickey, *J. Am. Chem. Soc.* , vol. 130, pp. 12570–12571 , 2008.

[240] S. J. Nichols, B. A. Callus, M. V. Baker, P. J. Barnard, S. J. Berners-Price, J. Whelan, G. C. Yeoh and A. Filipovska M. M. Jellicoe, *Carcinogenesis* , vol. 29, pp. 1124–1133, 2008.